HIGHWAY RESEARCH RECORD

Number 42

Extension of AASHO Road Test Concepts

4 Reports

Presented at the
42nd ANNUAL MEETING
January 7-11, 1963

HIGHWAY RESEARCH BOARD
of the
Division of Engineering and Industrial Research
National Academy of Sciences—
National Research Council
Washington, D. C.
1963

Department of Design

T. E. Shelburne, Chairman
Director of Research, Virginia Department of Highways
Charlottesville

Harold Allen, Chief, Division of Physical Research, Office of Research, U. S. Bureau of Public Roads, Washington, D. C.

Glenn Anschutz, Engineer of Aerial Surveys and Photogrammetry Section, Kansas State Highway Commission, Topeka

Robert F. Baker, Director, Office of Research and Development, U. S. Bureau of Public Roads, Washington, D. C.

Joseph Barnett, Deputy Director of Engineering, U. S. Bureau of Public Roads, Washington, D. C.

A. C. Benkelman, Altamonte Springs, Florida

Phillip P. Brown, Consultant, Soils, Mechanics and Paving Bureau of Yards and Docks, Department of the Navy, Washington, D. C.

J. N. Clary, Engineer of Bridges, Virginia Department of Highways, Richmond

C. N. Conner, Hollywood, Florida

Eric L. Erickson, Chief, Bridge Division, Office of Engineering, U. S. Bureau of Public Roads, Washington, D. C.

Wilbur J. Garmhausen, Chief Landscape Architect, Ohio Department of Highways, Columbus

A. T. Goldbeck, Chevy Chase, Maryland

John M. Griffith, Director of Research and Development, The Asphalt Institute, University of Maryland, College Park

Carl F. Izzard, Chief, Office of Research and Development, Hydraulic Research Division, U. S. Bureau of Public Roads, Washington, D. C.

R. E. Livingston, Planning and Research Engineer, Colorado State Highway Department, Denver

D. W. Loutzenheiser, Chief, Highway Standards and Design Division, U. S. Bureau of Public Roads, Washington, D. C.

Ralph A. Moyer, Research Engineer, Institute of Transportation and Traffic Engineering, University of California, Berkeley

Ernest T. Perkins, Executive Director, East Hudson Parkway Authority, Pleasantville, New York

Thomas B. Pringle, Chief, Civil Engineering Branch, Engineering Division, Military Construction, Office, Chief of Engineers, Department of the Army, Washington, D. C.

Gordon K. Ray, Manager, Paving Bureau, Portland Cement Association, Chicago, Illinois

K. A. Stonex, Assistant Engineer-in-Charge, General Motors Corporation, Warren, Michigan

William Van Breemen, Research Engineer, Engineering Research, New Jersey State Highway Department, Trenton

Eldon J. Yoder, Joint Highway Research Project, Purdue University, Lafayette, Indiana

COMMITTEE ON FLEXIBLE PAVEMENT DESIGN

R. E. Livingston, Chairman
Planning and Research Engineer
Colorado State Highway Department, Denver

Stuart Williams, Secretary
Supervisory Highway Research Engineer
U. S. Bureau of Public Roads, Washington, D. C.

A. C. Benkelman, Altamonte Springs, Florida
John A. Bishop, Director, Soils and Pavement Division, U. S. Naval Civil Engineering Laboratory, Port Hueneme, California
Thomas L. Bransford, Engineer of Research and In-Service Training, Florida State Road Department, Gainesville
W. H. Campen, Manager, Omaha Testing Laboratories, Omaha, Nebraska
George H. Dent, Benjamin E. Beavin Company, Baltimore, Maryland
James M. Desmond, Assistant State Materials Engineer, Wyoming State Highway Department, Cheyenne
T. V. Fahnestock, Bituminous Engineer, North Carolina State Highway Commission, Raleigh
Charles R. Foster, Coordinator of Research, National Bituminous Concrete Association, Texas A & M College, College Station
F. H. Gardner, Transportation Engineer Office, Transportation Research Command, Fort Eustis, Virginia
J. E. Gray, Engineering Director, National Crushed Stone Association, Washington, D. C.
John M. Griffith, Director of Research & Development, The Asphalt Institute, University of Maryland, College Park
R. A. Helmer, Research Engineer, Oklahoma Department of Highways, Oklahoma City
Frank B. Hennion, Assistant Chief, Civil Engineering Branch, Engineering Division, Military Construction, Office, Chief of Engineers, Department of the Army, Washington, D. C.
Raymond C. Herner, Consulting Engineer, Indianapolis, Indiana
W. S. Housel, University of Michigan, Ann Arbor
F. N. Hveem, Materials and Research Engineer, California Division of Highways, Sacramento
Charles W. Johnson, Engineer of Construction, New Mexico State Highway Department, Sante Fe
Henry J. Lichtefeld, Federal Aviation Agency, Airports Division, Washington, D. C.
Wallace J. Liddle, Chief Materials Engineer, Materials Testing Laboratory, Utah State Department of Highways, Salt Lake City
Chester McDowell, Supervising Soils Engineer, Texas Highway Department, Austin
Alfred W. Maner, Staff Engineer, The Asphalt Institute, University of Maryland, College Park
C. E. Minor, Materials and Research Engineer, Washington Department of Highways, Olympia
Carl L. Monismith, University of California, Berkeley
A. O. Neiser, Assistant State Highway Engineer, Kentucky Department of Highways, Frankfort
Frank P. Nichols, Jr., Highway Research Engineer, Virginia Department of Highways, Charlottesville
R. L. Peyton, Assistant State Highway Engineer, State Highway Commission of Kansas, Topeka
E. G. Robbins, Portland Cement Association, Chicago, Illinois
Rollin J. Smith, Engineer—Manager, Asphalt Department, Skelly Oil Company, Kansas City, Missouri

Fred Sternberg, Senior Highway Engineer—Research, Connecticut State Highway Department, Hartford
John H. Swanberg, Chief Engineer, Minnesota Department of Highways, St. Paul
B. A. Vallerga, Vice President, Golden Bear Oil Company, Bakersfield, California

COMMITTEE ON RIGID PAVEMENT DESIGN

William Van Breemen, Chairman
Research Engineer, Engineering Research
New Jersey State Highway Department, Trenton

Harry D. Cashell, Secretary
Chief, Concrete and Concrete Pavement Branch, Physical Research Division
U. S. Bureau of Public Roads, Washington, D. C.

Henry Aaron, Chief Engineer, Reinforced Concrete Pavement Division, Wire Reinforcement Institute, Washington, D. C.
Robert F. Baker, Director, Office of Research and Development, U. S. Bureau of Public Roads, Washington, D. C.
Phillip P. Brown, Consultant, Soils, Mechanics and Paving, Bureau of Yards and Docks, Department of the Navy, Washington, D. C.
Paul F. Carlton, Engineer, Headquarters, Army Materiel Command (AMCRD-RS-ED-E), Washington, D. C.
W. E. Chastain, Sr., Assistant Engineer of Research and Planning, Research Branch, Illinois Division of Highways, Springfield
E. A. Finney, Director, Research Laboratory Division, Michigan State Highway Department, Lansing
W. S. Housel, University of Michigan, Ann Arbor
F. N. Hveem, Materials and Research Engineer, California Division of Highways, Sacramento
W. H. Jacobs, Executive Secretary, Rail Steel Bar Association, Chicago, Illinois
C. D. Jensen, Director, Bureau of Materials, Pennsylvania Department of Highways, Harrisburg
Wallace J. Liddle, Chief Materials Engineer, Materials Testing Laboratory, Utah State Department of Highways, Salt Lake City
Ernest T. Perkins, Executive Director, East Hudson Parkway Authority, Pleasantville, New York
Thomas B. Pringle, Chief, Civil Engineering Branch, Engineering Division, Military Construction, Office of Chief of Engineers, Department of the Army, Washington, D. C.
Gordon K. Ray, Manager, Paving Bureau, Portland Cement Association, Chicago, Illinois
James P. Sale, Assistant Chief, Special Engineering Branch, Research and Development, Military Science Division, Department of the Army, Office of Chief of Engineers, Washington, D. C.
F. H. Scrivner, Pavement Research Engineer, Texas Transportation Institute, A & M College of Texas, College Station
M. D. Shelby, Research Engineer, Texas Highway Department, Austin
W. T. Spencer, Soils Engineer, Materials and Tests, Indiana State Highway Commission, Indianapolis
Otto A. Strassenmeyer, Associate Highway Engineer, Research and Development, Connecticut State Highway Department, Wethersfield
K. B. Woods, Head, School of Civil Engineering, and Director, Joint Highway Research Project, Purdue University, Lafayette, Indiana

Contents

Applications of a General Curve Fitting Procedure to AASHO Road Test Data

PAUL IRICK, Research Statistician, Highway Research Board

In most cases the mathematical models used for fitting AASHO Road Test data were not linear in the coefficients to be determined by the analysis. Since only least squares linear regression analysis was available at the Road Test, the summary equations that were developed and reported there were derived by a series of linearizations of the non-linear models. As a result, the coefficients that were obtained were not necessarily optimum with respect to particular criteria for the residuals from the equations.

This paper describes the application to Road Test data of a general curve fitting procedure that has been programmed for the Bendix G-15D computer. The new procedure can be used for linear or non-linear models and with any desired residual criterion; e.g., least squared residuals and minimum absolute residuals.

Results are given for applications of the new procedure to the derivation of present serviceability index formulas and pavement performance equations. Although the new results reflect only small differences from the corresponding results given in HRB Special Report 61E, the fit has been improved through the reduction of certain biases that were inherent in the previous methods of analysis.

The paper also presents results that are obtained when Road Test performance data are summarized with models that are simpler in form yet more comprehensive than those employed in previous Road Test reports.

An appendix to the paper gives detailed flow charts and illustrations that make it possible to code the procedures for other computers.

•A COMPUTATIONAL procedure has been evolved to fit experimental data with very general mathematical models. The procedure is described and illustrated in general terms, and an appendix presents rather complete details and illustrations for the procedure.

Apart from presenting the procedure itself, one objective is to show how the procedure, in the form of a Bendix G-15 computer program called MORC, can be used to provide a more unified analysis of AASHO Road Test pavement performance data than was possible when the Road Test performance equations were reported (1). Discussion and results are given to show how the MORC program can produce improved fits to the observed data, both with the models that were previously used and with considerably simplified forms of these models.

A final aim is to consider a somewhat different rationale for the analysis of pavement performance data than was used at the Road Test.

MORC PROCEDURE FOR GENERAL CURVE FITTING

There are many situations in which it is desirable to smooth or summarize experimental data by fitting a curve, or families of curves, to observed points that are plotted

Paper sponsored by Department of Design.

in a two dimensional diagram such as Figure 1. If only one curve is to be drawn then only two variables are involved; but if one or more families of curves must be used to represent the data properly, then more than two variables are involved and the curve fitting actually amounts to fitting a surface to the data after the coordinate system is expanded to include an axis for each variable.

Whether the curves are to be drawn by judgment or from the results of an automatic procedure, two questions must be answered: What geometrical properties shall the curves have, and what criterion shall be used to regulate discrepancies between points on the curves and corresponding data points? In automatic curve fitting these questions are settled by the selection of a mathematical model whose undetermined coefficients will be evaluated by the procedure and by the selection of a residual criterion that will lead to "best" values for the coefficients.

In Figure 1, the selected model is $X_1 = B_1 + B_2X_2$, the equation of a straight line, and the residual criterion to be minimized is the sum of squares of all vertical deviations from the line. One such residual is labeled r.

Whether this model and residual criterion are appropriate for the data shown is itself a question of judgment, and it is perhaps safe to say that there have been many attempts at automated (and manual) curve fitting where either the model or the criterion selection, or both, did not meet with universal approval. Perhaps the most that can be hoped is that models and criteria for fitting the models to experimental data will produce curves that are in accord with the judgment of those who are most experienced and knowledgeable in the field represented by the observations. Although this paper is concerned with automatic curve fitting, it seems appropriate to acknowledge that automation does not make the results valid. For example in Figure 1, the knowledgeable experimenter may know from theory or otherwise that the points shown are but a sample of observations that would ultimately tail out exponentially along the X_2 axis—so that a linear model is not really representative of the underlying relationship between X_1 and X_2. He may also know that some of the observations are suspect in that they probably represent a different set of conditions than do the remaining points; thus, the best residual criterion may involve lesser weights for residuals from these points than for the remaining residuals. Moreover, it may be that relative or percentage residuals are more appropriate to the problem than are the vertical deviations.

Generally speaking, most automatic curve fitting procedures have employed the techniques of least squares linear regression analysis where the models are linear combinations of unknown coefficients, where residuals are algebraic deviations parallel to one coordinate axis, and where the criterion to be minimized is the sum of squared residuals. These powerful procedures will probably remain the basis for most experi-

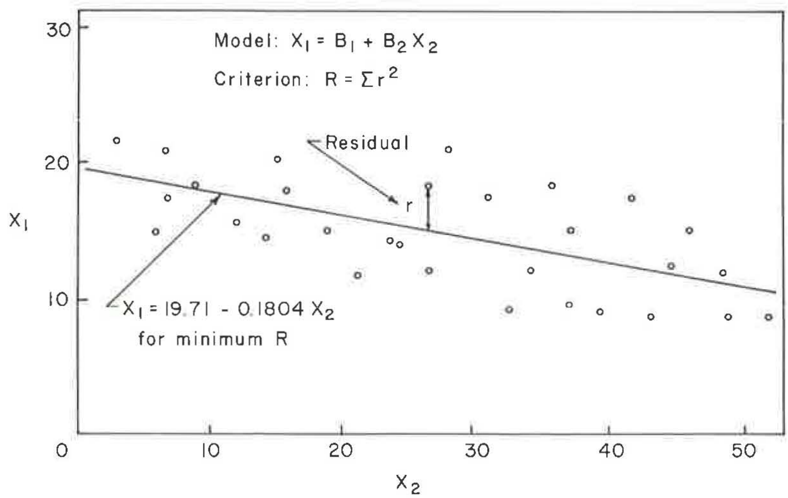

Figure 1. A simple linear regression problem.

mental designs and analyses, but compromises may be necessary in order to use them. For example, models non-linear in the coefficients are sometimes "linearized," perhaps by taking logarithms of one or more variables, or perhaps the non-linear models have to be fit piecemeal with subsets of the data or perhaps in successive stages of analysis. In some cases, the residuals have to be defined rather unnaturally so that the analysis only approximates what the experimenter might do by hand. Many algebraic forms are ruled out from the start because there are no appropriate linearizations.

MORC, an acronym for the minimization of residual criteria, is one of several automatic curve fitting procedures that have been evolved in recent years in order to fit almost any mathematical model to experimental data and to minimize almost any criterion based on residuals between the fitted curves and the observed points.

The general methods, including MORC, do not answer the two fundamental questions but they do permit a wide variety of permissible answers. At least in the case of MORC, the general procedures do not yield by-products, such as significance tests, standard errors, and correlation coefficients, that result from linear regression analyses, and may require long computations as well as thoughful intervention during the computation.

In Figure 1, a particular line is determined by values for B_1 and B_2, and these two values are the coordinates of a single point in the B_1B_2 plane of Figure 2. Corresponding to this point is an ordinate which is the residual criterion value, R, obtained from all residuals from the given line. Thus corresponding to every line in Figure 1 is an R value for Figure 2 and the locus of all criterion values will be called the criterion surface. For any specified region of the B_1B_2 plane there will be one or more least values for R, and the B_1 and B_2 values at this minimum will presumably yield the best fitting line to the data. The object of the MORC procedure for this problem is simply to start at an arbitrary point (B_1, B_2) and move over the criterion surface until the minimum is reached.

In terms of differential calculus, values are sought for B_1 and B_2 which satisfy the equations $\partial R/\partial B_1 = 0$ and $\partial R/\partial B_2 = 0$. In the B_1B_2 plane these equations have curves (lines in Fig. 2) which are projections of a valley system running through the criterion surface. All points denoted by letters in Figure 2 have been projected down, say, to the B_1B_2 plane from the overlying surface. Starting at A (above A), a parabola is fitted to the points A, a_1 and a_2, and the vertex of this parabola leads to the surface point (above) B which is hopefully in the neighborhood of the first valley. Points through B, b_1 and b_2 guide the next descent to C which is also supposed to be a valley point. The line from A through C determines a new origin at D and two more parabolas lead to E then F. Finally, a parabola whose plane contains the line CF is fitted at F and for the illustrative problem the vertex of the last parabola is at the minimum point G. Values

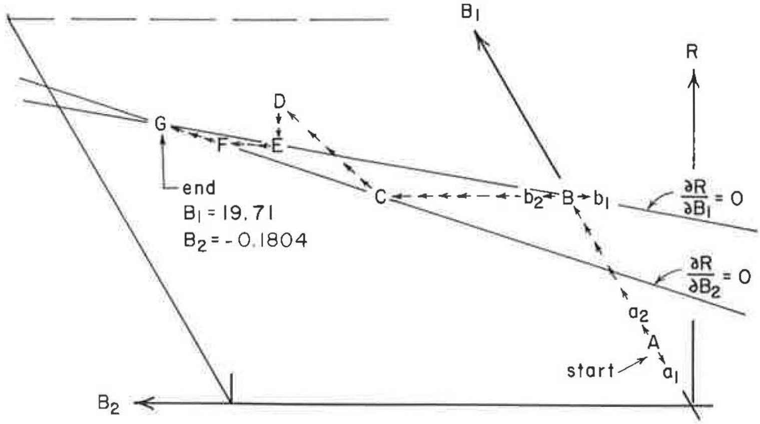

Figure 2. MORC path for simple linear regression.

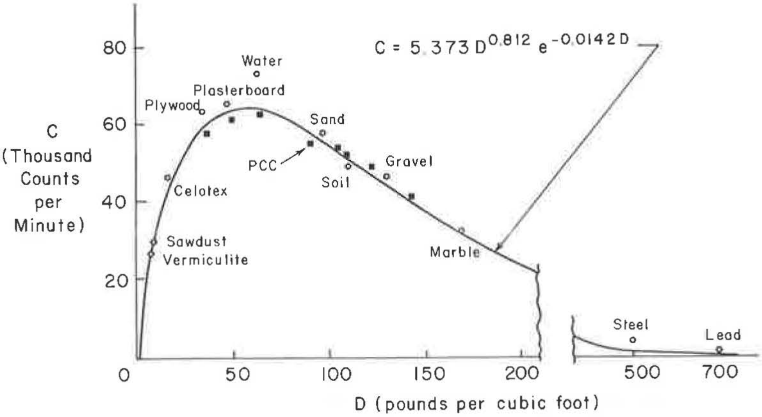

Figure 3. MORC fitting of nuclear density data.

of B_1, B_2 and R at G thus represent the problem's solution. When there are more coefficients or when the valley system is tortuous and cut off by constraints then the problem becomes much more complicated than in Figure 2 (see Appendix).

During the course of the Road Test nuclear devices were used to measure in-place densities of various materials. Before and during the field use, many laboratory experiments were performed, chiefly for calibration purposes. One such experiment, while perhaps not of any practical merit, resulted in the data plotted in Figure 3 in which the horizontal scale is for the densities of materials computed from weights and volumes. The vertical scale gives gamma ray counts, in thousands per minute, as the rays from a surface source traveled down through the material to be scattered and picked up by a surface detector only a few inches from the source. Many types of material were used in the experiment. The model selected for fitting the data was

$$C = B_1 D^{B_2} e^{-B_3 D}$$

where C and D are in the respective units of the vertical and horizontal scales of Figure 3. Residuals were considered to be vertical deviations of the observed counts from the corresponding curve values and the mean square residual was used as a criterion.

As is well known by those who use nuclear density gages, close calibration requires separate curves for different classes of materials. It is clear (Fig. 3) that the portland cement concrete data should be treated separately and that water seems to be in a class all by itself. Thus a complete model for the count-density relationship must include other factors and the curve can only be regarded as a broad generalization. The mathematical model is related, interestingly enough, to gamma functions in the field of mathematics, and has a maximum when $D = B_2/B_3$, at about 60 pcf. In this particular case it would be possible to use linear regression analysis to estimate the coefficients after taking logarithms. When MORC was applied to the data, no weight was given to the water data, and the result was the equation shown in Figure 3. The maximum horizontal deviation from the fitted curve is about 10 pcf in the range from D = 0 to D = 200, but most of the density deviations are less than 5 pcf.

APPLICATION OF MORC TO AASHO ROAD TEST PAVEMENT PERFORMANCE DATA

In order to discuss applications of the MORC program to AASHO Road Test pavement performance data it is helpful to review briefly some of the Road Test procedures. In Road Test Report 5 the model,

$$p = c_0 - (c_0 - c_1)(W/\rho)^\beta \tag{1}$$

in which $c_1 \leq p \leq c_0$, was used to fit the observed performance data of test sections. The present serviceability index, p, was evaluated by a formula that depended on surface deterioration and deformation measurements to yield an estimate of expert judgment as to the section's present ability to serve its intended use. The term c_0 was taken to be the average initial serviceability of the test sections, somewhat over 4.0, and $c_1 = 1.5$ represented a poor serviceability level at which sections were said to be out-of-test. W denotes axle load applications accumulated to the time that present serviceability is p, and in some analyses a seasonal weighting function was applied to actual applications to obtain weighted applications. The terms ρ and β in Eq. 1 are functions of pavement design and vehicle load parameters, there being three of the former and two of the latter in the main experimental designs used at the Road Test. Logically the seasonal weighting function should be applied to ρ and/or β, but it can be seen from the form of Eq. 1 that seasonal variation in the decrease of p will occur if a weighting function is applied to any of W, ρ, or β.

The model used for the function ρ was of the form

$$\rho = \frac{10^{A_0}(a_1D_1 + a_2D_2 + a_3D_3 + a_4)^{A_2}}{(L_1 + L_2)^{A_1}/L_2^{A_3}} \tag{2}$$

where L_1 is load (kip) on a single or tandem axle and where L_2 is one for single and two for tandem-axle vehicles. The terms D_1, D_2 and D_3 are respective thicknesses (inches) of surface, base, and subbase in the case of flexible pavements. For rigid pavements, D_2 and D_3 are respective thicknesses (inches) of slab and subbase, and D_1 is one or zero depending on whether or not the slab contains reinforcing mesh. Values for the remaining terms in Eq. 2 were either assumed or were obtained by fitting the model to observed performance data.

The function β was noted to depend upon design and load parameters and was of the general form

$$\beta = b_0 + f(D_1, D_2, D_3, L_1, L_2) \tag{3}$$

where the function f has the reciprocal form of ρ but with different values for the powers A_0, A_1, A_2 and A_3 than were determined for Eq. 2. Thus, in addition to the formulation of any weighting function for the applications, Eqs. 1, 2, and 3 required values for 16 constants. Values for c_0 and c_1 were assigned as described and a_4 was given the value 1. The minimum value for β, b_0, was taken to be 0.4 for flexible and 1.0 for rigid pavements—an assignment that permitted flexible pavement serviceability curves to have positive, negative, or zero curvature, and rigid pavement curves to have only negative or zero curvature. For rigid pavements, analyses of variance made before curve fitting indicated that the coefficients a_1 and a_3 were not significantly different from zero so these coefficients were taken to be zero in Eqs. 2 and 3. Thus the Road Test pavement performance models contained 12 or 10 coefficients to be determined by fitting the models to flexible or rigid pavement performance data. The curve fitting procedures are described in Appendix G of Road Test Report 5, and detailed flow charts have been given in a paper by Hain and Irick (2).

The models were fitted to performance data given in Appendix A of Report 5 for Design 1 (factorial experiment) flexible and rigid pavement test sections. Data for each section consist of from 5 to 10 pairs of values for p and log W for whichever of the following serviceability levels in evidence for the section while in test: p = 3.5, 3.0, 2.5, 2.0, 1.5 and p after 11, 22, 33, 44, 55 biweekly periods (called index periods). Thus a section that reached p = 1.5 in 30 weeks would have 6 pairs of performance data values, whereas a section whose p = 2.8 after 110 weeks (end of test) would have 7 pairs of data values for p and log W.

In essence, the residual criterion used to evaluate the undetermined constants in Eqs. 2 and 3 was an average of the discrepancies between log W values as given in the data and as calculated from Eqs. 1, 2, and 3.

Coefficients obtained for the Road Test models have been given in Road Test Report 5. Although the MORC procedure has been applied to Road Test performance data, there are several reasons for not presenting the coefficients that have been obtained. The MORC applications to date deal only with samples of the data because the computer used is not presently equipped with magnetic tape storage. Most of the work leading up to this paper has been in the development of MORC itself, and much more time would have been necessary to completely minimize any residual criterion over all the Road Test performance data. More important, perhaps, the work to date with MORC has been exploratory, with an aim to infer the kind of results the procedure will produce rather than to determine new coefficients for Road Test models.

To obtain samples of the Road Test performance data, test sections in the factorial experiments were split into three sets of 90 sections each for flexible pavements and two sets of 84 sections each for rigid pavements. Flexible pavement sets were divided according to the factorial separation (2), and rigid pavement sets were separated according to subbase thickness after deleting all sections having the thickest slabs in each of the eight heaviest load lanes.

Performance data for any section were selected at two points on the section's serviceability curve, at p = 3.0 and p = 2.0, if the latter value was reached before the end of test traffic. Otherwise the two data points were taken at 33 and 55 index days. Thus, any sample set of flexible pavement data had 90 sections and 180 data points, whereas either sample of rigid pavement data consisted of 84 sections and 168 data points. The MORC procedure was then applied to successive data sets, and after each cycle (see Appendix) coefficients were averaged to give a start for the next cycle of MORC. With greater computer storage capacity neither the sampling nor the averaging would have been necessary.

The residual criterion was the root mean square discrepancy between log W at observed points and log W as predicted by the performance model. In addition to this criterion value, Table 1 gives average algebraic and absolute log W residuals as well as the 5th and 95th percentiles of the sample residual distributions that arise when various models and procedures are used. Values shown for the Road Test models and procedures are for the sample data and do not cover the full range of data for which residuals were summarized in Road Test Report 5. In Tables 11 and 47 of Report 5 mean absolute and root mean square residuals were 0.23 and 0.31 for flexible pavements, and 0.17 and 0.22 for rigid pavements. Corresponding values in Table 1 are somewhat higher because the samples contain sections whose log W residuals were not included in the Report 5 summary tables.

Starting with coefficients as reported from the Road Test, Table 1 gives residual summary statistics for the sample data after four cycles of the MORC procedure. While none of the residual summary statistics were greatly changed, all moved in a favorable direction, and in particular, the algebraic means were more nearly zero—a condition for unbiased predictions from the equations. On the other hand the coefficients themselves were unaltered to any significant degree as far as their practical use might be concerned. It is possible of course, that more cycles of the MORC procedure would produce closer fits to the sample data than indicated in Table 1, but this was not attempted.

The remaining summary statistics (Table 1) are the result of applying several cycles of the MORC procedure to the sample performance data using the same criterion as before but with a modification of the Road Test models. In section 1.4.1 of Road Test Report 5, it was suggested that the models for ρ and β as given in Eqs. 2 and 3 might be put into shorter forms:

$$\rho = 10^6 \left[\frac{(a_1D_1 + a_2D_2 + a_3D_3 + a_4)^2}{(L_1 + L_2)/L_2^{A_2}} \right]^{A_1} \tag{4}$$

TABLE 1

STATISTICS FOR LOG W RESIDUAL DISTRIBUTIONS

Data	Procedures	Residual Summary				
		Mean Alg.	Mean Abs.	RMS	Percentile 5	95
Flexible pavements: 270 test sections, 540 data points	AASHO Road Test performance equations	0.03	0.25	0.33	-0.49	0.53
	Road Test models, MORC	-0.01	0.23	0.31	-0.46	0.46
	Modified models, MORC	-0.01	0.22	0.29	-0.45	0.47
Rigid pavements: 168 test sections, 336 data points	AASHO Road Test performance equations	0.10	0.23	0.33	-0.36	0.85
	Road Test models, MORC	0.03	0.21	0.30	-0.40	0.53
	Modified models, MORC	-0.01	0.19	0.26	-0.40	0.46

$$\beta = b_0 + \frac{b_1}{\rho^{b_2}} \tag{5}$$

Thus, for a specified ρ the "structure index," $a_1D_1 + a_2D_2 + a_3D_3 + a_4$, is assumed to be proportional to the square root of the load term, $(L_1 + L_2)/L_2^{A_2}$, and β is assumed to be directly related to ρ through Eq. 5. These modifications, together with Eq. 1, were used as a model to fit the sample data by the MORC procedure. Eqs. 4 and 5 have four fewer coefficients to be determined than do their counterparts, Eqs. 3 and 4.

The residual statistics (Table 1) for the modified models indicate rather clearly that the modifications do not lead to any sacrifice in closeness of fit to the sample data. When pavement design versus log W curves were drawn from the resulting equations, there was practically no difference between these curves and those given in Figures 23, 26, 116 and 117 of Road Test Report 5. This illustration shows rather clearly that no particular serviceability-performance model is likely to be superior to all other models that could be used.

Percentiles 5 and 95 have been included in Table 1 to indicate the degree to which the various distributions are symmetrical about zero and also to locate 90 percent limits for the horizontal scatter of points about curves that might be drawn over a log applications scale. In general, it can be seen that these limits lie about two mean absolute deviations from zero.

In summary, MORC applications to AASHO Road Test performance data are quite limited to date, but the results obtained seem to indicate that the MORC procedure can be useful in any further fitting of these data. In the light of the results obtained by fitting simpler models to the data, however, it would appear that more attention needs to be given to the original problems—selection of model and criterion for the curve fitting procedure.

SERVICEABILITY AND PERFORMANCE MODELS OF EXPONENTIAL FORM

It is assumed in this paper that it is both possible and useful to evolve and evaluate models that aim to predict pavement serviceability when sufficient information is given about pavement design, environmental factors and traffic experience. Since there are several manifestations of serviceability decline and since any one may reflect the combined effects of a rather large number of factors, it seems clear that performance models based on serviceability cannot be of much utility unless they conform in principle with fundamental knowledge about pavement behavior. For example, if established theories predict stresses, strains and deflections that will lead to serious pavement cracking because of existing factors, then it should be expected that the same factors will lead to a prediction of serviceability loss by the performance model. Moreover, it should be expected that the performance model will reproduce satisfactorily the prediction successes that have been attained from existing design methods for the provision of adequate and economic pavements.

Although it may be virtually impossible for any serviceability performance model to fulfill such a difficult assignment, a limited beginning was made at the AASHO Road Test and further progress is expected from research efforts in Area 1 of the National Cooperative Highway Research Program. A major aim of this continuing research is to evolve the AASHO Road Test pavement performance models and equations into forms that apply to wider conditions and at the same time conform with current knowledge of pavement behavior. It seems reasonable to suppose that much collective effort will be required to satisfy this goal, and that many past and current ideas should be tested with the results that emanate from the various satellite projects. It may be that ultimate models for pavement serviceability and performance will have different forms than those used at the AASHO Road Test, and the remainder of this paper is devoted to several considerations that might lead to the use of exponential forms.

A recent nationwide survey (3) of pavements about to undergo major maintenance shows the average terminal serviceability level to be in the neighborhood of $p = 2.2$, and it seems reasonable to suppose that this level is about one-half its original value. Thus it would seem appropriate to arrange present serviceability models so that when p is one-half its original value a critical point is reached in the algebraic formulation. For example, Eq. 1 gives the Road Test terminal serviceability of $p = 1.5$ when the applications W are equal to the expression for ρ. If exponential models of the form $p = p_0 2^{-x}$ are used for serviceability and performance, where p_0 is initial serviceability, $x = 1$ is critical in the sense that p will then be at one-half its original value—in the neighborhood of terminal serviceability.

Present serviceability at the AASHO Road Test was calculated from index formulas derived by linear regression analyses that optimized the multipliers but not the exponents of measurements on pavement deterioration and deformation. Moreover, the linear model was not constrained to give values between 0 and 5 which were limits on the rating scale used for subjective serviceability evaluations.

Painter (4) has shown that exponential type models for present serviceability index can be fitted to the serviceability data used in deriving the Road Test index formulas (see AASHO Road Test Report 5, Appendix F), and that the fit will be as good as with the linear models, and the boundary conditions will be met. When these models are used, each measurement value is changed to a multiplier whose value is between 0 and 1, and the index is obtained from the product of 5.0 with all multipliers. Extending this concept somewhat and incorporating the result of the nationwide terminal serviceability survey, the model

$$p = 5.0 \times 2^{-\left[B_1 X_1^{C_1} + B_2 X_2^{C_2} + \dots\right]} \tag{6}$$

may have advantages over other models for calculating present serviceability index values. The non-negative variables X_1, X_2, ... represent "detractor" items such as slope variance, roughness index, and cracking and the exponents C_1, C_2, ... determine the shape of the serviceability decline curves for X_1, X_2, ... The undetermined constants B_1, B_2, ..., C_1, C_2, ... are constrained to be non-negative during the fitting of Eq. 6 to observed serviceability data. The model can be represented as a product of 5.0 and multipliers of the form $2^{-B_i X_i^{C_i}}$, and when $X_i = 0$, the multiplier is 1. When X_i is large enough to cause $B_i X_i^{C_i}$ to be 1, then the multiplier is ½, and if all remaining X-values are 0, then X_i has resulted in near-terminal serviceability through its own weight. If the fitted data do not imply such a situation to be possible, then the coefficients B_i and C_i will presumably reflect this impossibility. Figures 4 and 5 show multiplier curves that were obtained when Eq. 6 was fitted by the MORC procedure to the flexible and rigid pavement serviceability data given in Appendix F of AASHO Road Test Report 5.

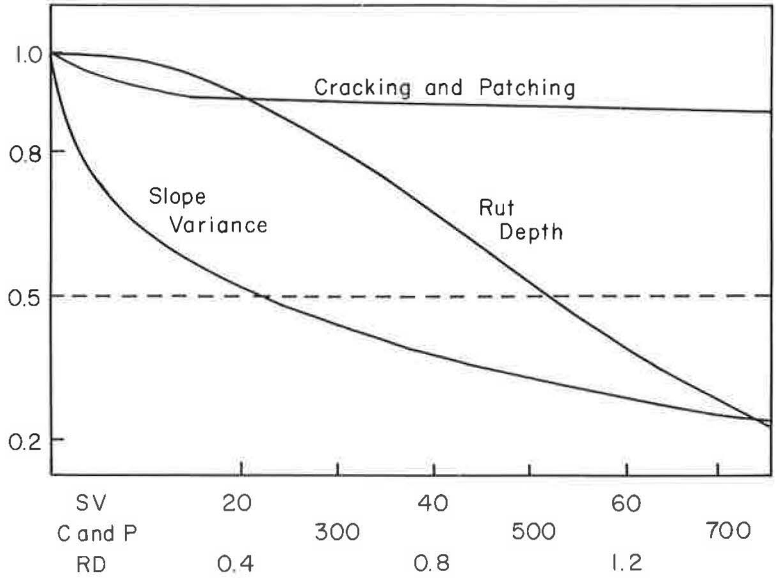

Figure 4. Flexible pavement illustrative multipliers for psi.

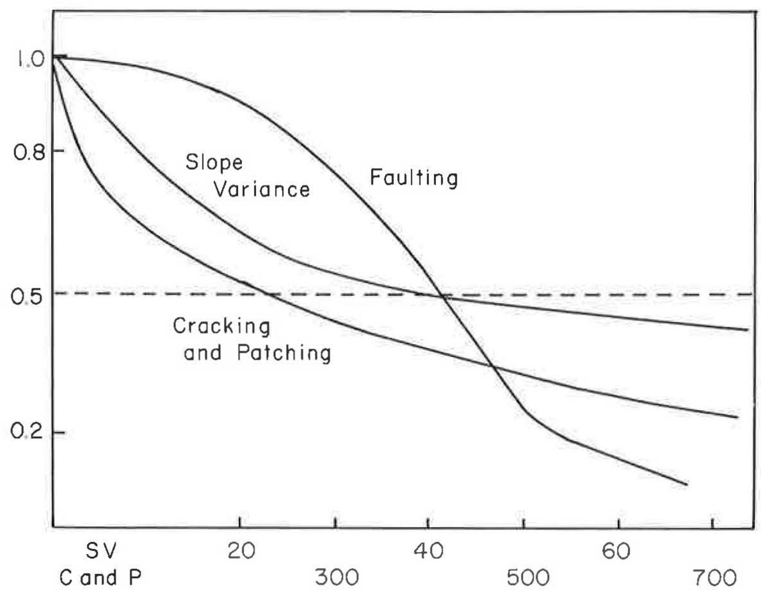

Figure 5. Rigid pavement illustrative multipliers for psi.

Results obtained after about 12 cycles of MORC are given in Table 2, but these as well as Figures 4 and 5 must be regarded as only illustrative because more cycles would have been required to reach a minimum for the criterion, the mean square residual between actual serviceability ratings and calculated serviceability index values. At the point where MORC was stopped, however, mean residuals were about the same as those given by Painter (4) and in Road Test Report 5.

TABLE 2

ILLUSTRATIVE MORC RESULTS FOR EXPONENTIAL PSI MODELS

Serviceability Element	B_i	C_i	Residuals
74 Flexible Pavements[a]:			
X_1 = Slope variance (× 10^6)	0.18	0.56	Mean absolute = 0.28
X_2 = Cracking and patching (ft^2/1,000 ft^2)	0.027	0.29	RMS = 0.36
X_3 = Rut depth (in.)	0.93	02.1	
49 Rigid Pavements[a]:			
X_1 = Slope variance (× 10^{-6})	0.11	0.58	Mean absolute = 0.26
X_2 = Cracking and patching[b]	0.043	0.58	RMS = 0.32
X_3 = Faulting (in./1,000 ft)	0.00002	02.91	

[a]Data from AASHO Road Test Report 5, Appendix F.
[b]As defined in Road Test Report 5, Appendix F.

When the exponents C_i (Eq. 6) are left to the curve fitting procedure, quite a variety of shapes become available for the various multipliers that represent pavement deterioration and deformation. If C_i is more than 2, say, then the corresponding X_i does not detract much until a critical value is reached at which point the multiplier drops quite rapidly. When C_i is less than 1, the loss rate is greater for small than for large values of X.

If a model similar to Eq. 6 was used to determine present serviceability index values, then the counterpart performance model might also be assumed to have an exponential form. Exponential models for performance might be considered to be analogous to those that are used for probabilistic models in fatigue and other failure theories, and have been used by Painter (5) in analyses of the AASHO Road Test flexible pavement performance data. A number of exponential models were fit to performance data at the Road Test before Eqs. 1, 2 and 3 were finally selected, and there were no strong indications that the exponential forms were less acceptable than the reported models. The concluding discussion revolves about a performance model of the form

$$p_t = p_{t-1} \, 2^{-S_t} = p_0 2^{-\Sigma S_t} \qquad (7)$$

in which $p_t = p_0/2$ whenever $\Sigma S_t = 1$.

In this model, the time scale t is divided into intervals so that the "stress" function S_t is essentially constant for the period from t - 1 to t. Changes in S_t from one interval to another may result from a change in loading rate or from a change in environmental stress conditions. For simplicity of discussion, it is assumed that S_t depends on three other functions, n_t, v_t, and ν. The first of these is a "loading" index for the number of equivalent axle-load applications received by the pavement during the interval and where the equivalency is relative to, say, 18-kip single-axle loads. The positive function v_t is a "relative support" index whose values are high or low whenever the environment leads to relatively high or low pavement support, respectively. The reference point for v_t might be, for example, initial environmental conditions at the AASHO Road Test since these are well documented. Then at the Road Test or elsewhere, v_t is >1 for conditions such as frozen structure and <1 for adverse conditions that might result from thawing or excessive moisture. Finally, ν might be called a "performability" index whose value depends on strengths and thicknesses of pavement components, and corresponds to the number of equivalent axle-load applications that are expected from the pavement when serviceability is one-half the initial serviceability and when all applications occur with $v_t = 1$. For example, two possibilities for S_t are

$$S_t = \left(\frac{n_t}{\nu}\right)^{v_t} \qquad (8)$$

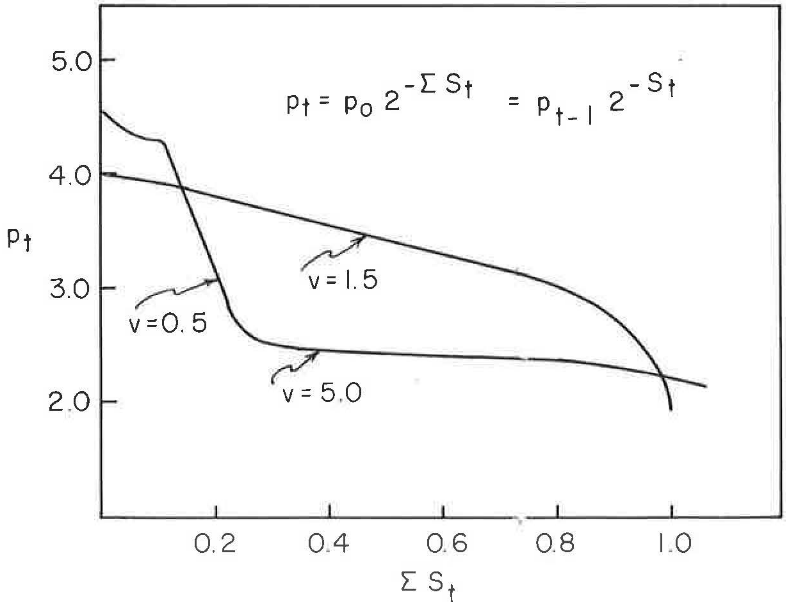

Figure 6. An exponential performance model.

$$S_t = \frac{n_t}{v_t \nu} \qquad (9)$$

For either Eq. 8 or 9, if v_t is always 1, then $S_t = 1$ when the accumulation of n_t is ν, and the pavement is then expected to have only one-half its initial serviceability. If v_t is sufficiently large, practically no serviceability will be lost from t - 1 to t, but if v_t is quite small, then S_t may become nearly 1 as a result of the applications during a single period. For Eq. 8, Figure 6 indicates how the serviceability history of a pavement might have almost any configuration as v_t changes.

Preliminary exploration with Eq. 8 on a very small sample of Road Test flexible pavement data suggests that a reasonable set of values for v_t are given by the ratios of initial (Benkelman beam) deflections to deflection during interval t. These ratios are more or less independent of pavement design so that v_t can be approximated by climatic measurements alone. This possibility is supported by Painter's results wherein a design-free weighting function based on time since spring thaw was used as a multiplier for n_t.

It is expected that the MORC procedure will be used with available data in further studies of exponential models such as Eqs. 7, 8 and 9. The ultimate goal is to provide a broad and valid basis for the prediction of pavement performance from pavement design, loading, and environmental parameters.

REFERENCES

1. "The AASHO Road Test: Report 5—Pavement Research." HRB Special Report 61E, Sections 2.2 and 3.2 (1962).
2. Hain, R. C., and Irick, P. E., "Fractional Factorial Analysis for Flexible Pavement Performance Data." The AASHO Road Test: St. Louis Conference Proceedings, HRB Special Report 73, 208-223 (1962).
3. Rogers, C. F., Cashell, H. D., and Irick, P. E., "Nationwide Survey of Pavement Terminal Serviceability." Highway Research Record 42 (1963).
4. Painter, L. J., "An Alternate Analysis of the Present Serviceability Index." Proc. of International Conf. on Struct. Design of Asphalt Pavements, Univ. of Michigan (Aug. 1962).

5. Painter, L. J., "Analysis of AASHO Road Test Data by the Asphalt Institute." Proc. of International Conf. on Struct. Design of Asphalt Pavements, Univ. of Michigan (Aug. 1962).

Appendix

MORC—A PROGRAM FOR THE MINIMIZATION OF RESIDUAL CRITERIA

This program aims to solve quite general minimization problems without using subroutines for partial differentiation, solution of simultaneous equations or the fitting of linear and quadratic surfaces. Only one tool, a three point parabola, is used with various strategies to descend a specified surface. The program has been developed through computer experiments with problems whose solutions were verifiable. Some of these problems have been used to illustrate minimization methods in references (A1, A2, A3, and A4), and a number of new examples have been constructed to provide a wider variety of problem situations.

For other problems there is no assurance that the program will find the required solution, but extensive experimentation suggests that MORC can be a useful alternative to available minimization procedures. Convergence time varies considerably from problem to problem. In some cases, it can be expected that this program will have to evaluate a disappointingly large number of surface points if a precise solution is required.

Problem specification and flow charts that are meant to be adequate for the coding of MORC for any computer are also presented. A few experimental problems are discussed in order to show some operating characteristics of the program.

Problem Specification

When MORC is used in data processing applications the data comprise a matrix of observations $[X_{jk}]$ where $j = 1, \ldots, J$ sets of observations have been taken on $k = 1, \ldots,$ K experimental variables. It is assumed that the data analysis should produce estimates for I coefficients, $B_1, \ldots, B_i, \ldots, B_I$, in a specified function

$$F_1(X_1, \ldots, X_K; B_1, \ldots, B_I) = 0 \qquad \text{(A1)}$$

and that the B_i must satisfy a set of constraints

$$C'_m \leq C_m(B_1, \ldots, B_I) \leq C''_m \text{ for } m = 1, \ldots, M. \qquad \text{(A2)}$$

In the simplest case, the functions $C_m = B_m$ and $M = I$ so that C'_m and C''_m are numerical limits for the coefficient B_m. In other cases, C_m may be a more complicated function of one or more of the coefficients.

Let $B^{(v)}$ represent a set of current values for the B_i and let $r_j^{(v)}$ be the residual for the j^{th} set of observations when $B^{(v)}$ is used in Eq. A1, that is

$$r_j^{(v)} = F_1(X_{j1}, \ldots, X_{jK}; B_1^{(v)}, \ldots, B_I^{(v)}) \qquad \text{(A3)}$$

Depending on the algebraic arrangement of F_1, it is possible for r_j to represent one of a wide variety of different assumptions or requirements on the form and allocation of experimental error. Ordinarily the r_j will be either absolute or relative deviations that measure discrepancies between what is observed for a particular X_k and what Eq. A1 gives for X_k upon substitution of $B^{(v)}$ for the B_i and other observations for the remaining variables.

Let R be a criterion function of the residuals,

$$R = F_2(r_1, \ldots, r_J) \qquad \text{(A4)}$$

where R might be a sum (or weighted sum) such as Σr_j^2, $\Sigma|r_j|$, or a criterion such as $|r_j|_{max}$, $|\Sigma r_j| + \Sigma|r_j|$, etc. Inasmuch as the observations X_{jk} do not vary during the MORC program, R varies only as the B_i are changed and the criterion may be expressed as

$$R = F_3(B_1, \ldots, B_I) \tag{A5}$$

Whether or not there are experimental data, Eq. A5 is the equation of a surface in $I + 1$ dimensions and the problem is to determine a sequence of points $P^{(v)}$, with ordinates $R^{(v)}$ and coordinates $B^{(v)}$, such that a minimum for R will be reached within the coordinate region defined by the constraints (Eq. A2). The user must infer whether the sequence of points leads to a relative or an absolute minimum or whether the process has simply gotten stuck. Ordinarily this inference can be made by comparing results obtained by starting the sequence from several different points in the constraint region.

MORC Descents

Before discussing the main flow of MORC it is helpful to describe subroutines that are used to make particular descents along a three point parabola. For any number of coordinate axes, the plane of the parabola is normal to $R = 0$ and is either parallel to a coordinate axis, for an axial descent, or contains the line joining $P^{(v)}$ to a previously evaluated point $P^{(u)}$ which is not lower than $P^{(v)}$, for a general descent. Figure A1 shows the trace of Eq. A5 in the plane of the parabola. The parabola is determined by ordinates at $B^{(v)}$ and at $B^{(v)} \pm tD$, in which D has components yet to be defined and t is not large enough to violate the constraints C' and C''.

From the three ordinates that determine the parabola, quantities L and Q are calculated so that the parabola vertex is at $B^{(v)} + (L/Q)tD$. If the vertex is not out of bounds and if the parabola has positive curvature, then the criterion ordinate at the parabola vertex is generally the end result of a MORC descent. Exceptions will be discussed later.

Details for the descent process are given in Figure A2. For completeness the general nature of the subroutine for computing criterion values is shown in a special box at the lower right of the figure. In the $R^{(v)}$ subroutine either Eq. A4 or Eq. A5 is used to compute $R^{(v)}$, and if $R^{(v)}$ is lower than $R^{(u)}$, then $P^{(v)}$ is copied into $P^{(u)}$. After the last computation of $R^{(v)}$ in the descent subroutine, $P^{(u)}$ is again copied into $P^{(v)}$ so that the end point of a descent is always the first point encountered such that no succeeding point is lower.

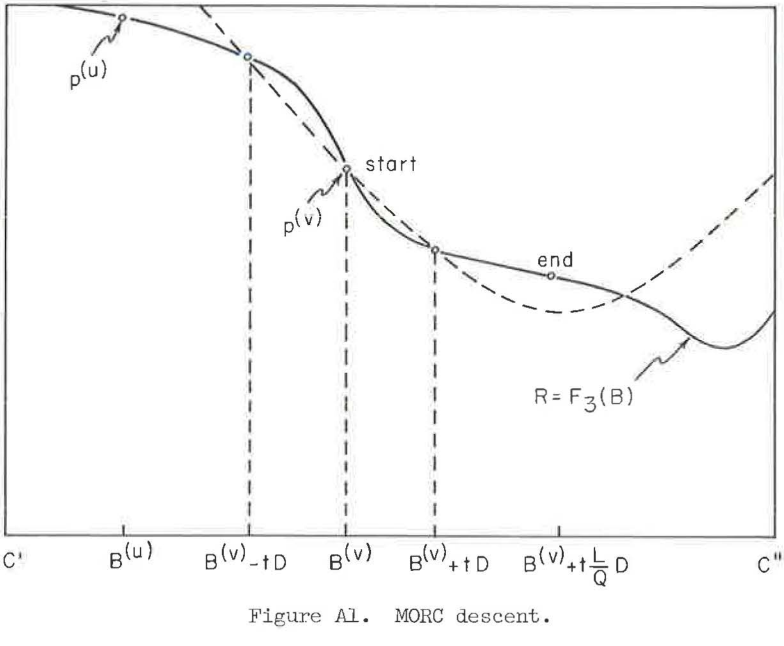

Figure A1. MORC descent.

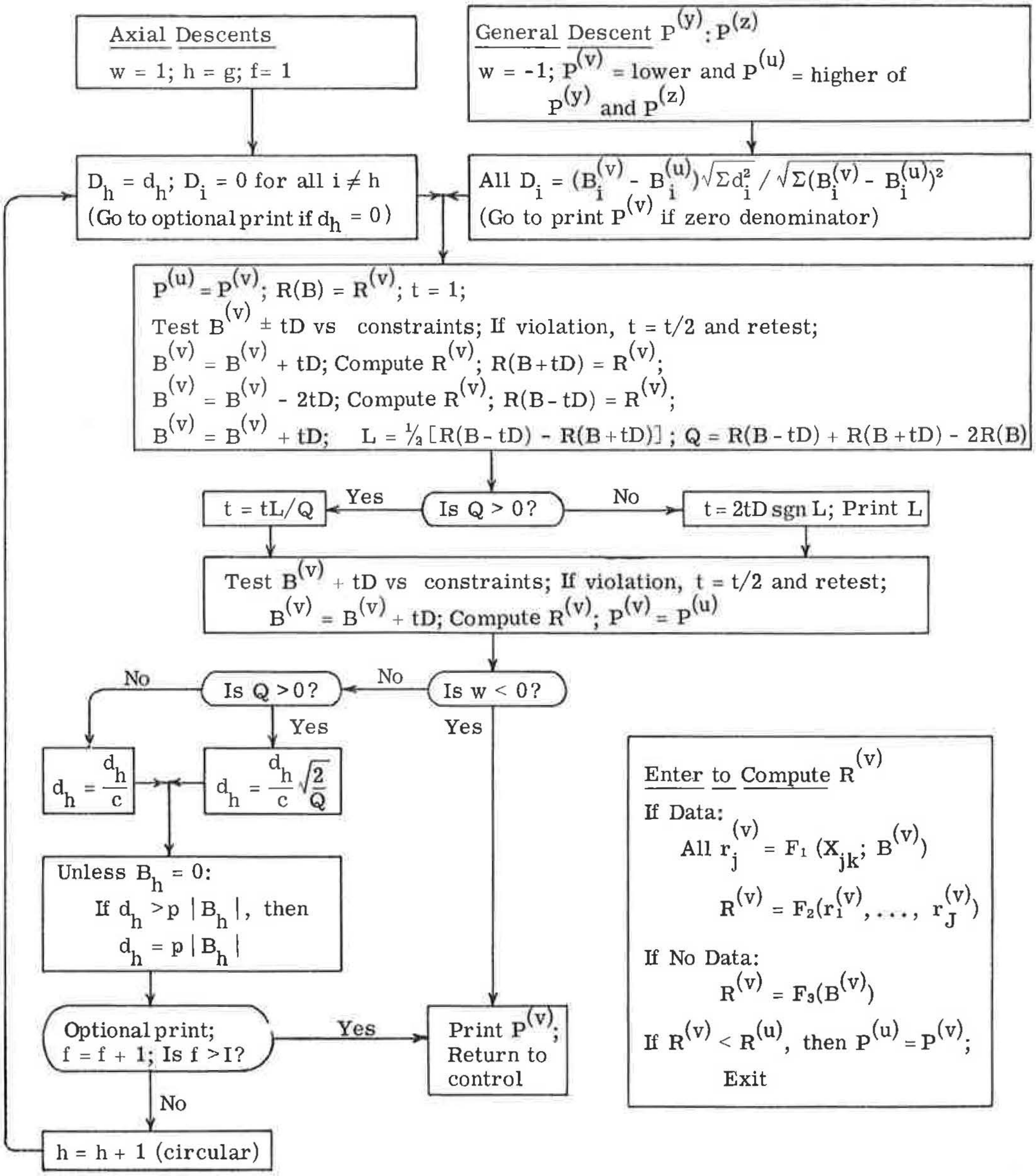

Figure A2. Flow charts for MORC subroutines.

For an axial descent parallel to the B_h axis, the increment D has only one non-zero component, d_h, which is called a basic increment for B_h. Whenever it is desired that B_h should no longer be varied during MORC, then the program is interrupted to set $d_h = 0$. Initial values for the d_i are set on a percentage basis to be discussed, and as shown at the bottom left of Figure A2, d_h is subject to change after each axial descent parallel to the B_h axis.

For a general descent the notation $P^{(y)}$: $P^{(z)}$ means that the parabola's plane is to contain the line through $P^{(y)}$ and $P^{(z)}$ and that the descent starts with $P^{(v)}$ the lower of $P^{(y)}$ and $P^{(z)}$ and $P^{(u)}$ the higher. The increment D then has components proportional to the direction cosines of the line through $B^{(u)}$ and $B^{(v)}$.

After the parabola's direction is determined a test is made to see if any constraint is violated by any component of $B^{(v)} \pm tD$ with $t = 1$. If a violation occurs then $t = t/2$ and the test is repeated until all constraints are satisfied. Linear and quadratic terms L and Q are next calculated from ordinates at $B^{(v)}$ and $B^{(v)} \pm tD$ and if $Q > 0$ (positive curvature) the parabola vertex is at $B^{(v)} + (L/Q)tD$. If the latter point is out of bounds t is halved until the constraints are satisfied and the final calculation of R is at the modified point. If $Q \leq 0$, R is computed at $B^{(v)} + 2tD \operatorname{sgn} L$ so that a linear descent is attempted to one increment beyond the previous exploration—unless t has to be modified to fit the constraints. The print of L enables the user to recognize linear descents. If the descent is general, the subroutine ends by printing the lowest point encountered during the descent.

Axial descents progress parallel to all I coordinate axes in succession and when an axial descent with $Q > 0$ is completed parallel to axis B_h, d_h is modified to $\frac{d_h}{c}\sqrt{\frac{2}{Q}}$, where c is initially 1, and is then doubled each time a general descent fails to make sufficient gain. This rule essentially gives basic increments that are proportional to "valley widths" in the direction of the coordinate axes, and in data processing applications the adjusted d_h are more or less proportional to the standard errors of the B_i. If the descent is linear, then d_h becomes d_h/c, but in no case is any d_h permitted to exceed $p|B_h|$ where p is 0.25, say. After all I axial descents are completed the final result is printed and the subroutine ends.

Main Flow for MORC

The general strategy in MORC is to satisfy the equations

$$\frac{\partial R}{\partial B_g} = 0 \qquad \text{for } g = 1, \ldots, I \tag{A6}$$

without actually forming the equations. Equation A6 for each condition is considered to be the projection on R = 0 of a valley running through the criterion surface and MORC descents are supposed to follow, but not too closely, the various valleys until a common valley point is reached—unless constraints bar the way. Figure A3 shows curves that

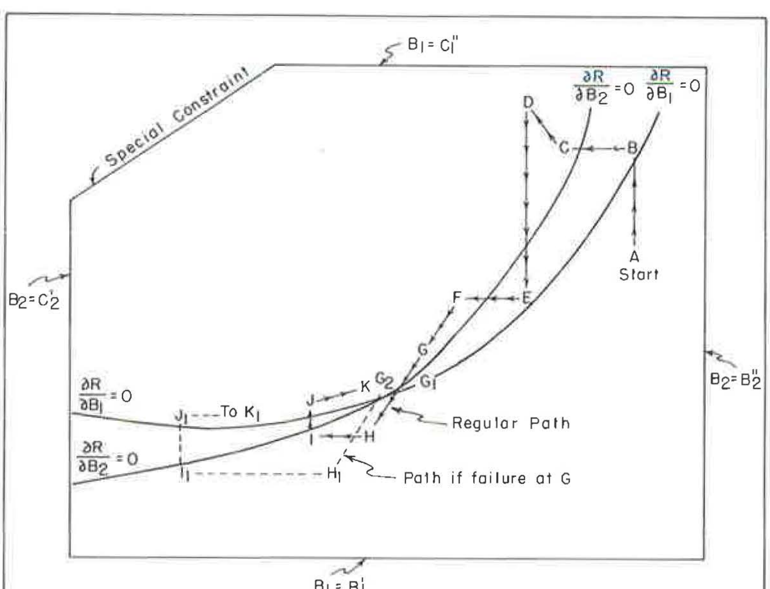

Figure A3. Illustrative MORC path.

might represent Eq. A6 when I = 2 and letters in the figure represent coordinate points that might be reached during the MORC program. Starting from an initial origin A, an axial descent is made towards the valley represented by Eq. A6 with g = 1 and from thence towards the next valley and so on until I axial descents have occurred, from A to B to C in Figure A3. Depending on how well the parabolas fit the criterion surface, the initial round of axial descents may end in the neighborhood of $\partial R/\partial B_I = 0$. This completes cycle zero.

Cycle one begins with a new origin about half as far from C as was A but on the other side of C. Then another round of axial descents progresses from D to E to F. The line through C and F is presumed to indicate the local direction of descent in the valley system, so a general descent is made to G from the lower of the two points and in the plane containing the line joining them. If G represents sufficient gain over C, cycle one is complete and a new origin is formed by extending CG to H. Axial descents in cycle two begin parallel to the B_2 axis and proceed from H to I to J whence a general descent to K is determined by the points G and J.

If G had not been sufficiently lower than the previous low, c would be doubled and cycle one would continue into an extra round of axial descents from G to G_1 to G_2. The origin for cycle two would then be at H_1, about half as far from G_2 as was C. Axial descents in cycle two would then be from H_1 to I_1 to J_1, followed by a general descent to K_1 in the direction determined by the points J_1 and G_2 and starting from the lower of these points.

The general purpose of new origins is to provide each cycle with a fresh start that tends to prevent the process from getting stuck. General descents are "between" valleys until insufficient gain is encountered, then the extra round of axial descents sets up the next general descent to be "within" a particular valley. Both between and within situations can have special advantages from one problem to another and so MORC strategy provides a mixture that can be governed to a large degree by the definition of sufficiency for gain made in the general descents.

The procedures that have just been sketched are shown more formally in Figure A4 where notation is introduced for points that were represented by letters in Figure A3.

The symbols $P^{(s)}$ and $P^{[s]}$ denote the origin and final point in cycle s where s = 0, 1, 2, ... After memory is loaded with program and data, initial coordinates $B^{(o)}$ are entered in $B^{(v)}$. Following a breakpoint $R^{(v)} = R^{(o)}$ is computed and the point $P^{(o)}$ is stored in space allotted to $P^{[s-1]}$. Initial basic increments are formed by the rule $d_i = p\ |B_i^{(o)}|$, but if $B_i^{(o)} = 0$ then $d_i = p$, and any d_i that has been preset to zero is left unchanged. The initial point is then printed, and all printouts show the basic increments in current use.

With g = 1 and c = 1, a round of axial descents produces the points $P^{(v)} = P^{[s,h]}$ for h = g, g + 1, ..., g - 1 circularly, that is, g - 1 = I if g = 1 and g + 1 = 1 if g = I. The I^{th} axial descent ends with $P^{(v)} = P^{[s,g-1]}$ which is printed. Brackets are used on the superscripts since this round of axial descents always completes a cycle, both for cycle zero and for any other cycle whose general descent was insufficient. Thus $P^{[s,g-1]} = P^{[s]}$ becomes $P^{[s-1]}$ after s is incremented to s + 1.

Cycle s > 0 is begun by printing s, g, and c. As shown Figure A4 coordinates for the cycle origin are formed in such a way that the new origin is in the opposite direction from the current low point than was the previous low. Moreover, $P^{(s)}$ is about half as far from $P^{[s-1]}$ as was $P^{[s-2]}$ although basic increments are added to the components of this distance to insure that the origin will be at a new point on the criterion surface. The constraint test may reverse the usual direction for a new origin to provide for those cases where it is profitable to back away from one or more constraint surfaces. By coming to constraint surfaces from different origins MORC has the opportunity to follow boundaries that may contain the required solution.

Just before computing $R^{(v)} = R^{(s)}$, $P^{(u)}$ is copied to $P^{[s-1]}$ then $P^{(v)} = P^{(s)}$ is determined and printed. Next a round of axial descents is made from $P^{(v)} = P^{(s)}$ to $P^{(v)} = P^{(s,h)}$ for h = g, ..., g - 1 circularly and $P^{(s,g-1)}$ is printed. The points $P^{(s,g-1)}$ and $P^{[s-1]}$ are now $P^{(y)}$ and $P^{(z)}$ for the flow chart of Figure A2 and a general descent is made to $P^{(v)}$ which will become $P^{[s]}$ if $R^{(v)}$ is less than $qR^{[s-1]}$. Otherwise c is doubled, and if c is not then greater than c′ the current cycle is completed with an

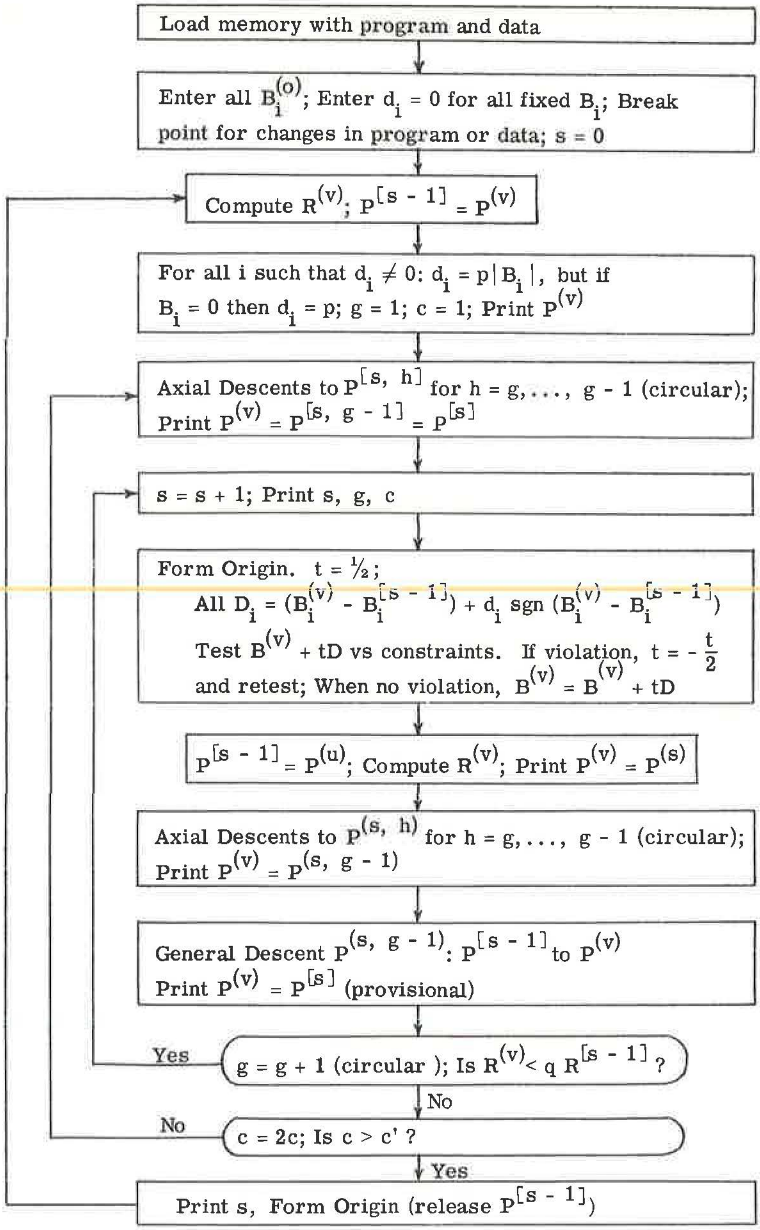

Figure A4. Flow chart for MORC control.

extra round of axial descents from $P^{(v)}$ to $P^{[s,g-1]}$ as before. When c exceeds c′ a new origin is formed and the program returns to the point where $P^{[s-1]}$ is replaced by the new origin and wide basic increments are again formed. Thus, the lowest point reached by MORC will generally be within a cycle where c′ changes back to 1, but not necessarily at the most recent change. This rule enables MORC to release $P^{[s-1]}$ periodically in order to start out on a somewhat different path. In all cases the index g is incremented circularly before starting a new cycle. Thus the first axial descent in a new cycle will head first toward successive valleys represented by Eq. A6.

The subroutine that tests for constraint violations will not be discussed since all that must be done is to form the functions $C_m(B^{(v)} \pm tD)$, or just $C_m(B^{(v)} + tD)$ for the one sided test; then determine whether C_m is less than C'_m or greater than C''_m for m = 1, ..., M.

In addition to memory requirements for program and for storing the matrix $[X_{jk}]$, if any, I + 1 locations are needed for each of $P^{(u)}$, $P^{(v)}$ and $P^{[s-1]}$; I locations for each set D_i and d_i; and M locations for each set C'_m and C''_m.

Space must be reserved for p, q, c', c, t, L, Q, R(B), R(B-D), R(B+D), w, and about two temporary storage locations are needed. Finally, there must be index registers for s, f, g, h, i, j (if data) and possibly k. The program is presently coded only for the Bendix G-15 computer and in the Intercom 500 code for this machine. In this form the program leaves from 300 to 400 memory locations for data storage, depending upon the length of the compute $R^{(v)}$ subroutine.

After completing cycle s there will have been s + 1 origins, s general descents, and I(s + s' + 1) axial descents where s' is the number of cycles in which there was insufficient gain. Since each descent calls for the evaluation of three new surface points, the total number of points evaluated through cycle s is

$$n = (4s + 1) + 3I(s + s' + 1) + s'' \qquad \text{(A7)}$$

in which s'' is the number of cycles having one extra origin due to 2c > c'.

In general, most of the computing time is used to evaluate $R^{(v)}$, so lower and upper bounds for running time through s cycles can be estimated by multiplying n times the computing time for $R^{(v)}$, using suitable estimates for s' and s''. Allowance must be made for those cases where repeated constraint violations occur and cause the program to spend unusual amounts of testing time.

There are obviously many arbitrary strategies employed in MORC and a number of variations have been tried during the program development. For example, the descent parabola might always be given the direction of steepest descent, but this approach seems to give no advantage over the present procedure. From all the alternatives that have been investigated the procedures given in Figures A2 and A4 seem to work reasonably well for the problems that have been used. The remainder of this paper describes results obtained for some of these problems. Wherever appropriate, the results include the number of criterion points, n, that have been evaluated.

Linear Regression Problems

If $r_j = X_{j1} - B_1 - B_2X_{j2} - \ldots - B_KX_{jK}$ and if $R = \Sigma r_j^2$ the minimization of R for variations in the B_i is a least squares linear regression problem for which elegant methods have long been established. When there are no critical constraints there is little point in using MORC for problems where r_j is linear in the coefficients—unless the user wishes to investigate other than least squares criteria, or perhaps wishes to minimize first with the linear model then with models that are non-linear in the B_i.

For least squares linear regression the criterion surface is parabolic in every direction so MORC ultimately solves these problems, although the search becomes quite prolonged as K increases. Table A1 shows some pertinent statistics for MORC applications to least squares linear regression problems. For K = 2 the solution is theoretically reached at the end of cycle one since any valley, $\partial R/\partial B_g = 0$, is a parabola whose vertex is at the minimum point on the criterion surface. The first problem shown in Table A1 has been partially discussed in the main text of this paper (see Figs. 1 and 2). Table A1 includes an orthogonal regression problem where for K = 4 all $\Sigma X_{jk}X_{jk'} = 0$ for $k \neq k'$. For problems of this class, the criterion paraboloid is untwisted with respect to the coordinate axes, and each axial descent produces in theory the correct value for a coefficient. Thus the solution should be reached at the end of the zero cycle. Since MORC is presently coded for only single precision arithmetic the theoretical results are not always realized as can be seen in Table A1.

The third example for K = 5 and J = 27 is used extensively by Anderson and Bancroft (A1) to explain conventional least squares linear regression analysis. Although MORC

TABLE A1

MORC STATISTICS FOR LEAST SQUARES LINEAR REGRESSION PROBLEMS

Problem and Statistics[a]		i = 1	i = 2	i = 3	i = 4	i = 5	R	n
I = K = 2	$P^{(0)}$	10.000	0.000				39.333	1
J = 30	$P^{[1]}$	19.712	-0.18034				10.116	17
	Solution	19.711	-0.18035				10.116	
	d_i	1.000	0.032					
	e_i	0.393	0.013					
I = K = 4	$P^{(0)}$	1	1	1	1		30.333	1
J = 6	$P^{[0]}$	5.001	3.999	3.000	2.000		0.66666	13
X_k orthogonal to $X_{k'}$	$P^{(1,4)}$	5.000	4.000	3.000	2.000		0.66667	26
	Solution	5	4	3	2		2/3	
	d_i	1.000	1.000	1.225	0.707			
	e_i	0.408	0.408	0.500	0.289			
I = K = 5	$P^{(0)}$	75	6	-90	2	-40	574.57	1
J = 27	$P^{[2]}$	83.43	5.91	-34.74	0.588	-23.54	87.275	79
(A1, ch. 15)	$P^{[12]}$	85.41	2.55	-74.56	1.15	-1.85	83.168	406
	$P^{[22]}$	82.01	2.457	-75.95	1.605	-1.040	83.067	749
	$P^{[32]}$	82.07	2.478	-75.17	1.591	-1.428	83.065	1,091
	Solution	82.174	2.464	-75.371	1.584	-1.379	83.065	
	d_i	1.000	0.513	3.624	0.130	1.921		
	e_i	2.015	0.468	3.878	0.309	2.107		

[a]Obtained with p = 0.25, q = 0.99, c' = 10 and $R = \Sigma r_j^2/J$.

eventually reaches the solution for this problem, it can be inferred from Table A1 that a great many points are required. The starting coordinates for this problem were obtained by judgment from plots of X_1 vs X_2, X_3, X_4 and X_5. The conventional analysis shows that only B_1 and B_3 have statistical significance relative to the residual mean square.

Table A1 includes "unit valley widths"; that is, d_i values obtained when c = 1 after axial descents and when there is no restriction on the size of d_i. If c were always 1, these values would remain essentially constant over the criterion surface. For comparison, standard error factors, e_i are given where e_i times the residual standard deviation gives the standard error estimate for B_i as determined by conventional regression analysis. It can be seen that the d_i give a certain amount of relative information about the standard errors of the coefficients. In the orthogonal case it can be shown that $d_i = e_i\sqrt{J}$ for all i.

Results shown in Table A1 are peculiar to p = 0.25, q = 0.99, and c' = 10. If any of p, q or c' are changed MORC will follow a somewhat different path over the criterion surface. In fact, each problem seems to have its own optimum values for these three input parameters, and it is sometimes desirable to interrupt the program to try different values.

An Example for I = 1

To illustrate MORC when there is only one coefficient to determine, the data shown in Table A2 were constructed for the model $X_1 = X_2^{B_1}$. In this case MORC consists of a series of origins and parabolas fitted to the criterion curve, there being no distinction between axial and general descents.

TABLE A2
DATA FOR I = 1 EXAMPLE

j	X_{1j}	X_{2j}
1	9	2
2	60	4
3	200	6
4	568	8
5	910	10
J = 6	1,800	12

If the model is linearized by taking logarithms, and if residuals are considered to be discrepancies between log X_{j1} and B_1 log X_{j2} then it turns out that the least squares estimate for B_1 is 2.9979. For the illustration, however, relative residuals

$$r_j = 1 - \frac{X_{j1}}{X_{j2}^{B_1}}$$

are used in connection with several criteria. If $R = \Sigma r_j^2/J$, the criterion curve has the form shown in Figure A5. If the initial point is set too far to the right the curvature is negative and MORC makes linear descents until $Q > 0$. Although the close neighborhood of the solution $R = 0.00777$, $B_1 = 3.0030$ is reached after about 30 points have been evaluated, even if $B^{(o)} = 1$ or 5, as many as 100 more points may be needed to reach five digit accuracy for B_1 when $q = 0.80$. Other criteria for this problem and corresponding MORC solutions are: $R = \Sigma|r_j|/J = 0.08215$ when $B_1 = 3.0162$, and $R = \max|r_j| = 0.11552$ when $B_1 = 3.0122$.

Fitting a Normal Curve with MORC

While not a practical application, one of the experimental problems consists of J = 7 relative frequencies, X_{j1}, at $X_{j2} = 1, \ldots, 7$ such that all

$$r_j = X_{j1} - \left(\exp\left[-(X_{j2} - B_2)^2/2B_1^2\right]\right)\Big/\sqrt{2\pi}\, B_1$$

are zero when $B_1 = 1.0468$ and $B_2 = 4.000$. If the criterion is $R = \Sigma r_j^2/J$ the criterion surface has a rather peculiar valley system. As long as B_2 is greater than about 0.5 there are only two main valleys such that $\partial R/\partial B_1 = 0$ is the straight line $B_1 = 4$, and $\partial R/\partial B_2$ has the appearance of a normal curve whose peak is at the solution. For $B_2 \ll 0.5$ however, there is a network of valleys and relative minima which can prevent MORC from reaching the solution if B_2 is not constrained to be greater than 0.2, say. It is clear for the data, however, that the standard deviation B_2 must be greater than 0.5 so there is no practical problem.

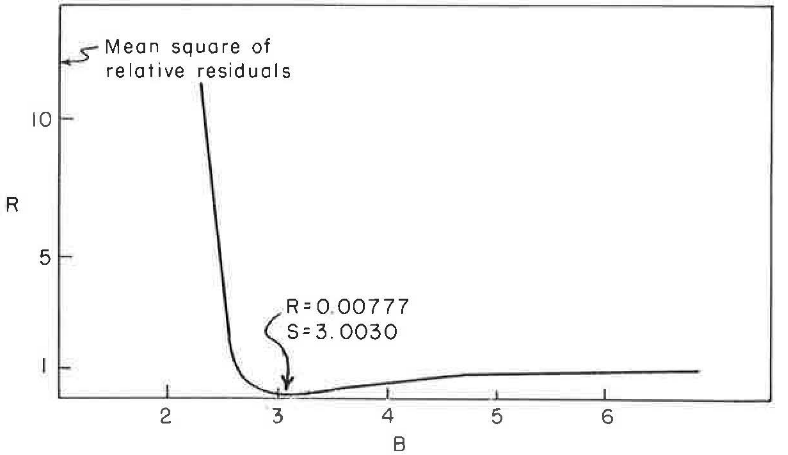

Figure A5. Criterion curve for an example with I = 1.

Starting from $P^{(o)}$ with $B_1 = 6$, $B_2 = 2$, and $R = 0.0218$, MORC reaches $P^{[5]}$ at $B_1 = 3.9997$, $B_2 = 1.0330$, $R = 0.000003$ after $n = 69$ points and comes to the solution in about twice as many points.

Some Minimization Problems Cited in the Literature

Development of MORC originated after the author had read reference (A2) which gives an example used by Hartley to illustrate his modified Gauss-Newton procedure. In this problem $J = 6$ sets of values are given for X_1 and X_2 which are assumed to be related through

$$X_1 = B_1 + B_2 \exp (B_3 X_2)$$

Residuals and the residual criterion are defined by

$$r_j = X_{j1} - B_1 - B_2 \exp (B_3 X_{2j}), \quad R = \Sigma r_j^2$$

Starting from the same origin as did Hartley, Table A3 shows how different choices for p, q, and c′ can affect the MORC path of descent. As has been mentioned, optimum values for these constants can change considerably from problem to problem. It is thus suggested that there may be optimizing strategies yet to be worked out.

The following problem is used to illustrate a minimization procedure given by Beale (A3):

Let $r_j = X_{j1} - B_1(1 - B_2^{X_{j2}})$ where $X_{j1} = 3(1 - 2^{-j})$ and $X_{j2} = j$. Then minimize $R = \Sigma r_j^2$ for $j = 1, 2, 3 = J$. For this problem the solution is $R = 0$ when $B_1 = 3$, $B_2 = 0.5$, and the derivative valleys project on the B_1B_2 plane in the pattern shown in Figure A3. Table A4 gives points reached by MORC when three different starts are used. It also indicates Beale's result after 27 points had been evaluated, three of which were the MORC starts given in Table A4.

A minimization procedure developed by Rosenbrock (A4) includes results given by that method when $R = 100(B_2 - B_1^2)^2 + (1 - B_1)^2$ is to be minimized. The valley system has a sweeping curve in the B_1B_2 plane and when the start is at $B_1 = -1.2$, $B_2 = 1.0$ the descent moves in the direction of (0, 0) then out to the solution at $B_1 = 1$, $B_2 = 1$, $R = 0$. Table A5 shows MORC results which seem to reach the solution in about the same number of points that are required by the Rosenbrock method. If more opportunities are given for general descents within derivatives, say with $q = 0.6$, $c' = 2$, then the solution is reached somewhat faster as is shown in Table A5.

Another interesting problem given by Rosenbrock is the maximization of the function $B_1B_2B_3$ subject to the constraints $0 \le B_i \le 42$ for $i = 1, 2, 3$ and $0 \le B_1 + 2B_2 + 2B_3 \le 72$.

TABLE A3

STATISTICS FOR THE HARTLEY EXAMPLE

Points		B_1	B_2	B_3	R	n
p = 0.10	$P^{(0)}$	580	-180	-0.16	27377	1
q = 0.99	$P^{[3]}$	546.6	-181.9	-0.1796	13507	49
c′= 64	$P^{[6]}$	523.2	-157.0	-0.1996	13390.1	88
p = 0.25	$P^{(0)}$	580	-180	-0.16	27377	1
q = 0.80	$P^{[3]}$	545.9	-181.0	-0.1812	13500	58
c′= 32	$P^{[6]}$	530.2	-165.1	-0.1924	13402	106
	$P^{[12]}$	524.2	-157.9	-0.1988	13390.2	238
Solution (A2)		523.3	-156.9	-0.1997	13390.2	

TABLE A4

STATISTICS FOR THE BEALE EXAMPLE

Points (p = 0.25, q = 0.90, c′ = 8)		B_1	B_2	R	n
First start	$P^{(0)}$	13.0	0.9	0.8948	1
	$P^{[5]}$	3.516	0.724	0.1056	69
	$P^{[10]}$	3.000	0.500	10^{-8}	131
Second start	$P^{(0)}$	0	0.9	14.20	1
	Same results as for first start				
Third start	$P^{(0)}$	13.0	0	355.45	1
	$P^{[2]}$	2.967	0.491	0.0002	33
	$P^{[6]}$	3.000	0.500	10^{-7}	85
Solution (A3)		3	1/2	0	
		2.905	0.4944	0.0091	27

TABLE A5

MORC MINIMIZATION OF

$R = 100(B_2 - B_1^2)^2 + (1 - B_1)^2$

Point		B_1	B_2	R	n
p = 0.25	$P^{(0)}$	-1.2	1.0	24.2	1
q = 0.8	$P^{[6]}$	-0.519	0.269	2.31	103
c′ = 32	$P^{[12]}$	0.632	0.394	0.138	163
	$P^{[18]}$	0.999	0.998	10^{-6}	235
p = 0.25	$P^{(0)}$	-1.2	1.0	24.2	1
q = 0.6	$P^{[5]}$	-0.435	0.189	2.06	87
c′ = 2	$P^{[10]}$	0.945	0.887	0.006	143
	$P^{[15]}$	0.999	0.998	10^{-6}	211
Solution		1	1	0	

TABLE A6

STATISTICS FOR THE ROSENBROCK CONSTRAINT PROBLEM

Points		B_1	B_2	B_3	R	$B_1B_2B_3$	n	s″
p = 0.50	$P^{(0)}$	1	1	1	4999	1	1	
q = 0.99	$P^{[5]}$	21.72	13.74	11.40	1600	3400	75	
c′ = 4	$P^{[10]}$	22.91	13.98	10.57	1616	3384	177	1
	$P^{[15]}$	21.23	13.12	12.25	1589	3411	289	3
	$P^{[22]}$	24.029	12.022	11.964	1544.0	3456.0	426	5
Solution (A4)		24	12	12	1544	3456		
		23.794	12.257	11.842	1546.2	3453.8	337 through 600	

TABLE A7

SIMULTANEOUS EQUATION PROBLEMS

Problem and Statistics		B_1	B_2	B_3	R	n
Two equations:	$P^{(0)}$	0	0		74	1
$B_1 + 2B_2 = 7$	$P^{[2]}$	1.037	3.005		0.0083	27
$2B_1 + B_2 = 5$	$P^{[4]}$	1.0000	3.0000		10^{-9}	53
Solution (A4)		1	3		0	
		1.040	2.970		0.0028	44
		0.996	3.009		0.00001	59
Three equations:	$P^{(0)}$	0	0	0	6	1
$B_1 + B_2 + B_3 = 5$	$P^{[3]}$	2.472	0.708	1.896	0.634	68
$B_1 = B_3 \exp(1 - B_2)$	$P^{[6]}$	1.984	1.024	2.008	0.063	116
$B_1 = B_3 + (B_2 - 1)^2$	$P^{[12]}$	2.000	1.000	2.000	0.00083	212
Solution		2	1	2	0	

The solution is $B_1 = 24$, $B_2 = B_3 = 12$, $B_1B_2B_3 = 3,456$ and lies on the constraint surface $B_1 + 2B_2 + 2B_3 = 72$. When MORC was applied to this problem the criterion used was $R = 5,000 - B_1B_2B_3$ and results are given in Table A6. Linear descents are the rule in this problem and much time is spent in backing off the effective constraint surface.

Release of $P^{[s-1]}$ after c exceeded c′ produced higher values of R for a few cycles, but succeeding cycles soon brought the MORC path back to the correct neighborhood.

Solution of Simultaneous Equations

Given a system of J simultaneous equations in I unknowns,

$$E_j(B_1, \ldots, B_I) = 0 \text{ for } j = 1, \ldots, J$$

where the B_i may be subject to constraints, then a criterion such as $R = \Sigma E_j^2$ or $R = \Sigma |E_j|$ can be minimized in order to find "best" values for the unknowns in the region of constraint. If the criterion minimum turns out to be zero when I = J, then the equations have been solved. The last two examples illustrate MORC performance for this type of problem.

Rosenbrock's method (A4) is applied to the two linear equations, $B_1 + 2B_2 = 7$ and $2B_1 + B_2 = 5$. The Rosenbrock and MORC results are given in the top part of Table A7 where $R = (B_1 + 2B_2 - 7)^2 + (2B_1 + B_2 - 5)^2$.

The bottom part of Table A7 shows the MORC solution of three equations of different forms. For variety this problem was solved using the criterion

$$R = |B_1 + B_2 + B_3 - 5| + |B_1 - B_3 \exp(1 - B_2)| + |B_1 - B_3 - (B_2 - 1)^2|$$

Conclusion

Four references (A1, A2, A3, A4) represent only that part of the literature from which illustrative problems were used in the development of MORC. Spendley et al. (A5) and its bibliography has been selected for two reasons. First it provides a rather comprehensive survey of existing minimization (or maximization) procedures when all criterion values can be generated from the data at hand. But it also gives and cites techniques for the generation of criterion points by means of experimental design and for the exploration of criterion surfaces that have no definite algebraic representation. These sequential designs for experimentation yield successive points that are likely to be on the path to the desired minimum (or maximum).

Conceivably the MORC origins and parabola vertices could be used to predict where new experimental points should be observed, but it is clear from the size of n in the examples of this paper that experimental designs based on a process like MORC would require far too much experimentation.

References

A1. Anderson, R. L., and Bancroft, T. A., "Statistical Theory in Research." Ch. 15, McGraw-Hill (1952).

A2. Hartley, H. O., "The Modified Gauss-Newton Method for the Fitting of Non-Linear Regression Functions by Least Squares." Technometrics, 3:2 (1961).

A3. Beale, E. M. L., "On an Iterative Method for Finding a Local Minimum of a Function of More than One Variable." Technical Report No. 25, Stat. Tech. Res. Group, Princeton Univ. (1958).

A4. Rosenbrock, H. H., "An Automatic Method for Finding the Greatest or Least Value of a Function." Computer Journal 3:168 (1960).

A5. Spendley, W., Hext, G. R., and Himsworth, F. R., "Sequential Application of Simplex Designs in Optimisation and Evolutionary Operation." Technometrics, 4:4 (1962).

Nationwide Survey of Pavement Terminal Serviceability

C. F. ROGERS and H. D. CASHELL, Bureau of Public Roads, and
P. E. IRICK, Highway Research Board

During the late fall and early winter of 1961-62, three survey teams traveled a total of 12, 000 miles in gathering data on the condition of highway pavements scheduled for resurfacing. In less than three months these teams, using instrumentation and techniques developed by the AASHO Road Test staff, surveyed 134 pavements projects in 35 States. The projects were selected for survey by a special subcommittee of the AASHO Highway Transport Committee from about 1, 100 projects submitted by the States.

The nationwide survey was conducted for the aforementioned special subcommittee by the Bureau of Public Roads in cooperation with the Highway Research Board and the State highway departments. Its purpose was to establish a serviceability index for pavements with surfaces no longer considered acceptable to traffic. This index, called the terminal serviceability index, was needed to make the AASHO Road Test equations usable in predicting the life of new pavements and the remaining life of pavements in service.

Nationwide, the average terminal serviceability index was determined to be 2. 2 for primary rigid pavements, 2. 1 for primary flexible pavements and 1. 9 for secondary flexible pavements. Secondary rigid pavements were not included in the survey because of the scattered locations of the relatively few such pavements scheduled for resurfacing.

Nearly 60 percent of the selected projects had terminal serviceability indexes of 1. 5 to 2. 5. For 8 percent of the projects the index was above 3. 0, indicative of resurfacing for reasons other than poor riding quality. For 16 percent of the projects the index was less than 1. 5, the value at which the AASHO Road Test sections were declared out of test.

When all classes of pavement were considered, no particular region could be singled out as consistently resurfacing at either a higher or lower serviceability index than any other region. A slight indication existed that there was more variation in resurfacing practices among States than within States.

•A SURVEY of the condition of highway pavements at the time they had been scheduled for resurfacing was conducted. This determination of terminal serviceability was required to establish procedures for the conduct of a pavement evaluation survey using the findings of the AASHO Road Test. The pavement evaluation survey would implement a determination of the structural capability of existing highway pavements and provide a reasonable basis for the regulation of motor-vehicle axle loads. Along with other sources of information, it would assist in the formulation of policy recommendations

Paper sponsored by Department of Design.

concerning the maximum weights and dimensions of motor vehicles permitted to operate on the highway systems of the United States.

The method of evaluating test section performance at the AASHO Road Test was decided by the Highway Research Board with the approval of its National Advisory Committee. From the several methods available the decision was reached to hinge the evaluation on "The Pavement Serviceability-Performance Concept" (1, 2) developed by the AASHO Road Test staff.

This concept of evaluating pavement performance utilizes serviceability formulas based on physical measurements. The formulas were derived from a statistical correlation with subjective performance ratings that defined the ability of road pavements to serve high-speed, high-volume, mixed traffic as of a certain time.

The analytical equations developed for the rigid and flexible pavement structures of the AASHO Road Test describe the probable decline in serviceability of pavements of known thickness when subjected to loads of known magnitude and frequency. Valid for the conditions existing at the test site in Illinois, these equations are susceptible to modification for conditions in other areas. They permit prediction of the service life of new pavements and the remaining life of pavements in service.

Use of the Road Test equations for such purposes requires the determination of a reasonable value for a factor designated as the terminal serviceability index, which defines the condition of pavements no longer capable of providing acceptable traffic service. To fill this need, a nationwide survey, using performance evaluation techniques developed at the Road Test, was undertaken on pavements scheduled for improvement in State programs.

This report describes the background, scope and procedure of the survey and presents the results. A final section, in reference to some of the implications drawn from the survey, discusses future applications and research needs.

BACKGROUND OF SURVEY

As one measure to conserve the investment in the National System of Interstate and Defense Highways, the 84th Congress in 1956 fixed certain limitations on the weight and width of vehicles permitted use of that system. The intent of the Congress was to place a "freeze" on existing limits, pending more objective determination of road capabilities based on the results of the AASHO Road Test. Subsection 108(k) of the 1956 Act also directed the Secretary of Commerce to make recommendations to the Congress with respect to the maximum desirable weights and dimensions for vehicles operated on the Federal-aid highway systems.

Concurrently, the AASHO Executive Committee authorized its Committee on Highway Transport to undertake a full-scale review of the 1946 Policy on motor-vehicle weights and dimensions and, upon conclusion of the AASHO Road Test, to develop a revised draft of recommended sizes and weights.

Throughout the development of these recommendations, the Bureau of Public Roads on behalf of the Department of Commerce has worked closely with the AASHO Highway Transport Committee. The same basic data have been jointly developed and utilized to bring about conformity in the separate determinations, to the end that the limits recommended to the Congress be consistent with those contained in the revised policy of AASHO.

On April 19, 1961, a special subcommittee of the AASHO Highway Transport Committee, on which the Bureau of Public Roads is represented, initiated a resolution calling for a pavement evaluation survey to provide information needed to assist in formulating the policy recommendations. The resolution, subsequently transmitted to the AASHO Executive Committee, was approved by that body on June 28, 1961. It was resolved that each State should evaluate the load-carrying capacity of its highways, making use of the equations produced by the AASHO Road Test. It provided that the request for this evaluation would be made by the Bureau of Public Roads, which would also collect, compile, and analyze the evaluation data submitted by the States.

At a meeting held in Chicago on August 16, 1961, attended by representatives of AASHO, HRB, and BPR, a number of committees were formed to carry out special features of the work. One group was assigned the task of preparing the manual for the pavement evaluation survey. A second group was designated to provide reasonable bases for modification of the Road Test equations applicable to other conditions. Another special group was given the task of determining typical average terminal values for the present serviceability index (PSI) for use in applications of the AASHO Road Test findings.

In the serviceability scale, ranging in value from 5 to 0 for pavements varying in condition from very good to very poor, newly constructed pavements have an initial index of about 4.5. At the Road Test, sections were considered "out-of-test" when the index value reached 1.5. This value, representing a condition approximating unsafe for traffic use, was chosen with the intent that it would be below the terminal value at which pavements are usually resurfaced or reconstructed.

From a structural viewpoint, to what extent does a road in normal use deteriorate--how diminished is its ability to serve traffic—before it is resurfaced or reconstructed? Typically, what is the terminal serviceability index of road pavements which the States schedule for improvement?

To answer this question the Bureau of Public Roads, in cooperation with HRB and AASHO, undertook in the fall of 1961 a nationwide survey of the terminal serviceability of highway pavements. Projects selected for survey included both rigid and flexible pavement types on the primary system and flexible pavement type on the secondary system.

SCOPE OF SURVEY

As the first step in the nationwide survey, a map was requested from each State showing the location and type of all primary and secondary rural pavement projects, two miles or more in length, that were scheduled for resurfacing in 1962. The States reported 244 primary rigid, 504 primary flexible, 49 secondary rigid and 306 secondary flexible pavement projects in this category. These ranged in length from 2 to 52 miles and averaged approximately 8, 9, 10 and 9 miles in the four classes, respectively.

On receipt of the State maps, the projects scheduled for resurfacing were plotted on a master map which was divided into the four AASHO regions. When this map was completed, the Special Subcommittee of the AASHO Highway Transport Committee selected the itinerary and survey projects. Secondary rigid pavement projects were excluded because only a few of the relatively small number of such projects were near the designated routes of travel. Projects with chip-seal bituminous surfacing and those that were to be reconstructed because of geometrics were also excluded. In addition, only those projects within about 25 miles of the selected travel routes were considered for the survey.

About 60 primary rigid, 60 primary flexible, and 20 secondary flexible pavement projects were selected for the nationwide terminal serviceability survey. Actually, 134 projects were surveyed. Table 1 shows the number of projects in each pavement class that were surveyed in each of the four AASHO regions, as well as the States in which the projects were located. Not listed, are ten special projects that were included in the 134 projects. Six of the special projects were previously resurfaced rigid pavements; 4 were newly constructed pavements; 3, flexible; and 1, rigid.

SURVEY PROCEDURES

The survey was conducted by three teams[1], each headed by a Bureau of Public Roads junior engineer assisted by an engineer technician. One team covered the east and the other two teams conducted surveys in the central and western parts of the country, respectively. The three teams began their tours in November and the last project was surveyed in early February. These teams traveled a total of approximately 12,000 miles.

[1] J. R. Huff, G. S. Lehman and F. D. Swaim, Bureau of Public Roads junior engineers; P. J. Heath, K. H. Severson, engineer technicians from the AASHO Road Test; Frank Russo, Bureau of Public Roads engineering technician.

TABLE 1

CLASSIFICATION OF SURVEY PROJECTS

AASHO Region	Class 1 Primary Rigid Pavement		Class 2 Primary Flexible Pavement		Class 3 Secondary Flexible Pavement	
	No.	State	No.	State	No.	State
1	8	N. H., N. J., Pa., Vt.	10	Conn., N. H., N. Y., Pa., Vt.	5	Conn., N. H., N. J., N. Y., R. I.
2	13	Ark., Fla., Ga., La., S. C., Tenn., Va., W. Va.	17	Ark., Fla., Ky., La., Miss., S. C., Tenn., Va.	7	Fla., Ga., Ky., La., Miss., W. Va.
3	18	Ill., Iowa, Kan., Mich., Minn., Neb., Okla., Wis.	12	Ind., Kan., Minn., Neb., Ohio, S. Dak.	4	Mich., Ohio, Wis.
4	8	Cal., Colo., Ore., Tex.	16	Ariz., Cal., Colo., Idaho, Ore., Wyo., Tex.	6	Ariz., Cal., Tex., Idaho, Wyo.
Totals	47	24	55	26	22	19

With the request for the previously mentioned map, each State highway department was asked to furnish certain personnel when the terminal serviceability survey was made within their State. Likewise, each division office of the Bureau was requested to furnish a representative. About two weeks before the arrival of the survey team, both agencies received detailed instructions relating to their part in the survey including a meeting place for the participants, which was usually the beginning of the first project in the State. As far in advance as possible, the survey team notified the Bureau's division office of the exact date and time that it would be at the designated meeting place. The division office in turn notified the State.

While awaiting the maps from the States, the teams were equipped and thoroughly instructed in the use of the instrumentation and techniques for obtaining data needed to determine the serviceability index of rigid and flexible pavements. These data included slope variance (3) as measured with the CHLOE profilometer (Fig. 1), cracking and patching for both rigid and flexible pavements, and rut depth for flexible pavements. For rigid pavements, the teams were also trained to obtain additional data consisting of faulting at transverse joints and cracks and scaling.

The following five steps were taken to provide what was believed to be the best coverage of the condition of the selected projects in the time allotted to the survey:

1. A 500-ft, single-lane section of pavement was chosen as the basic unit for PSI measurements.

2. If both roadways of a divided highway were scheduled for resurfacing, the outer lane of the roadway in the direction of travel of the survey team was designated for PSI measurements; if only one roadway of a divided highway was to be improved, the measurements were taken in the outer lane; for 2-lane highways, the measurements were taken in the lane in the direction of travel of the team.

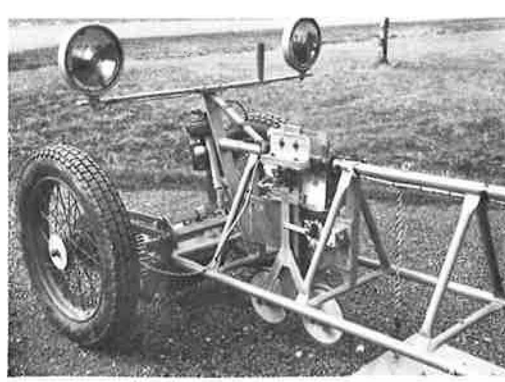

Figure 1. Rear of CHLOE profilometer.

3. The number of sections subject to measurement was set as 6 for projects 5 miles or less in length, 8 for projects between 5 and 15 miles, and 10 for those greater than 15 miles.

4. Equidistant spacing of the 500-ft sections in a given project, by odometer, was specified to insure random selection of pavement condition.

5. Slope-variance values were required to be obtained alternately in the outside and inside wheelpaths of successive 500-ft sections, rut-depth measurements at 50-ft intervals alternately in the outside and inside wheelpaths of a given section, and cracking and patching over the entire section.

Both men and slow-moving equipment occupied one lane of the pavement while making measurements. This necessitated traffic control similar to that required for patching or other repairs to the pavement. For this control, and in the interest of safety, the maintenance divisions of the State highway departments provided the necessary trained personnel, signs, barricades, etc. In some States the maintenance divisions furnished two traffic-control crews, functioning in leap-frog fashion. As soon as the survey team completed observations on a 500-ft section, it would then move to the next section and begin observations without the delay of transferring and setting up paraphernalia. The time required to obtain measurements on a 500-ft section varied from 20 to 30 minutes.

From the data collected by the survey teams, a value for the present serviceability index was computed for each project from the following AASHO Road Test PSI formulas:

Rigid pavement formula:

$$PSI = 5.41 - 1.80 \log (1 + \overline{SV}) - 0.09\sqrt{\overline{C}_c + \overline{P}_c}$$

Flexible pavement formula:

$$PSI = 5.03 - 1.91 \log (1 + \overline{SV}) - 0.01\sqrt{\overline{C}_f + \overline{P}_f} - 1.38\ \overline{RD}^2$$

in which

- PSI = present serviceability index;
- $\overline{SV}$ = slope variance in wheelpath, average for all sections of the project;
- $\overline{C}_c$ = total lin ft of Class 3 and 4 cracks per 1,000 sq ft of pavement surface (4), average for all sections of the project;
- $\overline{C}_f$ = area in sq ft per 1,000 sq ft of pavement surface exhibiting Class 2 and 3 cracking (4), average for all sections of the project;
- $\overline{P}_c$ = bituminous patching in sq ft per 1,000 sq ft of pavement surface, average for all sections of the project;
- $\overline{P}_f$ = skin or deep patching in sq ft per 1,000 sq ft of pavement surface, average for all sections of the project; and
- $\overline{RD}$ = rut depth in wheelpath in in., average for all sections of the project.

SURVEY RESULTS

Terminal Serviceability Data

Terminal serviceability indexes for all projects and for each 500-ft section of every project are given in Tables 6, 7, and 8 (Appendix). As previously indicated, the project PSI values were computed from project average measurements, and are not necessarily the same values that would result from averaging section PSI values.

Frequency distribution of the project terminal serviceability indexes are given in Table 2 for each of the three classes of pavement. About 60 percent of the 124 regular projects had serviceability indexes of 1.5 to 2.5. Eight percent of the projects were in the "good" category of serviceability (3.0 to 4.0 PSI), and it may be presumed that most of these were scheduled for maintenance for reasons other than unacceptable riding quality. Sixteen of the projects had serviceability indexes less than 1.5, the value at which the AASHO Road Test sections were declared out of test.

TABLE 2

FREQUENCY DISTRIBUTIONS OF PROJECT TERMINAL SERVICEABILITY INDEXES

Serviceability Index Range	Class 1 Primary Rigid Pavement	Class 2 Primary Flexible Pavement	Classes 1, 2 All Primary Pavement	Class 3 Secondary Flexible Pavement	Classes 2, 3 All Flexible Pavement
3.5 - 4.0	—	1	1	1	2
3.0 - 3.5	5	3	8	—	3
2.5 - 3.0	14	6	20	1	7
2.0 - 2.5	15	18	33	9	27
1.5 - 2.0	5	20	25	6	26
1.0 - 1.5	5	7	12	3	10
0.5 - 1.0	2	—	2	2	2
0 - 0.5	1	—	1	—	—
No. of Projects	47	55	102	22	77

TABLE 3

AVERAGE TERMINAL SERVICEABILITY INDEX

AASHO Region	Class 1 Primary Rigid Pavement	Class 2 Primary Flexible Pavement	Classes 1, 2 All Primary Pavement	Class 3 Secondary Flexible Pavement	Classes 2, 3 All Flexible Pavement
1	2.2 (8)[a]	1.6 (10)	1.9 (18)	1.3 (5)	1.5 (15)
2	2.6 (13)	2.1 (17)	2.3 (30)	1.8 (7)	2.0 (24)
3	2.1 (18)	2.0 (12)	2.1 (30)	2.4 (4)	2.1 (16)
4	1.8 (8)	2.3 (16)	2.2 (24)	2.3 (6)	2.3 (22)
All	2.2 (47)	2.1 (55)	2.1 (102)	1.9 (22)	2.0 (77)

[a]Figures in parentheses are the number of projects included in the averages.

Average terminal serviceability indexes for the four AASHO regions and for all regions in each pavement class are given in Table 3, which shows that the average terminal serviceability index was 2.2 for primary rigid pavements, 2.1 for primary flexible pavements and 1.9 for secondary flexible pavements. Table 3 does not give an average terminal serviceability index of 2.3 for the 6 previously mentioned resurfaced rigid pavements and an average initial serviceability index of 4.3 for the 4 newly constructed pavements. This latter value is very nearly the same as the average initial serviceability index of all test sections at the AASHO Road Test.

The survey produced information on PSI variability in four categories: section-to-section within projects; project-to-project within States; State-to-State within regions; and region-to-region within the country. Analysis of these variations shows the magnitude of the different variances and brings out certain nonhomogeneities that exist in the various categories.

Table 4 gives the summary results of an analysis of the variances or mean squares for the terminal serviceability indexes. Line A shows the average variance of project PSI's about their respective class means. These variances are 0.48, 0.33 and 0.43 for primary rigid, primary flexible, and secondary flexible pavements, respectively, and the overall average is about 0.4 when weighted with degrees of freedom. Thus the standard deviation of the projects is between 0.6 and 0.7.

In lines B through E (Table 4), the mean squares serve for comparison purposes only and are not to be used to derive standard deviations. A particular mean square can be compared either with other mean squares in the same line or with corresponding mean squares in the line just below.

TABLE 4

ANALYSIS OF VARIANCE FOR PROJECT PSI DATA

Line	Type of Variation	Class 1 Primary Rigid Pavement		Class 2 Primary Flexible Pavement		Class 3 Secondary Flexible Pavement	
		df[a]	MS[b]	df	MS	df	MS
A	Total	46	0.48	54	0.33	21	0.43
B	Among regions	3	1.04	3	1.07	3	1.37
C	Among States in regions:	20	0.64	22	0.40	15	0.24
C_1	Region 1	3	1.29	4	0.42	4	0.13
C_2	Region 2	7	0.52	7	0.45	5	0.29
C_3	Region 3	7	0.66	5	0.27	2	0.18
C_4	Region 4	3	0.23	6	0.43	4	0.27
D	Among projects in States:	23	0.26	29	0.21	3	0.37
D_1	Region 1	4	0.28	5	0.04		
D_2	Region 2	5	0.04	9	0.39	1	0.03
D_3	Region 3	10	0.05	6	0.07	1	0.04
D_4	Region 4	4	1.03	9	0.22	1	1.04
E	Among sections in projects:		0.30 (0.23)[c]		0.24 (0.17)[c]		0.17
E_1	Region 1		0.23		0.14		0.11
E_2	Region 2		0.24		0.24		0.13
E_3	Region 3		0.21		0.36		0.34
E_4	Region 4		0.67		0.23		0.15

[a]df = Degrees of freedom.
[b]MS = Mean square or variance.
[c]Three projects having extreme section-to-section variance were excluded.

Line B (Table 4) gives the project variance among the regional means for each class of pavement. Comparison of line B variances with those of line C leads to the conclusion that, in each pavement class, there is appreciably more variation from region-to-region than might be expected in view of the State-to-State variation within regions.

Since Class 1 and Class 2 regional means are based on an average of about 12 projects, and those of Class 3 on about 5 projects, regional means are rather heavily influenced by projects that have relatively extreme PSI values. Although there appears to be significant region-to-region variances, Table 3 gives little reason to suppose that a particular region can be singled out as having projects whose terminal serviceability indexes average either consistently high or consistently low in all three classes of pavement.

Line C (Table 4) gives the average variance among State means when the States are in the same region, and lines C_1, C_2, C_3 and C_4 give the regional values that are averaged to obtain line C mean squares, using df's as weights. For Class 1, Region 1, the State-to-State variance is at least twice any other mean square in lines C. Table 6 (Appendix) shows that this is the result of three projects having PSI's less than 1.0. Mean squares in lines C can be compared with corresponding mean squares in lines D to judge whether State-to-State variation is significant relative to project-to-project variation within States. In general, corresponding variances are greater in lines C than lines D, suggesting that there may be somewhat more variation among States than within States.

Line D gives the average variance among project PSI's in the same State, and lines D_1, D_2, D_3 and D_4 give the regional mean squares whose averages are shown on line D. It can be seen that project-to-project variances within States are not very homogeneous from one region to another. In nearly two-thirds of the cases, however, the variances in lines D are not much larger, if at all, than the corresponding variances in lines E. Since the line E variances reflect differences from section-to-section within projects, there is, on the average, no more variation among projects within the same State than can be expected in view of the internal variations within any one project.

Measurement Data

Project slope variances are given in Tables 9, 10, and 11 (Appendix) for each class of pavement. These variances are averages of the previously mentioned measurements

TABLE 5

AVERAGES FOR MEASURED DATA[a]

AASHO Region	Class 1 Primary Rigid Pavement				Class 2 Primary Flexible Pavement			Class 3 Secondary Flexible Pavement		
	SV	C + P	F	Sc	SV	C + P	RD	SV	C + P	RD
1	32	76	2.7	43	49	316	0.21	71	217	0.27
2	18	48	2.6	22	32	173	0.19	41	140	0.17
3	26	83	2.8	3	31	496	0.18	18	309	0.12
4	27	184	2.4	6	22	407	0.16	23	350	0.14
All	25	90	2.7	11	32	338	0.18	39	246	0.17

[a]Units of measurement are as follows:

SV = slope variance in wheelpath (actual multiplied by 10^6);

C = total linear ft of Class 3 and 4 cracks per 1,000 sq ft of pavement surface for rigid pavement, and area in sq ft per 1,000 sq ft of pavement surface exhibiting Class 2 and 3 cracking for flexible pavement;

P = patching in sq ft per 1,000 sq ft of pavement surface;

F = faulting in wheelpath at transverse joints and cracks in in. per 1,000 lin ft of pavement;

Sc = scaling in sq ft per 1,000 sq ft of pavement surface; and

RD = rut depth in wheelpath in in.

taken alternately in the outer and inner wheelpaths of successive 500-ft sections. In general, variances in the outer wheelpath were somewhat greater than those in the inner wheelpath. For each project the difference in variance between the two wheelpaths was used to adjust the section PSI's of Tables 6, 7, and 8 to a comparable basis.

Tables 9, 10, and 11, also give average values of cracking and patching for all projects in each pavement class. Tables 12 and 13 (Appendix) give the project average rut depth for all of the flexible pavement projects. Table 14 (Appendix) shows the average values of faulting and scaling for all of the rigid pavement projects.

The measurement data given in the Appendix are shown in Table 5 as regional and overall averages for each of the three classes of pavement. The number of projects for each average is the same as given in Table 3.

Based on the projects included in the survey, Table 5 indicates that (1) slope variances of pavements scheduled for resurfacing are greatest in Region 1 for all three classes of pavement, (2) the combination of cracking and patching is most extensive in Regions 3 and 4, and (3) rigid pavements are scaled most in Regions 1 and 2, this condition being caused by two pavements in these regions having 75 percent of the total scaling recorded for the 47 pavements included in the survey.

Table 5 also indicates that the average depth of the wheelpath ruts in the flexible pavements was quite small. Actually, rut depths of the magnitude encountered in the survey had only a slight influence on the terminal serviceability index values.

RESULTS

The data recorded in the nationwide survey have provided a sound basis for the computation of typical terminal serviceability indexes for highway pavements in need of resurfacing. But not all of the significant variables were included in the survey. Without specific supporting data, it was nonetheless apparent that the survey projects were representative of a considerable range of traffic volumes and compositions. It was also observed that these projects varied substantially in type and thickness of pavement structure. Moreover, differences in fiscal capability were evident among the several States and regions. It seems logical to conclude, therefore, that the variance which characterized the values for terminal serviceability was in some degree the product of the relation between the pavement structures and their traffic, and was influenced also by budget considerations.

This raises the question of whether the level of serviceability at which pavements are usually scheduled for improvement is, in fact, the critical level at which they should be improved. Similarly, a question exists as to whether the improvement of pavements of greater traffic service may be scheduled at higher levels of serviceability, and conversely, as to whether the improvement of the pavements of lesser traffic importance is delayed by fiscal limitations beyond the desirable level of terminal serviceability.

FUTURE APPLICATIONS AND RESEARCH NEEDS

The scheduling of projects for construction, reconstruction or resurfacing is part of a logical sequence of steps in the programming process. The initial need is for improved classification of roads in accordance with the type of traffic service rendered. It is suggested that this would provide a preferred means to the development of more appropriate improvement standards for the roads in each class of service. The development of such standards is a condition precedent to the adequate pricing of future improvement programs. Within the fiscal budget limitations, pricing is the key to the orderly establishment of construction project priorities. The extent to which the programs may embrace the mileage of lesser importance should be more readily indicated.

Application of the pavement serviceability-performance concept to the scheduling of the priority order of project improvements is suggested as a potentially fruitful area of future research. The need is indicated for more precise, and more rapid means to determine pavement conditions which warrant improvement and to insure that the improvements made will be compatible with the anticipated traffic. Serviceability histories, developed and maintained on projects or control sections, would result from a more extensive use of rating procedure to establish the current serviceability of existing pavements. This type of determination would take better account of the traffic use which has occasioned decline in pavement serviceability and permit improved predictions to be made of remaining service life.

Inasmuch as such predictions depend on traffic use, means must be developed, for the mileage in each class of traffic service, to portray more accurately the volumes, compositions, and axle-load distributions to which particular pavements will be subjected. This is an area of development which appears ideally suited to the greatly expanded use of such means as the electronic scale for weighing vehicles in motion and automatically recording the needed load-distribution data. The mass recording of more representative data, over a wider range of traffic volumes and compositions, would be possible by such means.

CONCLUSION

The nationwide terminal serviceability survey has provided usable index values which define the condition of highway pavements scheduled for improvement by reason of their structural condition. Since the procedures of the pavement evaluation survey involved the use of the AASHO Road Test equations, the availability of these typical index values for terminal serviceability has contributed to the derivation of information relative to the load-supporting ability of highways. This information is important to the formulation of sound policy recommendations concerning the maximum desirable weights and dimensions of motor vehicles permitted use of the highway system. This sequence of steps would therefore appear to constitute a valid application of the AASHO Road Test findings.

Equally valid applications of the road test equations are indicated in other areas. These areas of actual and potential application have been demonstrated and discussed. By the program of satellite tests, the AASHO Road Test findings can be translated to conditions in other areas and the equations can be modified by experience. By simulation of the rating procedure in other applications, the highway engineer in effect has been equipped with a new set of tools. Capable of reproducible results, these tools can be used in the solution of problems in the areas of design, regulation, and programming. Used with judgment and improved with use, they can provide more solid bases of resolution in the future.

REFERENCES

1. Carey, W. N., Jr., and Irick, P. E., "The Pavement Serviceability-Performance Concept." HRB Bull. 250, 40-58 (1960).

2. "The AASHO Road Test—History and Description of Project." HRB Special Report 61A, p. 13, 34, 35, and 39 (1961).
3. Carey, W. N., Jr., Huckins, H. C., and Leathers, R. C., "Slope Variance as a Measure of Roughness and the CHLOE Profilometer." HRB Special Report 73, 126-135 (1962).
4. "The AASHO Road Test: Report 5—Pavement Research." HRB Special Report 61E, p. 23 and 142 (1962).

Appendix

TABLE 6

PROJECT AND SECTION PSI DATA — PRIMARY RIGID PAVEMENTS

Project		Project PSI	PSI for Individual 500-ft Sections									
			1	2	3	4	5	6	7	8	9	10
AASHO	N. H.	2.3	1.7	2.5	2.7	2.2	2.8	2.9				
Region	N. J.	1.6	1.9	1.8	1.8	1.3	1.3	2.0				
1	N. J.	2.8	2.9	3.2	2.6	2.7	3.1	2.6				
	N. J.	1.9	2.1	2.1	1.6	1.5	2.3	2.2				
	Pa.	2.3	2.3	2.5	1.6	3.0	3.2	2.5				
	Pa.	3.2	3.3	3.2	3.4	3.3	3.1	4.0	2.6			
	Pa.	2.6	2.1	2.8	3.4	2.6	3.3	2.3				
	Vt.	0.4	0.0	1.0	1.0	1.7	0.0	0.2				
AASHO	Ark.	2.9	2.7	3.6	2.8	3.1	2.9	2.7				
Region	Ark.	2.6	3.0	2.4	2.7	2.9	3.0	3.0	4.1	1.7		
2	Fla.	3.4	3.7	3.2	3.2	3.9	3.9	3.3				
	Ga.	2.9	3.1	3.2	2.6	3.1	3.2	2.9	3.5	2.1		
	Ga.	3.1	3.2	2.7	3.1	3.1	3.6	3.4				
	La.	2.1	1.6	2.5	1.7	2.8	2.2	2.5	1.8	2.0		
	La.	1.8	2.3	2.2	2.5	2.2	2.5	1.4	1.2	1.3		
	S. C.	3.3	4.0	3.9	2.2	4.2	3.3	3.8				
	S. C.	2.8	2.3	3.3	3.0	2.8	2.4	3.8				
	Tenn.	1.5	1.4	1.9	1.0	1.5	0.6	1.5	2.2	2.4		
	Va.	2.6	3.2	2.6	2.0	2.3	2.7	3.4				
	Va.	2.5	2.7	2.8	2.4	2.9	2.4	2.1				
	W. Va.	2.3	2.3	3.0	2.1	3.0	2.7	1.4				
AASHO	Ill.	1.7	1.9	1.5	2.0	2.0	1.9	1.7	2.5	2.4		
Region	Ill.	1.4	1.3	1.3	0.9	0.9	1.7	2.5	1.6	1.7	2.2	0.6
3	Iowa	2.9	2.7	2.9	2.7	3.2	3.1	2.4	3.2	3.5		
	Iowa	2.5	2.4	2.3	3.8	2.8	2.4	2.2	2.5	2.4		
	Iowa	2.9	2.4	3.8	2.6	3.3	2.9	3.8	3.1	2.7		
	Kan.	2.5	2.4	2.5	2.3	3.0	2.5	2.7	2.4	2.8		
	Kan.	2.1	1.9	2.1	2.1	2.1	2.1					
	Mich.	2.1	1.8	2.2	2.6	2.5	2.0	1.7	2.2	2.2		
	Mich.	2.2	2.3	1.6	2.3	2.2	2.1	2.4	2.8	2.3		
	Minn.	2.2	1.9	2.6	2.1	2.6	2.4	1.8				
	Minn.	2.5	2.6	3.0	2.5	2.5	2.2	2.8				
	Neb.	2.3	2.0	2.8	1.7	2.1	2.7	3.1				
	Neb.	2.6	2.5	2.9	2.4	2.7	2.2	4.6	2.6	2.3		
	Okla.	2.1	1.3	2.0	2.5	2.4	2.2	2.6				
	Okla.	2.2	3.0	2.6	2.2	2.4	2.1	2.6	2.1	1.3		
	Okla.	2.1	2.4	2.5	1.3	3.3	2.7	1.6	2.5	2.0		
	Wis.	0.8	0.6	0.6	1.0	1.0	0.8	0.7				
	Wis.	1.4	1.3	2.0	1.8	2.0	1.3	1.5	0.9	0.6		
AASHO	Cal.	1.9	2.1	1.8	1.5	2.3	2.3	1.9				
Region	Cal.	2.3	1.6	2.4	3.5	3.7	1.5	2.6				
4	Colo.	2.0	1.9	0.9	1.9	2.6	2.4	2.2	2.7	3.0		
	Ore.	1.1	1.3	2.1	3.2	0.2	0.4	0.8				
	Tex.	3.4	3.8	3.4	3.4	3.5	2.9	3.3				
	Tex.	2.1	3.3	1.9	2.8	1.6	3.1	1.1				
	Tex.	0.6	0.0	0.3	0.4	2.2	2.3					
	Tex.	1.3	2.1	2.1	1.8	1.8	2.0	0.0				

TABLE 7

PROJECT AND SECTION PSI DATA — PRIMARY FLEXIBLE PAVEMENTS

Project		Project PSI	PSI for Individual 500-ft Sections									
			1	2	3	4	5	6	7	8	9	10
AASHO	Conn.	2.0	1.7	2.1	1.9	2.1	1.9	2.5				
Region	N. H.	1.8	1.1	1.8	1.3	3.2	1.8	2.9				
1	N. H.	2.0	2.3	2.2	1.9	2.5	1.8	1.6				
	N. Y.	1.7	2.0	1.6	1.4	1.8	1.9	1.6	1.5	1.6		
	N. Y.	1.3	1.1	1.8	1.4	1.8	0.5	1.6	1.0	1.7		
	N. Y.	1.1	1.6	1.2	1.9	1.1	0.3	1.9				
	Pa.	1.1	1.1	1.7	1.1	0.6	1.0	1.4	0.8	1.1		
	Pa.	1.1	1.5	0.7	1.2	1.0	1.1	1.1				
	Vt.	2.2	2.4	2.1	2.1	2.4	2.1	2.3				
	Vt.	2.1	1.8	2.3	2.0	2.1	2.2	2.5				
AASHO	Ark.	1.5	1.1	1.3	1.5	1.3	2.4	2.7				
Region	Ark.	1.7	1.3	1.3	2.0	2.1	1.8	1.9	1.7	1.7		
2	Fla.	2.6	2.5	3.2	3.3	2.1	2.2	2.6	2.7	3.5		
	Fla.	2.0	2.4	1.9	2.0	2.1	2.0	1.9				
	Ky.	1.9	1.5	1.7	1.6	2.2	1.6	2.2	1.7	3.0		
	La.	3.6	3.5	4.0	4.0	4.2	2.9	3.8	3.5	3.6		
	Miss.	2.1	2.7	1.9	2.8	2.8	2.1	2.1	2.0	1.5		
	Miss.	2.7	2.8	2.5	2.5	2.3	3.5	2.7	4.1	2.7		
	Miss.	2.0	1.6	2.0	2.0	1.9	1.3	2.6	2.2	3.0	1.7	3.1
	S. C.	2.4	2.8	2.7	2.3	2.2	2.4	2.2				
	S. C.	1.9	4.0	4.5	2.2	1.5	1.7	1.6	1.7	2.1	1.2	2.3
	S. C.	1.4	1.6	1.2	2.0	1.2	1.2	1.4	1.1	2.0		
	S. C.	1.8	1.4	2.1	1.4	2.7	1.6	2.5				
	Tenn.	1.9	1.7	2.3	2.7	1.5	2.1	2.0	0.7	2.1		
	Va.	1.1	1.5	0.9	1.6	0.8	0.8	1.1				
	Va.	2.2	1.9	2.4	1.8	2.4	2.2	2.7				
	Va.	3.3	3.1	3.1	3.4	4.0	3.2	3.5				
AASHO	Ind.	1.5	1.2	2.2	1.6	1.9	1.2	1.4				
Region	Ind.	1.6	1.6	1.8	1.1	2.0	2.2	1.2	1.7	1.8		
3	Kan.	2.2	2.7	2.8	2.2	1.8	2.3	2.1	2.5	2.0		
	Kan.	2.4	2.7	2.2	2.2	2.8	2.1	2.6				
	Kan.	1.7	1.8	1.8	2.5	1.3	2.4	1.1				
	Minn.	2.0	2.2	1.9	1.3	1.8	2.3	2.6	1.9	2.3	2.5	2.8
	Neb.	1.8	1.9	2.0	1.4	2.1	1.4	2.8	1.7	1.9		
	Neb.	1.6	1.2	1.8	1.3	1.5	1.6	1.8	2.1	1.6		
	Ohio	2.5	2.0	3.6	2.1	3.5	3.6	1.6	3.0	3.2		
	Ohio	2.6	2.1	2.7	2.1	3.3	2.9	3.0	2.8	2.8		
	S. Dak.	1.9	1.6	2.7	2.1	1.8	1.9	1.9	1.8	1.9		
	S. Dak.	1.6	1.6	1.1	1.0	1.7	2.9	4.6				
AASHO	Ariz.	2.4	2.3	3.0	2.0	2.9	2.3	2.5	2.4	2.8		
Region	Ariz.	2.2	2.3	2.2	2.0	2.2	2.4	2.1				
4	Cal.	2.4	3.3	2.5	3.1	1.9	2.0	2.6	2.5	2.1		
	Cal.	3.2	3.1	3.7	2.6	3.6	2.9	3.3	3.4	4.5		
	Cal.	3.0	3.0	1.9	4.8	3.9	4.9	3.1				
	Cal.	2.6	2.1	2.6	2.7	2.1	1.8	3.1	3.0	3.9	3.8	3.2
	Colo.	1.7	0.8	2.9	2.1	2.3	1.4	2.7	1.7	1.5		
	Colo.	1.3	1.9	1.3	2.1	0.5	1.4	1.2	1.2	1.8		
	Idaho	2.5	2.5	3.0	2.0	2.0	2.9	2.7				
	Ore.	2.3	2.2	2.5	1.8	2.5	2.7	2.2	2.2	2.4		
	Ore.	2.2	2.3	2.0	2.2	2.2	2.4	2.1	2.2	2.3		
	Wyo.	2.3	2.9	2.8	2.4	1.8	2.4	1.9	1.9	3.2		
	Wyo.	1.8	2.1	1.6	2.1	1.4	1.7	2.0	2.0	1.9		
	Tex.	1.7	2.4	1.6	1.5	1.4	2.1	1.6	1.8	1.9		
	Tex.	2.4	2.8	2.3	2.7	2.6	2.3	2.2				
	Tex.	3.4	3.1	3.4	3.5	3.7	3.3	4.4	3.1	3.1		

TABLE 8

PROJECT AND SECTION PSI DATA — SECONDARY FLEXIBLE PAVEMENTS

Project		Project PSI	PSI for Individual 500-ft Sections									
			1	2	3	4	5	6	7	8	9	10
AASHO	Conn.	1.6	1.1	2.0	1.4	2.2	1.2	1.9				
Region	N. H.	1.7	1.9	1.3	1.5	2.5	1.4	2.4				
1	N. J.	1.2	1.0	1.2	1.2	1.4	1.0	1.6				
	N. Y.	0.9	0.5	1.0	0.9	0.8	0.6	0.5				
	R. I.	1.0	0.5	1.2	0.8	1.2	0.8	1.8				
AASHO	Fla.	1.2	1.4	1.3	0.8	1.4	1.0	1.2	1.2	1.2		
Region	Ga.	1.7	1.9	1.8	1.8	2.2	2.3	1.3	1.5	1.3		
2	Ky.	2.2	1.8	2.4	2.1	2.3	2.4	3.0				
	Ky.	2.5	1.9	2.4	2.2	2.9	3.3	3.3				
	La.	2.2	2.0	2.2	2.1	2.5	2.6	2.2				
	Miss.	1.8	1.8	1.8	1.8	2.0	2.0	1.8	2.0	1.6		
	W. Va.	1.3	1.5	1.6	1.1	1.0	1.1	2.0				
AASHO	Mich.	2.9	1.6	3.1	3.8	3.5	3.3	3.4	4.1	3.8		
Region	Ohio	2.2	2.3	2.5	2.2	1.9	3.3	2.7	1.5	2.6		
3	Ohio	2.5	3.0	3.1	2.6	2.4	2.5	2.7	2.2	2.0		
	Wis.	2.1	2.8	2.2	2.8	1.8	1.8	2.2	2.1	1.8		
AASHO	Ariz.	2.0	2.1	1.9	1.8	1.9	2.1	2.0				
Region	Cal.	2.1	2.3	2.4	1.8	1.9	2.3	2.4	2.0	2.0		
4	Idaho	2.3	1.9	2.5	2.1	3.0	2.1	2.9				
	Wyo.	1.8	1.6	2.1	1.9	1.7	1.9					
	Tex.	3.6	3.4	3.7	3.5	2.7	4.8	4.7	3.1	4.6		
	Tex.	2.2	2.0	2.3	2.6	2.1	2.3	2.0				

TABLE 9

PROJECT MEASUREMENTS: SLOPE VARIANCE AND CRACKING AND PATCHING — PRIMARY RIGID PAVEMENTS

Project		Slope Variance	Cracking and Patching
AASHO	N. H.	31	16
Region	N. J.	67	30
1	N. J.	17	15
	N. J.	36	54
	Pa.	23	42
	Pa.	10	20
	Pa.	18	31
	Vt.	57	401
AASHO	Ark.	16	15
Region	Ark.	15	45
2	Fla.	9	4
	Ga.	17	11
	Ga.	10	22
	La.	21	110
	La.	31	92
	S. C.	8	27
	S. C.	14	35
	Tenn.	37	156
	Va.	18	31
	Va.	18	46
	W. Va.	27	34
AASHO	Ill.	23	199
Region	Ill.	52	112
3	Iowa	12	39
	Iowa	13	82
	Iowa	21	1
	Kan.	15	65
	Kan.	25	83
	Mich.	27	57
	Mich.	22	68
	Minn.	27	52
	Minn.	16	51
	Neb.	16	94
	Neb.	16	51
	Okla.	24	78
	Okla.	24	66
	Okla.	27	58
	Wis.	73	204
	Wis.	44	145
AASHO	Cal.	37	56
Region	Cal.	16	98
4	Colo.	27	70
	Ore.	15	559
	Tex.	7	23
	Tex.	14	183
	Tex.	73	248
	Tex.	31	235

TABLE 10

PROJECT MEASUREMENTS: SLOPE VARIANCE AND CRACKING AND PATCHING — PRIMARY FLEXIBLE PAVEMENTS

Project		Slope Variance	Cracking and Patching
AASHO	Conn.	29	277
Region	N. H.	42	109
1	N. H.	31	211
	N. Y.	46	104
	N. Y.	67	217
	N. Y.	71	637
	Pa.	77	616
	Pa.	84	261
	Vt.	22	386
	Vt.	25	338
AASHO	Ark.	53	217
Region	Ark.	44	244
2	Fla.	14	31
	Fla.	32	2
	Ky.	32	311
	La.	4	18
	Miss.	29	138
	Miss.	12	135
	Miss.	33	69
	S. C.	20	80
	S. C.	38	44
	S. C.	58	258
	S. C.	40	93
	Tenn.	34	196
	Va.	74	768
	Va.	24	30
	Va.	5	312
AASHO	Ind.	52	337
Region	Ind.	48	477
3	Kan.	20	617
	Kan.	17	318
	Kan.	37	309
	Minn.	24	806
	Neb.	33	673
	Neb.	35	835
	Ohio	17	62
	Ohio	14	177
	S. Dak.	28	790
	S. Dak.	44	552
AASHO	Ariz.	16	465
Region	Ariz.	19	820
4	Cal.	17	369
	Cal.	6	209
	Cal.	8	546
	Cal.	14	298
	Colo.	37	766
	Colo.	57	926
	Idaho	13	265
	Ore.	23	48
	Ore.	25	112
	Wyo.	18	704
	Wyo.	36	567
	Tex.	41	331
	Tex.	19	73
	Tex.	6	17

TABLE 11

PROJECT MEASUREMENTS: SLOPE VARIANCE AND CRACKING AND PATCHING — SECONDARY FLEXIBLE PAVEMENTS

Project		Slope Variance	Cracking and Patching
AASHO	Conn.	47	242
Region	N. H.	39	515
1	N. J.	65	774
	N. Y.	130	201
	R. I.	75	751
AASHO	Fla.	71	532
Region	Ga.	53	23
2	Ky.	21	267
	Ky.	17	137
	La.	24	118
	Miss.	40	239
	W. Va.	63	368
AASHO	Mich.	10	100
Region	Ohio	23	322
3	Ohio	16	260
	Wis.	25	552
AASHO	Ariz.	30	410
Region	Cal.	24	536
4	Idaho	20	290
	Wyo.	37	407
	Tex.	4	101
	Tex.	24	357

TABLE 13

PROJECT MEASUREMENTS: RUT DEPTH — SECONDARY FLEXIBLE PAVEMENTS

Project		Rut Depth (in.)
AASHO	Conn.	0.27
Region	N. H.	0.19
1	N. J.	0.17
	N. Y.	0.34
	R. I.	0.37
AASHO	Fla.	0.25
Region	Ga.	0.12
2	Ky.	0.19
	Ky.	0.16
	La.	0.12
	Miss.	0.11
	W. Va.	0.22
AASHO	Mich.	0.17
Region	Ohio	0.09
3	Ohio	0.11
	Wis.	0.10
AASHO	Ariz.	0.15
Region	Cal.	0.08
4	Idaho	0.14
	Wyo.	0.14
	Tex.	0.15
	Tex.	0.15

TABLE 12

PROJECT MEASUREMENTS: RUT DEPTH — PRIMARY FLEXIBLE PAVEMENTS

Project		Rut Depth (in.)
AASHO	Conn.	0.16
Region	N. H.	0.19
1	N. H.	0.11
	N. Y.	0.23
	N. Y.	0.31
	N. Y.	0.25
	Pa.	0.26
	Pa.	0.28
	Vt.	0.16
	Vt.	0.16
AASHO	Ark.	0.14
Region	Ark.	0.19
2	Fla.	0.27
	Fla.	0.26
	Ky.	0.27
	La.	0.12
	Miss.	0.15
	Miss.	0.14
	Miss.	0.15
	S. C.	0.09
	S. C.	0.13
	S. C.	0.22
	S. C.	0.18
	Tenn.	0.15
	Va.	0.30
	Va.	0.28
	Va.	0.24
AASHO	Ind.	0.17
Region	Ind.	0.13
3	Kan.	0.14
	Kan.	0.14
	Kan.	0.33
	Minn.	0.16
	Neb.	0.16
	Neb.	0.36
	Ohio	0.17
	Ohio	0.10
	S. Dak.	0.14
	S. Dak.	0.15
AASHO	Ariz.	0.15
Region	Ariz.	0.18
4	Cal.	0.18
	Cal.	0.20
	Cal.	0.14
	Cal.	0.06
	Colo.	0.17
	Colo.	0.19
	Idaho	0.39
	Ore.	0.16
	Ore.	0.19
	Wyo.	0.15
	Wyo.	0.11
	Tex.	0.13
	Tex.	0.07
	Tex.	0.08

TABLE 14

PROJECT MEASUREMENTS: FAULTING AND SCALING — PRIMARY RIGID PAVEMENTS

Project		Faulting (in./1,000 ft)	Scaling (ft^2/1,000 ft^2)
AASHO	N. H.	4.2	0
Region	N. J.	3.5	0
1	N. J.	1.3	0
	N. J.	1.7	0
	Pa.	1.8	4
	Pa.	1.8	7
	Pa.	0.9	333
	Vt.	6.1	0
AASHO	Ark.	2.2	37
Region	Ark.	2.3	54
2	Fla.	4.2	0
	Ga.	0.6	0
	Ga.	0.9	0
	La.	3.4	0
	La.	8.0	0
	S. C.	2.3	0
	S. C.	0.2	0
	Tenn.	6.8	104
	Va.	2.2	0
	Va.	0.0	0
	W. Va.	0.7	0
AASHO	Ill.	1.2	0
Region	Ill.	3.9	24
3	Iowa	1.3	0
	Iowa	2.1	0
	Iowa	8.2	0
	Kan.	3.2	0
	Kan.	1.6	0
	Mich.	3.3	7
	Mich.	0.7	0
	Minn.	2.3	2
	Minn.	4.2	0
	Neb.	1.5	0
	Neb.	2.0	0
	Okla.	5.3	0
	Okla.	3.3	0
	Okla.	4.6	0
	Wis.	0.7	9
	Wis.	1.7	16
AASHO	Cal.	4.5	0
Region	Cal.	5.5	0
4	Colo.	4.2	5
	Ore.	3.0	0
	Tex.	1.8	0
	Tex.	0.0	0
	Tex.	0.0	35
	Tex.	0.0	8

Use of Loadometer Data In Designing Pavements For Mixed Traffic

JAMES F. SHOOK, LOUIS J. PAINTER, and THEODORE Y. LEPP,
The Asphalt Institute

• MOST procedures now used for designing pavements do not consider directly the effect of numerous applications of loads of different magnitude. The first effort to design for the effects of mixed traffic was made by California in 1942. Subsequently, Kentucky and other states, and AASHO in its recently completed Interim Design Guide, have incorporated this feature. Other methods consider designing only for prevention of overstress due to single applications of a given load, or for "unlimited" repetitions of a design load.

A tremendous increase in both the number and weight of vehicles using the highways since World War II makes it necessary to evaluate the effect of mixed traffic on pavement design and performance. The AASHO Road Test had as one of its primary purposes the determination of the relative effects of loads of different magnitude. One outgrowth of the AASHO Road Test has been a renewed interest in techniques for designing pavements for mixed traffic.

One of the greatest drawbacks to proper applications of data such as those from the AASHO Road Test has been a shortage of information concerning the number and magnitude of the axle applications to which highways are actually subjected.

Most states are now making truck weight and loadometer studies. Data from these studies provide estimates of the number and magnitude of axle loads being applied to the major highway systems. However, for many highways and streets, sufficient data are not available. Limited studies of some of the available data are reported in this paper. The use of loadometer data in designing pavements for mixed traffic is discussed.

Results of truck weight and loadometer studies from Maryland, Ohio, Kansas, Missouri, Arizona, North Carolina, Washington and Mississippi have been collected and studied. Information was available for Interstate rural, Interstate urban, primary rural, primary urban and other classes of highway. Table 1 is a typical data report sheet, following Bureau of Public Roads practices. Each sheet summarizes data from several individual loadometer stations, usually collected over a 24-hr period. Axle weights are separated into categories by vehicle type and axle configuration (single or tandem).

It is possible, by using equivalency factors derived for some given design procedure (that is, California, AASHO Design Guide, or, as used in this paper, a method developed by the Asphalt Institute) to combine the effects of the various axle loads into a single summary statistic. Equivalent 18-kip single-axle applications are used in the paper.

A statistical analysis of the data from 7 states has shown that significant differences in equivalent applications for a given vehicle type exist between states and between classes of highway. Thus, one axle-weight distribution should not be used to represent all traffic in any state or large geographical area. Discussion of the significance of this, relative to pavement design, will be made later in the paper. It is pointed out also, as a consequence, that there is a need for valid and more complete data about the number and magnitude of axle applications to which pavements are being subjected.

Paper sponsored by Committee on Flexible Pavement Design.

TABLE 1

EXTRACT FROM TYPICAL 1961 LOADOMETER SURVEY REPORT
STATE OF MARYLAND

TABLE W-4 Other FA Primary Rural—Number of axle loads of various magnitudes of loaded and empty trucks and truck combinations of each type weighed and the probable number of such loads of each general type and of all types counted at 8 loadometer stations during the period from July 10, 1961 to August 1, 1961 compared to corresponding data for 1960*.

Axle Loads in Pounds	Single Unit Trucks				Trac. Semitrailer Comb.			Total All Trucks and Comb. Prob. No.
	Panel and Pickup Under 1 Ton	Other 2-Axle 4-Tired	Other 2-Axle 6-Tired	3-Axle	3-Axle	4-Axle	5-Axle or More	
(1)	(2)	(4)	(6)	(8)	(12)	(14)	(16)	(30)
SINGLE AXLES								
Under 3,000	225	79	62		1			9733
3,000 - 6,999	43	108	1038	64	239	332	2	10092
7,000 - 7,999		1	122	17	89	278	2	2092
8,000 - 11,999		2	247	49	224	762	14	5258
12,000 - 15,999			102	26	126	121	5	1540
16,000 - 17,999			44	5	50	101		805
18,000 - 19,999			28	1	41	181		996
20,000 - 21,999			19		30	173		878
22,000 - 22,399			3		7	25		138
22,400 - 23,400[1]			2		11	28		158
23,401 - 23,999			2		8	11		81
24,000 - 25,999					10	11		78
26,000 - 29,999			5		13	5		88
30,000 - 34,999					2			7
35,000 - 39,999					1			3
Total single axles weighed	268	190	1674	162	852	2028	23	
Total single axles counted	10418	1600	8144	793	2883	8020	47	31947
TANDEM AXLES								
Under 6,000						1		4
6,000 - 11,999				25		203	8	942
12,000 - 17,999				43		181	10	947
18,000 - 23,999				11		93	7	436
24,000 - 29,999				18		133	9	632
30,000 - 31,999				10		85	2	389
32,000 - 33,999				9		106	5	473
34,000 - 35,999				8		93	1	409
36,000 - 37,999				7		57	4	267
38,000 - 39,999				3		35		153
40,000 - 41,000[2]				2		12		57
41,001 - 41,999				3		5		35
42,000 - 43,999				1		6		29
44,000 - 45,999				4		3		32
46,000 - 49,999				7		1		38
50,000 - 54,999				7				34
55,000 - 59,999				3				15
60,000 - 64,999				1				5
65,000 - 69,999								
Total tandem axles weighed				162		1014	46	
Total tandem axles counted				793		4010	94	4897
ALL AXLES								
Under 3,000	225	79	62	2	1	4		9759
3,000 - 6,999	43	108	1038	139	239	897	29	12749
7,000 - 7,999		1	122	51	89	390	9	2716
8,000 - 11,999		2	247	102	224	1029	31	6607
12,000 - 15,999			102	71	126	576	26	3603
16,000 - 17,999			44	42	50	436	13	2339
18,000 - 19,999			28	22	41	388	7	1931
20,000 - 21,999			19	11	30	234		1173
22,000 - 22,399			3	2	7	38		199
22,400 - 23,400[1]			2	11	11	32		228
23,401 - 23,999			2	3	8	12		99
24,000 - 25,999				10	10	14		138
26,000 - 29,999			5	18	13	6		180
30,000 - 34,999				2	2			17
35,000 - 39,999					1			3
Total axles weighed	268	190	1674	486	852	4056	115	
Total axles counted	10418	1600	8114	2379	2883	16040	235	41741
Total vehicles counted	5209	800	4057	793	961	4010	47	15898

[1] State legal limit: single axle 22,400 lb plus 1,000-lb tolerance (non-statutory).
[2] State legal limit: tandem axles 40,000 lb plus 1,000-lb tolerance (non-statutory).
*Corresponding 1960 data deleted from this extract because of space limitations.

Recognizing the fact that significant differences exist between certain traffic classifications, it is still possible to reduce a complicated array of data from loadometer studies to simplified factors for converting numbers of vehicles of each type to equivalent applications. Procedures for deriving such factors from the loadometer data are shown. Further simplifications permitting the conversion of percent trucks to total equivalent applications for use in design are also made.

Results of state loadometer studies are shown to be of help to city, county and other engineers who do not have facilities for making their own surveys. By using factors derived from state highway loadometer surveys and traffic counts (by vehicle type), it is possible for these engineers to design pavements based on reasonable estimates of mixed traffic.

EQUIVALENT APPLICATIONS CONCEPT

The concept of using equivalent applications to reduce mixed traffic to a single parameter for use in pavement design is not new. Hveem and Carmany (1) postulated in 1948 that the required thickness of a flexible pavement was proportional to the logarithm of the number of load repetitions to which the pavement would be subjected, and that repetitions for mixed traffic could be expressed as repetitions of an equivalent 5,000-lb wheel load. Using equivalent wheel load (EWL) constants adopted by California in 1942, and results of loadometer studies and traffic counts, a procedure was developed for designing flexible pavements which, with modifications, is still in use.

Sherman (2) reported in 1958 on changes in the California wheel-load factors for computing EWL, based on continued highway experience and data from test tracks. Hveem and Sherman (3) proposed additional modifications in 1962 after a study of the results of the AASHO Road Test. Present California procedures (4) make full use of the EWL concept for designing flexible pavements, and for selecting slab thicknesses and minimum strengths of cement-treated base for rigid pavements.

As explained by Sherman (2), one application of a given load (L) is equivalent, in "terms of potential damage" to the pavement, to some number of applications of a base load. Using a base wheel load of 5,000 lb, the EWL constant is thus defined as the number of repetitions of a 5,000-lb wheel load divided by the number of repetitions of load L which causes the same amount of damage to a pavement of constant thickness.

EWL constants used by California have been defined by the following relationships:

$$1942 \text{ EWL constant} = 2^{L-5}$$
$$1957 \text{ EWL constant} = (L/5)^{5.0}$$
$$1962 \text{ EWL constant} = (L/5)^{4.2}$$

As a result of work with AASHO Road Test data, Scrivner (5) and Scrivner and Duzan (6) have published studies of the concepts involved in combining effects of applications of axle loads of different magnitude. Scrivner concluded that the shape of the deterioration (as measured by decrease in present serviceability index) vs applications curve is important in combining effects of mixed traffic. Thus, if the shape of the curve is a function of design and load (as it is in the AASHO Road Test equations, 7), the equivalency of different axle loads applied to a pavement is a function of the order in which they are applied. The equivalent applications concept assumes that the effects of different axle loads are independent of the order in which the loads are applied.

The equivalent applications concept was shown by Scrivner and Duzan (6) to be essentially the same as the Scrivner mixed-traffic theory for flexible pavements having D = 4.0 [$D = 0.44D_1 + 0.14D_2 + 0.11D_3$ (7); D_1, D_2 and D_3 = thicknesses in inches of surfacing, base and subbase, respectively.] or thicker, and for rigid pavements having slab thicknesses of 7.0 in. or greater.

The equivalent applications concept embodies these assumptions:

1. Load effects are independent of the shape of the performance vs load applications curve.

2. Load effects are independent of the order in which loads of different magnitude are applied.

3. The effect of a single application of load L_i may be expressed as a constant times the effect of some base load L_b.

4. Equivalency is expressed as the ratio of the number of applications of L_b required to produce the same performance as a single application of L_i.
5. Pavement thickness required to maintain a given level of performance is a function of the sum of the applications of mixed axle loads expressed as equivalent applications of L_b.

These assumptions are hypothetical. As far as the authors know, there is no direct experimental evidence to confirm or deny them.

The above statements imply that equivalency factors are dependent on the mathematical form of the relationship between design and load applications. This will be illustrated.

In the original work in California, the equivalency relationship was first assumed, and the general design relationship was built around this relationship. As indicated above, modifications in the equivalency relationship were later made in order to adjust the entire design relationship. Work by the AASHO Committee on Design (8, 9, 10) was based on the assumption that load equivalency factors were defined by the relationship between design on one hand and number of applications and magnitude of load on the other. Equivalency factors based on deflection measurements, equal subgrade stresses or other than some direct measure of pavement performance are not considered to be within the equivalent applications concept.

Derivation of load equivalency factors can be illustrated by the following. It is assumed that the thickness required to maintain a given level of performance is defined by the relationship

$$\log t = a + b \log W_i + c \log L_i \tag{1}$$

in which

t = total thickness of pavement;
W_i = applications of load L_i;
L_i = single-axle load; and
a, b and c = factors which may or may not be functions of L or t.

By replacing $a + c \log L_i$ with a', Eq. 1 may be reduced to the following:

$$\log t = a' + b \log W_b$$

in which

$W_b = \Sigma (L_i/L_b)^{c/b} W_i$ over all loads.

Individual load factors are equal to $W_b/W_i = (L_i/L_b)^{c/b}$ and may be tabulated for convenience of use.

The 1957 California factor had the form $W_b/W_i = (L_i/L_b)^{c/b} = (L_i/5)^{5.0}$.

Shook and Finn (11) derived the following relationships for flexible pavements from AASHO Road Test data:

$$T = -8.50 + 5.53 \log W_{18} \tag{2}$$

in which

T = thickness factor, defined as a linear combination of surfacing, base and subbase thicknesses in inches;
$T = 2.0D_1 + 1.0D_2 + 0.75D_3$;
$W_{18} = \Sigma W_L F_L$;
W_{18} = equivalent 18-kip single-axle applications required to reduce present serviceability of pavement to 2.5 level;
W_L = applications of load L;
F_L = load factor for load L;
$F_L = 10^{0.12088(L-18)}$; and
L = single-axle load or ($1.14 \div 2 \times$ tandem-axle load), in kips.

The basic relationship is of the form

$$T = a + b \log W + cL$$

which can be reduced to

$$T - a = b \log W_b + cL_b = b \log W_i + cL_i$$

$$\left(\frac{W_b}{W_i}\right)^b = \frac{10^{cL_i}}{10^{cL_b}} = 10^{c(L_i - L_b)}$$

$$\frac{W_b}{W_i} = 10^{c/b\,(L_i - L_b)} = F_L$$

Figure 1 shows the relationship between a set of thickness-applications curves for individual loads and the load factors derived from them. The Shook and Finn design relationship (Eq. 2) consists of a set of parallel straight lines; hence, the load factors are independent of design. A set of parallel straight lines on a log-log plot (for example, Eq. 1) would also result in load factors independent of design. Load factors from design curves that are not linear or parallel would depend on design. Such is the case with those of the AASHO Design Guides (9, 10).

Obviously, these load factors are not all identical, either in mathematical form or in value (Table 2). California factors have been recomputed for an 18,000-lb base load; otherwise, they are the same as previously indicated. AASHO Design Guide factors are given for p = 2.5 and D = 5.0 for flexible pavements, and D = 9.0 for rigid pavements. They will vary somewhat with the actual design used.

Evaluation of the effects of the differences among load factors can be made by comparing designs computed for realistic traffic situations. It is not within the scope of the paper to discuss this, but it should be borne in mind that designs for mixed traffic usually depend more on the character of the design-applications relationship than on the magnitude of the load factors used.

COMPUTATION OF EQUIVALENT APPLICATIONS

Table 1 is an extract from a typical loadometer survey report. Data from 1960 and certain other values have been deleted because of space limitations. The combined results of one 24-hr survey made at each of eight loadometer stations on Maryland Federal-aid primary rural highways (excluding Interstate) in 1961 are given.

Data from similar loadometer studies have been reduced to summary statistics by computing separate factors for each vehicle type and a weighted mean factor for all trucks as a group. The vehicle factor is the long-term average number of equivalent 18-kip single-axle applications contributed by one passage of a given vehicle of any

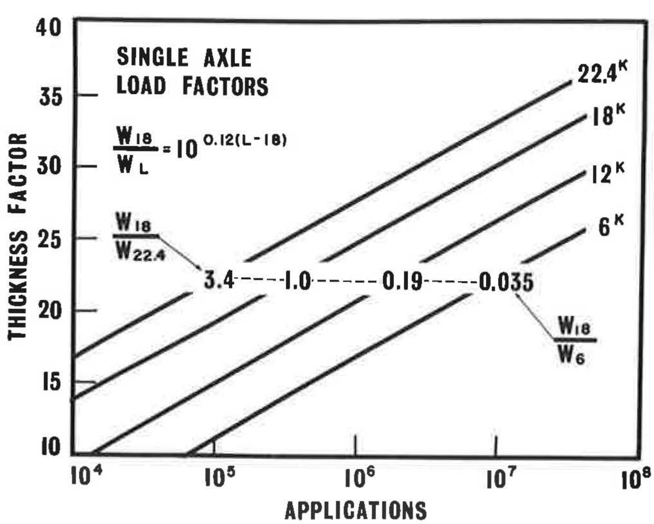

Figure 1. Load factors (Shook and Finn).

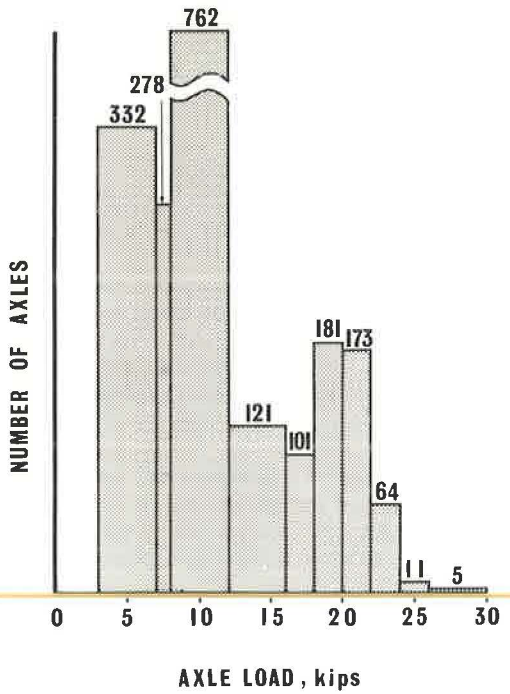

Figure 2. Distribution of single-axle loads (1961 Maryland OR).

particular type. The weighted mean truck factor is the long-term average number of equivalent 18-kip single-axle applications contributed by one passage of a truck of any type.

The design procedure used for computing equivalent applications and the various factors are those described by Shook and Finn (11). Their thickness design chart is reproduced (see Fig. 3), and load factors are given in Table 3. All computations followed the procedure which would be used in making a study for design purposes except that passenger vehicles, autos or buses, were not included. All comparisons were, therefore, made for trucks only.

It should be stated here that similar studies can be made using other design procedures, for example, the new AASHO Design Guides. Values will certainly be different, and conclusions possibly so. However, one purpose of this paper is to shed light on the many problems involved in pavement design for mixed traffic, and the foregoing is an example of one problem.

TABLE 2

EQUIVALENT AXLE LOAD FACTORS[a]

Single-Axle Load (kips)	California[b] 1942 2^{L-18}	California[b] 1957 $\left(\frac{L}{18}\right)^5$	California 1962 $\left(\frac{L}{18}\right)^{4.2}$	Shook and Finn $10^{0.12(L-18)}$	AASHO Flexible[c] D = 5.0	AASHO Rigid[c] D_2 = 9.0
2	0.000	0.000	0.000	0.012	0.0002	0.0002
4	0.008	0.001	0.002	0.020	0.003	0.002
6	0.016	0.004	0.010	0.035	0.01	0.01
8	0.31	0.017	0.033	0.062	0.03	0.03
10	0.062	0.053	0.085	0.108	0.09	0.08
12	0.125	0.132	0.180	0.188	0.19	0.18
14	0.250	0.286	0.348	0.328	0.36	0.34
16	0.500	0.556	0.610	0.573	0.62	0.60
18	1.00	1.00	1.00	1.00	1.00	1.00
20	2.00	1.69	1.56	1.74	1.51	1.57
22	4.00	2.72	2.32	3.04	2.18	2.34
24	8.00	4.23	3.35	5.31	3.03	3.36
26	16.00	6.30	4.68	9.27	4.09	4.67
28	32.00	9.10	6.40	16.2	5.39	6.29
30	64.00	12.8	8.55	28.2	6.97	8.28

[a] Load factors are given as ratios of an 18-kip single-axle load.
[b] Axle loads less than 10 kips were not considered in computation of EWL for design of pavements.
[c] Pavement Design Guide.

An example of a typical axle-load distribution is given in Table 4. Figure 2 is a frequency distribution plot for this problem. The distribution appears to be a combination of two overlapping distributions, one composed of steering axles and another of rear axles, from both loaded and unloaded trucks. Information as to the distribution within axle-load groups was not studied in this report and is not available in the data reported to the Bureau of Public Roads.

If the distribution in Table 4 represented all of the axles for a given design situation, the total equivalent 18-kip single-axle applications would be computed from $W_{18} = \Sigma$ (number of axles per group × load factor for the mean load of each group).

To compute the equivalence factor for any particular vehicle, a similar procedure was used. The total equivalent applications were first computed for each truck type, and an average was obtained by dividing the total by the number of that type truck weighed. Using the problem in Table 4 as an example, the total equivalent applications contributed by the axles are 2,143. The average per axle passage is 0.705, and the average per vehicle passage is 2.11.

For design purposes, the contribution of 4-axle tractor semitrailer trucks to the total applications would be 2.11 times the number of these vehicles expected during the design life.

TABLE 3

LOAD FACTORS (SHOOK AND FINN)

Single Axles		Tandem Axles	
Axle Load (kips)	Factor[a]	Axle Load[b] (kips)	Factor[a]
2	0.01164	4	0.0126
3	0.01538	8	0.0237
4	0.02030	12	0.0448
6	0.03545	16	0.0843
7	0.04681	20	0.1590
8	0.06183	24	0.3005
10	0.1080	28	0.5650
12	0.1882	32	1.069
14	0.3285	36	2.017
16	0.5731	40	3.814
18	1.000	44	7.175
20	1.745	48	13.45
22	3.045	52	25.34
22.4	3.403		
24	5.312		
26	9.269		
28	16.17		
30	28.22		

[a] Load factor = $10^{0.12088(L-18)}$; L = single- or 1.14 ÷ 2 × tandem-axle load.
[b] Gross load on a set of tandem axles spaced approximately 40 in. apart.

Similar factors can be computed for all vehicle types. By using observed vehicle distributions, plus appropriate growth factors, estimates can be made of the total equivalent applications expected on the class of highway being studied.

COMPARISONS AMONG HIGHWAY SYSTEMS

Loadometer data from 8 states have been used for making comparisons among different highway systems. States were selected to provide samples from different areas of the United States. However, the samples do not provide means for generalization to the country as a whole. They do provide a preliminary look at some of the problems to be encountered in any future attempt at such a generalization.

Tables 5, 6, 7, 8 and 10 summarize much of the pertinent information gained from the studies of the data from the 8 states. Tables 5 through 7 contain summarizations of data and computed vehicle factors for 7 of the 8 states. Separate tabulations and computations are included for several types of highways within each state. Passenger vehicles (autos and buses) are not included.

A description of the types of highways, number of loadometer stations, number of vehicles counted and weighed, and the number of hours during which data were secured are given in Table 5.

Vehicle factors, as computed previously in the discussion of Table 4, are given in Table 6 for each highway shown in Table 5. Vehicle factors for each truck type and the weighted average factor per truck are included. For two states it was necessary to use

TABLE 4

COMPUTATION OF EQUIVALENT APPLICATIONS FOR 4-AXLE TRACTOR SEMITRAILER COMBINATIONS (1961 Maryland FAPR)

Axle Load Group	Mean Axle Load	Load Factor	No. Axles	Percent Axles	Equivalent Applications
		SINGLE AXLES			
Under 3,000	2,000	0.01165	0	0	0
3,000 - 6,999	5,000	0.02672	332	16.4	8.87
7,000 - 7,999	7,500	0.0538	278	13.7	14.96
8,000 - 11,999	10,000	0.108	762	37.6	82.30
12,000 - 15,999	14,000	0.3285	121	6.0	39.75
16,000 - 17,999	17,000	0.757	101	5.0	76.50
18,000 - 19,999	19,000	1.321	181	8.9	239.10
20,000 - 21,999	21,000	2.305	173	8.5	398.76
22,000 - 22,399 22,400 - 23,400 23,401 - 23,999	23,000	4.019	64	3.2	257.22
24,000 - 25,999	25,000	7.017	11	0.5	77.19
26,000 - 29,999	28,000	16.17	5	0.2	80.85
				Total	1,275.50
Total single axles weighed			2,028		
Total single axles counted			8,020		
		TANDEM AXLES			
Under 6,000	3,000	0.0108	1	0.10	0.0108
6,000 - 11,999	9,000	0.0278	203	20.02	5.64
12,000 - 17,999	15,000	0.0719	181	17.85	13.01
18,000 - 23,999	21,000	0.186	93	9.17	17.30
24,000 - 29,999	27,000	0.484	133	13.12	64.37
30,000 - 31,999	31,000	0.912	85	8.38	77.52
32,000 - 33,999	33,000	1.253	106	10.46	132.82
34,000 - 35,999	35,000	1.721	93	9.17	160.05
36,000 - 37,999	37,000	2.363	57	5.62	134.69
38,000 - 39,999	39,000	3.246	35	3.45	113.61
40,000 - 41,000	40,500	4.113	12	1.18	49.36
41,000 - 42,000	41,500	4.827	5	0.49	24.14
42,000 - 43,999	43,000	6.125	6	0.59	36.75
44,000 - 45,999	45,000	8.412	3	0.30	25.24
46,000 - 49,999	48,000	13.45	1	0.10	13.45
				Total	867.96
				Grand total	2,143.46
Total tandem axles weighed			1,014		
Total tandem axles counted			4,010		
				Avg. per axle	0.705
				Avg. per vehicle	2.114

TABLE 5

SAMPLE INFORMATION (1960 Data)

State	Type of Highway	No. Stations	No. Vehicles[a] Counted	No. Vehicles[a] Weighed	Percent[b] Weighed	Time (hr)
Ariz.	IR[c]	7	3,309	520	15.7	8
	IU[d]	1	2,427	194	8.0	
	OFU[e]	1	1,257	104	8.3	
Kan.	MR[f]	12	3,948	1,277	32.3	8
	OU[g]	2	1,531	124	8.1	
Md.	IR[c]	5	17,991	2,497	13.9	24
	IU[d]	1	1,322	280	21.2	
	OFR[h]	8	15,274	2,949	19.3	
	OFU[e]	1	1,784	183	10.3	
	FSR[i]	1	139	72	51.8	
Mo.	MR[f]	22	33,186	11,668	35.2	16-24
	OU[g]	4	11,788	2,289	19.4	
N. C.	IR[c]	8	5,153	3,439	66.7	8
	OR[j]	17	8,782	6,951	79.2	
Ohio	IR[c]	3	5,909	888	15.0	24
	OR[j]	7	10,997	1,885	17.1	
Wash.	IR[c]	2	1,970	620	31.5	24
	OMR[j]	5	4,637	2,447	52.8	
	OU[g]	1	2,187	466	21.3	

[a]Excluding passenger vehicles.
[b]Varies by vehicle type.
[c]Interstate rural.
[d]Interstate urban.
[e]Other Federal-aid primary urban.
[f]All main rural.
[g]Urban.
[h]Other Federal-aid primary rural.
[i]Federal-aid secondary (state).
[j]Other main rural.

data from the "all-axle" categories in substitution for separate single- and tandem-axle tabulations. For the design procedure used, it was sufficiently accurate to treat each set of tandem axles as two single axles. However, this procedure would not apply as a general rule, for example, to either of the AASHO Interim Guides.

The weighted mean factor per truck was computed by weighting each vehicle factor by its proportionate share of the total vehicles counted during the loadometer study period. The appropriate percentages from the loadometer study reports are given in Table 7. The proportion of the average contributed by each truck type is given in Table 8.

The number of equivalent applications contributed, on the average, by the passage of one truck is influenced by the distribution of axles within each truck type. Thus the information given in both Tables 6 and 7 has important bearing on the values in Table 10, and on any comparisons made among types of highway or states.

Design thicknesses are influenced by the same variables. An example will indicate to what extent such influences may be present. Assuming an estimated 1,000 trucks per day, or 7,300,000 trucks in 20 years, the designs in Table 9 may be selected from Figure 3 depending on the Interstate rural highway system being considered. Total equivalent applications were computed by multiplying 7,300,000 by the various factors. Similar computations made with other design procedures would not necessarily give the same thickness differentials, but would indicate similar important differences.

TABLE 6

VEHICLE FACTORS

(Equivalent Applications per Truck Passage, from Loadometer Data)

State	Type of Highway[a]	Single-Unit Trucks				Tractor Semitrailer Comb.			Comb. Plus Full Trailer			Weighted Mean per Truck
		Pickup	2-Axle 4-Tire	2-Axle 6-Tire	3-Axle	3-Axle	4-Axle	5-Axle or More	4-Axle or Less	5-Axle	6-Axle or More	
Ariz.	IR	0.0301	0.0384	0.0263	0.690	0.642	1.27	1.15	0.234	1.33	2.20	0.58
	IU	0.0286	0.0364	0.133	1.01	0.254	0.576	0.265	0.239	0.693	3.69	0.12
	OFU	0.0242	0.0233	0.0822	1.64	0.684	1.34	0.694	–	0.693	3.69	0.11
										Weighted average		0.34
Kan.	MR	–[b]	0.0273	0.238	0.428	0.627	1.06	0.611	0.944	0.585	–	0.35
	OU	–[b]	0.0307	0.202	0.384	0.854	1.24	0.832	0.944	–	–	0.13
										Weighted average		0.28
Md.	IR	0.0281	0.0411	0.797	0.994	1.01	2.45	1.14	–	–	–	1.54
	IU	0.0260	0.0422	0.928	1.57	1.22	2.21	1.18	–	–	–	1.02
	OFR	0.0283	0.0450	0.507	1.43	1.19	2.60	1.47	–	–	–	0.92
	OFU	0.0266	0.0374	0.238	0.855	0.502	1.99	–	–	–	–	0.22
	FSR	0.0278	0.0460	0.093	1.57	0.546	2.16	–	–	–	–	0.13
										Weighted average		1.19
Mo.	MR	0.0267	–[b]	0.238	0.327	0.560	0.876	0.644	0.283	–	–	0.37
	OU	0.0274	–[b]	0.169	0.416	0.289	0.749	0.511	0.283	0.378	–	0.20
										Weighted average		0.33
N. C.	IR[c]	0.0252	0.0355	0.132	0.575	0.383	0.749	0.760	–	–	–	0.28
	OR[c]	0.0247	0.0348	0.153	0.533	0.375	0.749	0.554	–	–	–	0.27
										Weighted average		0.27
Ohio	IR	0.0243	0.0404	0.189	0.331	0.665	1.42	1.32	0.753	1.35	0.425	0.93
	OR	0.0252	0.0429	0.148	0.374	0.595	1.05	1.38	2.15	1.83	0.950	0.55
										Weighted average		0.68
Wash.	IR[c]	0.0268	–[b]	0.098	0.131	0.471	0.357	1.06	0.535	1.03	0.864	0.39
	OMR[c]	0.0262	–[b]	0.174	0.346	0.638	0.713	1.61	0.535	1.03	0.864	0.51
	OU[c]	0.0250	–[b]	0.168	0.267	0.752	0.490	1.04	1.72	1.07	0.833	0.23
										Weighted average		0.49

[a] See notes, Table 5.
[b] Pickup, and 2-axle, 4-tire vehicles combined.
[c] Actual computations based on "all-axle" group.

TABLE 7

DISTRIBUTION OF COUNT BY TRUCK TYPE

(Percentages of Total Count Assigned to Each Vehicle Type, Based on Count Obtained During Loadometer Studies)

State	Type of Highway[a]	Single-Unit Trucks				Trac. Semitrailer Comb.			Comb. Plus Full Trailer		
		Pickup	2-Axle 4-Tire	2-Axle 6-Tire	3-Axle	3-Axle	4-Axle	5-Axle or More	4-Axle or Less	5-Axle	6-Axle or More
Ariz.	IR	38.56	0.85	11.30	1.78	8.73	7.95	23.24	0.30	6.74	0.55
	IU	56.03	6.76	22.66	3.30	2.51	1.65	4.33	0.33	2.35	0.08
	OFU	80.27	2.31	10.42	1.75	1.59	0.72	1.91	–	0.63	0.40
Kan.	MR	–[b]	43.56	20.79	1.82	7.73	15.51	8.59	1.87	0.13	–
	OU	–[b]	62.44	29.39	2.35	1.70	2.29	1.11	0.72	–	–
Md.	IR	14.94	2.14	18.21	1.41	11.50	51.45	0.35	–	–	–
	IU	27.39	2.87	31.16	6.13	8.55	23.60	0.30	–	–	–
	OFR	31.75	4.97	28.83	3.52	6.38	24.39	0.16	–	–	–
	OFU	47.31	9.36	32.85	3.64	2.97	3.87	–	–	–	–
	FSR	53.24	5.04	36.68	1.44	1.44	2.16	–	–	–	–
Mo.	MR	36.49	–[b]	20.99	2.56	8.41	20.45	11.04	0.06	–	–
	OU	44.29	–[b]	29.05	2.10	8.62	11.41	4.50	0.02	0.01	–
N. C.	IR[c]	21.37	15.10	30.33	4.07	4.33	24.66	0.14	–	–	–
	OR[c]	30.32	10.35	27.34	3.59	4.03	24.23	0.14	–	–	–
Ohio	IR	10.87	1.30	11.80	1.18	15.37	47.30	7.39	0.81	3.52	0.46
	OR	21.80	3.89	21.80	2.94	11.48	30.45	5.30	0.33	1.95	0.06
Wash.	IR[c]	32.69	–[b]	20.86	6.04	5.33	3.91	23.2	2.18	5.53	0.26
	OMR[c]	39.83	–[b]	14.90	11.43	3.17	2.16	22.6	1.41	4.42	0.08
	OU[c]	52.58	–[b]	25.74	2.38	3.02	4.71	8.83	1.28	1.37	0.09

[a] See notes, Table 5.
[b] Pickup, and 2-axle, 4-tire vehicles combined.
[c] Actual computations based on "all-axle" group.

TABLE 8

AMOUNT OF TOTAL EQUIVALENT APPLICATIONS ASSIGNED TO EACH VEHICLE TYPE
(Based on Count Obtained During Loadometer Surveys)

State	Type of Highway[a]	Single-Unit Trucks				Trac. Semitrail. Comb.			Comb. Plus Full Trailer			Total (Weighted Mean Factor per Truck)
		Pickup	2-Axle 4-Tire	2-Axle 6-Tire	3-Axle	3-Axle	4-Axle	5-Axle or More	4-Axle or Less	5-Axle	6-Axle or More	
Ariz.	IR	0.0116	0.0003	0.0297	0.0123	0.0560	0.1010	0.2669	0.0007	0.0896	0.0121	0.5802
	IU	0.0160	0.0025	0.0301	0.0333	0.0064	0.0095	0.0115	0.0008	0.0128	0.0015	0.1244
	OFU	0.0194	0.0005	0.0086	0.0287	0.0109	0.0096	0.0133	–	0.0038	0.0148	0.1096
Kan.	MR	–[b]	0.0119	0.0495	0.0078	0.0485	0.1644	0.0525	0.0177	0.0008	–	0.3464
	OU	–[b]	0.0192	0.0594	0.0090	0.0145	0.0284	0.0092	0.0068	–	–	0.1296
Md.	IR	0.0042	0.0009	0.1451	0.0140	0.1162	1.2605	0.0040	–	–	–	1.5449
	IU	0.0071	0.0012	0.2892	0.0962	0.1043	0.5216	0.0035	–	–	–	1.0231
	OFR	0.0090	0.0022	0.1462	0.0503	0.0759	0.6341	0.0024	–	–	–	0.9201
	OFU	0.0126	0.0035	0.0782	0.0311	0.0149	0.0770	–	–	–	–	0.2173
	FSR	0.0148	0.0023	0.0341	0.0226	0.0079	0.0467	–	–	–	–	0.1284
Mo.	MR	0.0097	–[b]	0.0499	0.0084	0.0471	0.1791	0.0711	0.0002	–	–	0.3655
	OU	0.0121	–[b]	0.0491	0.0087	0 0249	0.0855	0.0230	0.0001	0.00004	–	0.2034
N. C.	IR	0.0054	0.0054	0.0400	0.0234	0.0166	0.1847	0.0011	–	–	–	0.2766
	OR	0.0075	0.0036	0.0418	0.0191	0.0151	0.1815	0.0008	–	–	–	0.2694
Ohio	IR	0.0026	0.0005	0.0223	0.0039	0.1022	0.6717	0.0975	0.0061	0.0475	0.0020	0.9302
	OR	0.0055	0.0017	0.0323	0.0110	0.0683	0.3197	0.0731	0.0071	0.0357	0.0006	0.5469
Wash.	IR[c]	0.0088	–[b]	0.0204	0.0079	0.0251	0.0140	0.2459	0.0117	0.0570	0.0022	0.3912
	OMR[c]	0.0104	–[b]	0.0259	0.0395	0.0202	0.0154	0.3639	0.0075	0.0455	0.0007	0.5089
	OU[c]	0.0131	–[b]	0.0432	0.0064	0.0227	0.0231	0.0918	0.0220	0.0147	0.0007	0.2266

[a]See notes, Table 5.
[b]Pickup, and 2-axle, 4-tire vehicles combined.
[c]Actual computations based on "all-axle" group.

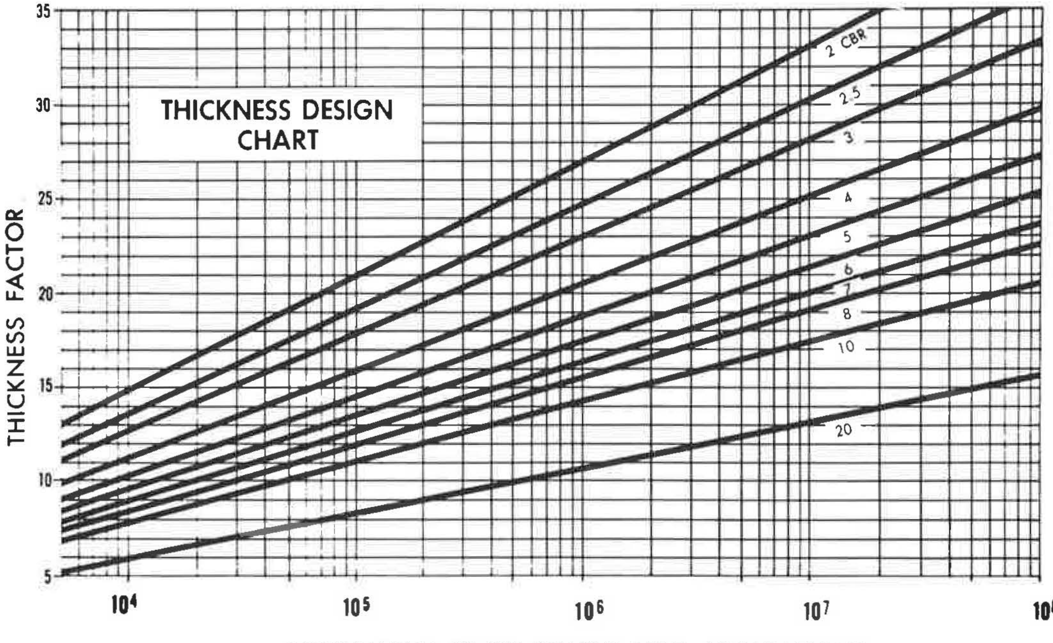

Figure 3. Thickness design chart.

Mean vehicle factors provide a convenient way in which to use results of loadometer studies for pavement design. For mainline pavements most design methods do not consider autos, and this simplifies computations. For city streets and highways where light vehicles make up more than 90 percent of the total vehicle count, it is likely that they will be an important factor. In this paper, however, their influence is neglected.

TABLE 9

DESIGN THICKNESS

State IR	Weighted Mean Factor per Truck	Total Equivalent Applications (millions)	T[a]	Design[a]
Md.	1.54	11.2	28.5	5-8-14
Ohio	0.93	6.8	27.5	5-8-13
Ariz.	0.58	4.3	26.5	5-8-11.5
Wash.	0.39	2.9	25.5	5-8-10
N. C.	0.28	2.1	25.0	5-8-9.5

[a] $T = 2.0D_1$ (surface) + D_2 (base) + $0.73D_3$ (subbase). CBR = 3.0 Design: surface-base-subbase, inches.

TABLE 10

DATA USED IN ANALYSIS OF 4-AXLE VEHICLE

State	No. of Axles	Avg. Equiv. 18-Kip Applic. per 4-Axle Veh.
Maryland	10,920	2.45
Ohio	3,848	1.29
Kansas	1,400	1.10
Mississippi	8,408	0.90
Missouri	18,872	0.88
North Carolina	10,952	0.75
Washington	544	0.64
Total	54,944	1.20
Total (excluding Md.)	44,024	0.89

As mentioned, variations in computed factors result from variations in both the axle-weight and the truck-type distributions. The vehicle factors in Table 6 show an expected difference in the number of equivalent applications contributed by one passage of different vehicles. However, these differences are not consistent for all states or highways. No doubt legal weight-limit variations, differences in the character of vehicle and load prevailing in a given area and many other factors account for these differences. An important point is that the differences exist and that they may have an influence on the pavement thickness selected for a given highway.

Similar points can be raised for the percentage distributions by truck type shown in Table 7.

It is interesting and significant (Table 6) that the vehicle factors for pickups and light trucks are essentially constant across all states and types of highway. On the other hand, the percentages for this type truck vary considerably (Table 7) and, in fact, are correlated to some extent with the weighted mean factor per truck. Thus the greatest influence on design is produced by 2-axle, 6-tire vehicles or larger.

The computations in Table 8 reflect the effects due both to the distribution of count and the distribution of axle weight. Here it appears that the 4-axle semitrailer combination contributes a significant amount, as much as one-half in many cases, to the

TABLE 11

EQUIVALENT 18-KIP SINGLE-AXLE APPLICATIONS

State	Per 4-Axle Semitrailer	Per Truck
Md.	2.45	1.19
Ohio	1.29	0.68
Kan.	1.10	0.28
Mo.	0.88	0.33
N. C.	0.75	0.27
Wash.	0.64	0.49

total weighted mean factor per truck. This is particularly so for Interstate rural highways. There does not appear to be any dominant vehicle in the urban classifications.

The possible influence of these variations on design has been mentioned. Since loadometer studies are expensive, it would be of great practical importance if the average loading pattern for each type of truck was reasonably constant throughout the United States. This would permit the simple counting of truck types in a traffic survey in lieu of full loadometer studies. The truck type counts could then be multiplied by their appropriate vehicle load factors to obtain as accurate a traffic-loading summary (equivalent 18-kip applications) as the full weighing study. It is not reasonable, of course, to expect that average truck axle weights are the same for all types of trucks.

The reported axle-load data for the 4-axle semitrailer trucks in 7 states were analyzed statistically to determine if there was, in fact, a single constant or average load factor which would accurately describe their loading pattern. The 4-axle vehicle was chosen because it was the principal contributor to total equivalent 18-kip axle loads in virtually all the states studied.

The statistical analysis showed highly significant variations between the various states. It was noted that Maryland had a higher (22.4 kip) legal single-axle load limit than the other states studied (18 kip). After eliminating the Maryland data, significant variations were still found.

A summary of the data used in this analysis is given in Table 10. Except for the substitution of Mississippi for Arizona, the states are the same ones previously discussed. Excluding the Maryland data, there is still a factor of two between the highest and lowest vehicle factors. About the same ratio also can be observed from Table 6 for the weighted mean truck factors. The statistical analysis showed that samples of 4-axle semitrailer trucks weighed in the several states could not be considered as samples from a single population. Although no statistical analysis was performed, it appears reasonable that the same would apply to the weighted mean factors computed for the data given in Tables 6, 7 and 8. Comparable data are given in Table 11.

Inasmuch as the equivalent applications per 4-axle semitrailer are not influenced by the percentage of 4-axle vehicles in the total count, it is to be expected that a direct correspondence might not hold in all cases. For instance, 4-axle vehicles in Kansas are apparently fairly heavy, but they do not constitute as great a percentage of the total truck count as they do in Ohio.

It may be that the significant variations found in the loading patterns are not important from an engineering standpoint. However, there is a decision to be faced by the design engineer as to how much simplification and generalization can be made from loadometer survey data. This requires a thorough knowledge of the many problems involved.

PROBLEMS

In the discussion of the equivalent applications concept and of load equivalency factors, it was pointed out that load equivalency factors secured from one source should not be applied to design procedures developed from another source. It is obvious that the load equivalency factors in Table 2 are not the same for all of the methods; yet designs developed for a given mixed-traffic situation may or may not be the same. Thus the design engineer must consider the end-result properties of his design system.

Examples using one thickness design system for asphalt pavements have been worked out and trends indicated. It is likely that certain properties or characteristics

TABLE 12

TOTAL EQUIVALENT APPLICATIONS FOR HYPOTHETICAL AXLE-LOAD GROUP

Axle Load	No. Axles	Load Factor	Total Equiv. 18-Kip Single-Axle Applic.
8	2	0.0618	
10	2	0.108	0.716
12	2	0.188	
8	1	0.0618	
10	2	0.108	0.842
12	3	0.188	
8	3	0.0618	
10	2	0.108	0.589
12	1	0.188	

of the axle-load or truck-type distributions will vary as a function of the design system rather than solely as a result of changes in the distributions themselves. However, the major points made in the paper will apply in general to those design methods in Table 2.

Actual use of any of these design procedures requires that some assumptions be made regarding the properties of the design method and in applying it to loadometer data. Specific examples are that the axle loads can be grouped into cells, that tandem-axle loads are evenly distributed between the two axles and that the equivalent applications concepts apply.

That such assumptions may require consideration can be illustrated by one example: the use of the load factor for the mean load of a group to represent the group. If the actual number of axles within a group is uniformly increasing or decreasing along a straight line, then the use of the equivalency factor for the mean load would result in either an underestimate or an overestimate of the total equivalent applications for the group. Other than straight-line distributions would do the same unless the distribution coincided with the shape of the load vs load-factor relationship.

How this might affect the total equivalent applications computed for a hypothetical axle-load group can be seen from Table 12. The values for the three computed cases can be compared to the number 0.648 obtained by multiplying the total number of axles (6) times the factor for the mean load (0.108).

One way to reduce the likelihood of errors of this type would be to summarize the data into load categories of narrower range. A more precise method would require that each weight axle be computed separately. It is understood that most of the data reported to the Bureau of Public Roads are on punched cards. It would be possible to compute and tabulate factors for each individual load with an electronic computer and to record this information on the same cards. Subsequent calculations would thus be relatively simple.

As with any similar study, the reliability of the sample is a most important factor. The authors suggest that there are many ways in which the reliability of the samples being obtained in loadometer studies could be checked. It is realized that there are many practical reasons why a more extensive sampling program might not easily be put into effect. Nevertheless, some discussion of the problems, as related to pavement design, is in order.

Most of the truck weight studies used in this paper reported data collected at each loadometer station for one 24-hr period during July or August. In a few cases only 8-hr periods were included in the study. Although the selection of a day during July or August may be advantageous from a practical standpoint, it is obvious that such surveys tell nothing about the distribution of axle loads or vehicles during the other months of the year. It would seem necessary that at least a few 24-hr study samples be obtained during these other months.

The time of the year at which samples are obtained is only one of the many factors which governs the reliability of the samples. Some of these factors are summarized in the following.

1. Size of sample:
   a. Percent of the daily total count which is weighed,
   b. Number of stations at which surveys are made,

   c. Number of stations included for each type of highway, and
   d. Number of observations made each year at each station for each highway type.
2. Method by which specific trucks are selected.
3. Time of day and time of year during which observations are made.
4. The specific locations of the loadometer stations:
   a. Relative to the character of the traffic, and
   b. Relative to type of highway they represent.

The reliability or unreliability of loadometer survey samples could have significant consequences. For example, factors to account for growth or the detection of trends with time are obviously influenced by the reliability of the data. Since pavements are usually designed for future traffic, the use of erroneous growth factors could lead to either under- or overdesign. Growth allowances for use in thickness design involve more than traffic volume or gross weight of vehicle. A study of reliable loadometer data would reveal how the average equivalent applications factors might be changing, which in turn would reflect changes in the number and type of vehicles using a particular type of highway.

If the results of loadometer studies taken at a few stations on a given class of highway are to be applied to traffic observed on other portions of the highway system, it is necessary that the axle-weight and truck-type distributions be reasonably constant. A proper sampling program would establish whether or not an assumption of constancy is justified. If, for instance, the design equivalent applications are to be determined from factors computed for each truck type, or if the weighted mean truck factor is to be used as indicated in the previous section, then the assumption must be made that these factors are applicable (constant). If this is not so, then a sampling program to detect trends should be devised.

As indicated earlier, neither the axle-load nor the truck-type distributions are the same for the seven states (Tables 6 and 7) nor for the different types of highway within a single state. Thus, it would seem that the collection and study of reliable data are necessary if pavement designs for mixed traffic are to reflect accurately the actual traffic to which they will be subjected. Securing reliable data is complex and expensive; however, it would seem only logical that programs be developed for securing the necessary information.

SUMMARY OF SUGGESTED PROCEDURES

Several procedures for using results of loadometer surveys in pavement design have been indicated. One method required the computation of equivalent applications from full loadometer studies made for, or assumed to apply to, a given design situation. Where sufficient information is available about a given area, this might be the most accurate procedure. However, it must be recognized that any factors normally considered to affect the traffic on a highway also might affect the character of the axle-weight distribution; therefore, the exclusive use of loadometer surveys might be not only expensive, but also misleading.

Another procedure was that loadometer studies be used to establish factors for vehicles of each type and that these factors then be weighted according to the percentage of each truck type determined for a given design problem. This has an advantage in that it permits use of count data from locations where there are no loadometer stations.

The most convenient procedure, but somewhat less reliable, would be that of using weighted mean truck factors to compute equivalent applications. These estimates are made by multiplying weighted mean factors times estimated numbers of trucks expected. Although this technique makes use of the same data as that computed by the previous method, it does require more stability in the truck-type distributions. It would seem that if a sufficient number of surveys indicate that there is not a great variation within a given class of highway in a state, then the use of this procedure would be justified.

In cases where no facilities are available for making loadometer studies, or where quick estimates are to be made, the last procedure has considerable merit. Either of the last two procedures could be adapted for use by agencies which do not have facilities for making full loadometer studies. Estimates of the axle-weight distributions could be made from data collected by state highway departments. Counts of the number of commercial vehicles, or counts by vehicle type, could be made by the lesser equipped agencies, and the information used for design purposes. This certainly would be more reliable than information based on no loadometer studies whatsoever.

CONCLUSION

Several important factors concerning the use of loadometer data in designing pavements for mixed traffic have been discussed. It has been pointed out that the equivalent applications concept provides a theory for combining the effects of different loads, but that there are still many areas which require further study. Among these are the validity of the theory itself, reliability of the data available, and amount of simplification to be permitted in using loadometer data.

REFERENCES

1. Hveem, F. N., and Carmany, R. M., "The Factors Underlying the Rational Design of Pavements." HRB Proc. 28:101-136 (1948).
2. Sherman, G. B., "Recent Changes in the California Design Method for Structural Design of Flexible Pavement." California Department of Public Works, Sacramento (1958).
3. Hveem, F. N., and Sherman, G. B., "California Method for the Structural Design of Flexible Pavements." Proc., International Conf. on Struct. Design of Asphalt Pavements, Ann Arbor, Mich. (1962).
4. "Planning Manual of Instruction, Part 7—Design." California Division of Highways, Sacramento, 2nd Ed. (April 1959).
5. Scrivner, F. H., "A Theory for Transforming the AASHO Road Test Pavement Performance Equations to Equations Involving Mixed Traffic." HRB Special Report 66, 39-46 (1962).
6. Scrivner, F. H., and Duzan, H. C., "Application of AASHO Road Test Equations to Mixed Traffic." HRB Special Report 73, 387-392 (1962).
7. "The AASHO Road Test: Report 5—Pavement Research." HRB Special Report 61E, 352 pp. (1962).
8. Langsner, G., Huff, T. S., Liddle, W. J., "Use of Road Test Findings by AASHO Design Committee." HRB Special Report 73, 399-414 (1962).
9. "AASHO Interim Guide for the Design of Flexible Pavement Structures." American Association of State Highway Officials (Oct. 1961).
10. "AASHO Interim Guide for the Design of Rigid Pavement Structures." American Association of State Highway Officials (Oct. 1961).
11. Shook, J. F., and Finn, F. N., "Thickness Design Relationships for Asphalt Pavements." Proc., International Conf. on Struct. Design of Asphalt Pavements, Ann Arbor, Mich. (1962).
12. "Truck Weight and Vehicle Classification Study." Maryland State Roads Commission, Baltimore (1960, 1961).
13. "Loadometer Study." Ohio Department of Highways, Columbus (1960, 1961).
14. "Truck Weight and Volume Study." Kansas State Highway Commission, Topeka (1960, 1961).
15. "Truck Weight and Vehicle Classification Study." Missouri State Highway Department, Jefferson City (1960, 1961).
16. "Comparative Loadometer Survey." Arizona Highway Department, Phoenix (1960, 1961).
17. "Report on Truck Weight Survey Data from Twenty-Five Survey Stations." North Carolina State Highway Commission, Raleigh (1960).
18. "Truck Weight Survey." North Carolina State Highway Commission, Raleigh (1961).
19. "Truck Weight Study." Washington State Highway Commission, Olympia (1959, 1960).
20. "Loadometer Study." Mississippi State Highway Department, Jackson (1960, 1961).

Comparison of Concrete Pavement Load-Stresses at AASHO Road Test with Previous Work

W. R. HUDSON,[1] Senior Designing Engineer, Highway Design Division, Texas Highway Department

Existing rigid pavement design equations spring primarily from the theories developed by Westergaard in 1925. Some of these design equations are based on empirical modifications of the original theory, others are merely simplifications. Several of the empirical modifications have been developed from strain measurements taken under static loads. Recent developments in electronic equipment allow more accurate dynamic strain measurement than was formerly possible. Such equipment was used to make approximately 100,000 individual strain gage readings under dynamic loads in conjunction with the AASHO Road Test (1958 to 1960).

The purpose of this paper is to discuss these strain measurements and to compare them with the static strain measurements used to develop existing empirical design equations. The stresses calculated from these strains will be compared with the original Westergaard theories. Such comparisons could provide the basis for modifying empirical design equations to include a dynamic load effect.

•THE primary results of the AASHO Road Test were performance equations relating pavement design, axle load, number of load applications, and pavement serviceability (1). These equations were developed with a great many other design variables held constant. Two methods will be helpful in analyzing these remaining variables to complete the general design equation: (a) additional road tests, and (b) development of a mechanistic model or equation relating the multitude of design variables. Judging from previous experience in structural research both approaches will ultimately be combined to provide the final solution of the problem.

This report is based on the idea that load-stresses offer an approach to a mechanistic model and that such a model will be helpful in extending the results of the AASHO Road Test equations.

It should be pointed out at this point that no stresses have been measured in this or any other study. Strains are measured and the corresponding stresses are calculated by use of elastic theory. Such stresses will be called "observed stresses" in this report. Theoretical stresses or those computed from empirical equations will be referred to as "calculated stresses." Symbols used in this report are defined where they first appear or where necessary for clarity, and for convenience in reference, are listed alphabetically in Appendix C.

EARLY HISTORY OF MATHEMATICAL AND THEORETICAL ANALYSES

In the early 1920's, A. T. Goldbeck and Clifford Older independently developed formulas for approximating the stresses in concrete pavement slabs under certain assumed conditions. The best known of these formulas is generally called the "corner formula" and is expressed

Paper sponsored by Committee on Rigid Pavement Design.

[1] Formerly, Assistant Chief, Rigid Pavement Research Branch, AASHO Road Test.

$$\sigma_c = \frac{3\ P}{h^2} \tag{1}$$

in which

σ_c = maximum tensile stress, psi, in a diagonal direction in the surface of the slab near a rectangular corner;
P = static load, in lb, applied at a point at the corner; and
h = depth of the concrete slab, in in.

Eq. 1 was derived using the assumptions of point load applied at the extreme corner and no support from the subgrade. The fiber stresses in the surface of the slab are assumed to be uniform on any section at right angles to the corner bisector.

Strain measurements taken on the Bates Road Test in 1922-23 appear to confirm the corner formula. Obviously, the assumptions of point load and load applied at the extreme corner were not correct for the Bates test sections. It is interesting that in spite of this there was reasonably good comparison. This good agreement could be partly due to the high impact transmitted to the slabs with the solid rubber tires used in the Bates test or to the possibility that subgrade support may have been very low as assumed by this formula.

In 1926, H. M. Westergaard completed a logical and scientific mathematical analysis of the stresses in concrete highway pavements. This analysis is concerned with the determination of maximum stresses in slabs of uniform thickness resulting from three separate conditions of loading:

1. Load applied near the corner of a large rectangular slab (corner load);
2. Load applied near the edge of a slab but at a considerable distance from any corner (edge load); and
3. Load applied at the interior of a large slab at a considerable distance from any edge (interior load).

In the solution of this problem, Westergaard made the following important assumptions:

1. The concrete slab acts as a homogeneous isotropic elastic solid in equilibrium.
2. The reactions of the subgrade are vertical only and they are proportional to the deflections of the slab.
3. The reactions of the subgrade per unit of area at any given point is equal to a constant k multiplied by the deflection at the point. This constant is termed "the modulus of subgrade reaction" or "subgrade modulus." The constant k is assumed to be constant at each point, independent of the deflection, and to be the same at all points within the area of consideration.
4. The thickness of the slab is assumed to be uniform.
5. The load at the interior and at the corner of the slab is distributed uniformly over a circular area of contact; for the corner loading, the circumference of this circular area is tangent to the edge of the slab.
6. The load at the edge of the slab is distributed uniformly over a semicircular area of contact, the diameter of the semicircle being at the edge of the slab.

The following expressions for stress were developed by Westergaard:

$$\sigma_i = 0.275\ (1 + \mu)\frac{P}{h^2}\left(\log_{10}\frac{Eh^3}{kb^4}\right) \tag{2}$$

$$\sigma_e = 0.529\ (1 + 0.54\mu)\frac{P}{h^2}\left(\log_{10}\frac{Eh^3}{kb^4} - 0.71\right) \tag{3}$$

$$\sigma_c = \frac{P}{h^2}\left[1 - \left(\frac{12\,(1-\mu^2)\,k}{E\,h^3}\right)^{0.15} (a\sqrt{2})^{0.6}\right] \tag{4}$$

in which

P = point load, in lb;
σ_i = maximum tensile stress, in psi, at the bottom of the slab directly under the load, when the load is applied at a point in the interior of the slab at a considerable distance from the edges;
σ_e = maximum tensile stress, in psi, at the bottom of the slab directly under the load at the edge, and in a direction parallel to the edge;
σ_c = maximum tensile stress, in psi, at the top of the slab, in a direction parallel to the bisector of the corner angle, due to a load applied at the corner;
h = thickness of the concrete slab, in in.;
μ = Poisson's ratio for concrete;
E = modulus of elasticity of the concrete, in psi;
k = subgrade modulus, in pci;
a = radius of area of load contact, in in.; the area is circular in case of corner and interior loads and semicircular for edge loads;
b = radius of equivalent distribution of pressure at the bottom of the slab ($= \sqrt{1.6\,a^2 + h^2} - 0.675\,h$).

As a part of his analyses and in order to simplify further the discussions, Westergaard introduced a factor called the radius of relative stiffness ℓ, defined as

$$\ell = \sqrt{\frac{E\,h^3}{12\,(1-\mu^2)\,k}} \tag{5}$$

Eq. 4 can be expressed in terms of ℓ as follows:

Corner loading:

$$\sigma_c = \frac{3P}{h^2}\left[1 - \left(\frac{a\sqrt{2}}{\ell}\right)^{0.6}\right] \tag{6}$$

If μ is set at 0.15, Eqs. 2 and 3, respectively, may be expressed in the form:

Interior loading:

$$\sigma_i = 0.31625\,\frac{P}{h^2}\left[4\log_{10}\left(\frac{\ell}{b}\right) + 1.0693\right] \tag{7}$$

Edge loading:

$$\sigma_e = 0.57185\,\frac{P}{h^2}\left[4\log_{10}\left(\frac{\ell}{b}\right) + 0.3593\right] \tag{8}$$

Modifications to the original 1926 equations were made by Westergaard in 1933, 1939 and 1947. The 1933 modifications were concerned primarily with interior loads and will not be discussed in this paper.

In the 1930's, F. T. Sheets introduced an equation containing a constant c which was equated to the value of k as employed by Westergaard. The Sheets equation can be written as follows:

$$\sigma_c = \frac{2.4\ P\ (c)}{h^2} \tag{9}$$

Eq. 9 is reported to give stresses which are in good agreement with those obtained at the Bates Road Test; however, it is no longer in general use and does not contain all the variables of interest to the designer.

The principal weakness of these early stress equations was the rather broad assumptions necessary to facilitate analysis. Furthermore, with techniques available at that time it was difficult to make the strain measurements necessary to verify these stresses. As a result, very few stress comparisons were actually performed. Subsequent stress equations are all based on some modification of the original Westergaard equation. The major work that resulted in these modifications will be more completely discussed later in this paper, including the Kelley equation developed as a result of the BPR Arlington Test, the Spangler equation developed as the result of the Iowa State College tests and the Pickett equations developed as the result of additional mathematical analysis. Finally, the Maryland Road Test strain measurements will be discussed with the AASHO Road Test measurements in an effort to summarize all recent works in this field.

EFFECT OF PHYSICAL CONSTANTS

The values for physical constants assumed in calculation of theoretical stresses and in computation of observed stresses from measured strains can greatly influence the apparent correlations. For example, a variation of E from 4,000,000 to 5,000,000 psi results in an increase of 25 percent in the stresses computed from observed strain values. Such variations in E can exist and must be closely examined. The modulus of elasticity of the concrete can vary with age, moisture content, temperature and other factors. At best, any value used in computations must be an average value.

Aside from these variations in the "true" modulus of elasticity, the indicated modulus of elasticity as obtained from static load tests or dynamic (sonic) measurements vary greatly, with the dynamic value usually being 20 to 30 percent larger than the so-called static value.

Poisson's Ratio

Poisson's ratio μ is extremely hard to measure; however, it has only a minor influence on theoretical stresses or calculated observed stresses.

Modulus of Subgrade Reaction

The modulus of subgrade reaction k has no influence on calculated observed stress, but it can have significant influence on theoretical stress. Being a property of a granular material or soil, k inherently possesses all variations associated with such heterogeneous materials. For example, k varies with the density and moisture content of the material; with the temperature due to the curling characteristics of the slab; with the size of loaded area (plate size) used in the determination; and probably with the intensity of load due to the greater deflection imposed by higher loads.

It will be recalled that k is a stiffness coefficient that expresses the resistance of the soil structure to deformation under load in pounds per square inch of pressure per inch of deformation. Furthermore, the ability of a subgrade to maintain its k over the life of the pavement is extremely important. There are indications that most pavements have sufficient supporting power at the beginning of their life. However, as load applications are applied to the pavement, the character of the subgrade support changes until the pavement in many cases becomes relatively unsupported, particularly in the corner area. Common causes of this loss of support are pumping, settlement, and permanent deformation of the subgrade or subbase material. In addition to these variations inherent in the "true k value" there are variations dependent on the method of measurement used to determine k. A multitude of methods exist. The three basic methods are (a) calculation of k from the deflection of a rigid steel plate usually 30 in. in diameter (values of k have been found to vary with diameter), (b) calculations of k from measurements of load-deflection characteristics of existing slabs (13) and (c) assignment of k-value based on other soil strength tests, such as CBR, and triaxial compression tests.

ROAD TEST LOAD-STRESS EXPERIMENT

In conjunction with the AASHO Road Test (1958-1960) two major pavement strain measuring experiments were conducted: (a) edge strains on normal test pavements were measured under moving loads, and (b) a special factorial experiment was provided on a spacial no-traffic loop for measurement of strains under a vibrating load.

All concrete strains were measured with etched foil SR-4 strain gages. The effective gage length was 6 in. and the nominal gage resistance was 750 ohms. The sensitivity of the gages was ± μin. per in. of strain. The gages were cemented to the upper surface of the pavement slab and were protected from weather and traffic. Details of the measurement system are reported in the AASHO Road Test Report No. 5 (2).

In order to use these strain measurements to the best advantage, the gage readings were converted to principal strains, major and minor. These principal strains were converted to stresses by elastic theory. The development and formulas are given in Appendix E of Report 5 (2). In these conversions, Young's modulus E was taken equal to 6.25×10^6 psi, the dynamic modulus measured for concrete pavement at the Road Test. The static modulus for the Road Test pavement was 5.25×10^6 psi. Poisson's ratio μ was taken as 0.28, the average measured for the Road Test pavements (see Appendix A herein, and also Report 5, Appendix D, p. 284-286).

Main Loop Stresses

Measurement of Strains.—During the course of the project, 13 rounds of main loop strain data were gathered. A round consisted of one set of measurements on the selected factorial experiment, and the test vehicles normally assigned to a given lane were used as the test load for that lane (Fig. 1). Each round of strain data is representative of (a) the early morning pavement condition (pavement corners and edges curled up); (b) the period from 10:00 AM to 4:00 PM (pavements curled down); or (c) the period from 6:00 AM to 12:00 PM (pavements relatively flat). By varying this time of measurement, normal load-stress variations due to temperature differential within the slab could be studied. Several studies of pavement strain were also made continuously around the clock to provide more definitive information about strain variation with temperature differential.

No data from cracked slabs were used as a part of this experiment. Inspections were made to insure the uncracked condition of the slab being tested throughout the life of the project. When a crack occurred in the selected slab, a new slab was chosen and the gages relaid. When all slabs in a section cracked or a section was removed from the test, no further measurements were made on that section. Two gages were installed in each pavement section, one on each side of the joint (Fig. 2). Gages on 15-ft panels (nonreinforced section) were placed at the center of the panels, 7.5 ft from each joint. Gages on the 40-ft panels (lightly reinforced sections) were placed 10 ft from the joint. Output from the strain gages was recorded continously on paper tape as the test vehicles passed by. The strain value representative of one section for one round consisted of an average of 6 values, a minimum of 3 measurements on each of 2 strain gages. These measurements were made when the centroid of the loaded area (load wheels) was located opposite the gage and 20 in. (-3 to + 2 in.) from the pavement edge. (This biased tolerance was selected as the result of special studies of the distribution of the placement of

AASHO ROAD TEST

RIGID PAVEMENT MAIN LOOP EXPERIMENT

Loop	Traffic Load	Subbase Thickness	2.5 R	2.5 N	3.5 R	3.5 N	5.0 R	5.0 N	6.5 R	6.5 N	8.0 R	8.0 N	9.5 R	9.5 N	11.0 R	11.0 N	12.5 R	12.5 N
3	12k S	3			X	X	●	X	X	●	X	X						
		6			X	X	X	●	●	X	X	X						
		9			X	X	X	X	X	X	X	X						
	24k T	3			X	X	●	X	X	●	X	X						
		6			X	X	X	●	●	X	X	X						
		9			X	X	X	X	X	X	X	X						
4	18k S	3					X	X	●	X	X	●	X	X				
		6					X	X	X	●	●	X	X	X				
		9					X	X	X	X	X	X	X	X				
	32k T	3					X	X	●	X	X	●	X	X				
		6					X	X	X	●	●	X	X	X				
		9					X	X	X	X	X	X	X	X				
5	22.4k S	3							X	X	●	X	X	●	X	X		
		6							X	X	X	●	●	X	X	X		
		9							X	X	X	X	X	X	X	X		
	40k T	3							X	X	●	X	X	●	X	X		
		6							X	X	X	●	●	X	X	X		
		9							X	X	X	X	X	X	X	X		
6	30k S	3									X	X	●	X	X	●	X	X
		6									X	X	X	●	●	X	X	X
		9									X	X	X	X	X	X	X	X
	48k T	3									X	X	●	X	X	●	X	X
		6									X	X	X	●	●	X	X	X
		9									X	X	X	X	X	X	X	X

X Denotes a Test Section
● Denotes Replicate (2) Test Sections

Figure 1. AASHO Road Test, rigid pavement main loop experiment.

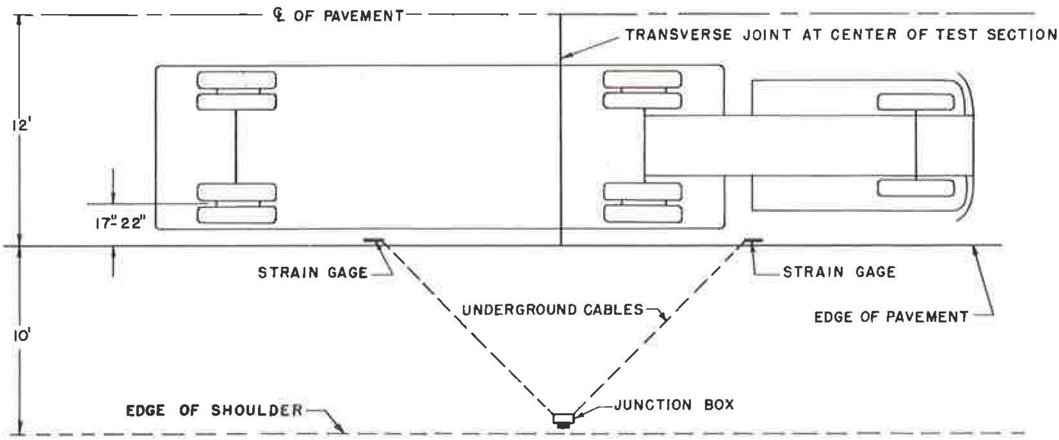

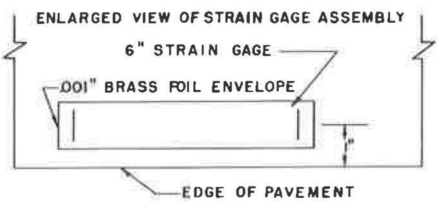

Figure 2. Location of gages for main loop experiment.

vehicles whose operators were attempting to drive at a specified distance of 20 in. from the pavement edge.) This placement resulted in the outer edge of the dual wheels being located at approximately 6 to 9 in. from the pavement edge.

Analysis of Data—Main Loops.—In early studies it became apparent that several variables should be isolated in order to simplify the study of strain data. Two of these variables were load and temperature.

Load Effects.—Several load-strain studies conducted early in the Road Test indicated that for a given pavement at a given time, strain varies linearly with load. This was substantiated many times. As a result of these studies the general mathematical model adopted for strains was

$$\frac{\text{strain}}{\text{axle load}} = f \text{ (design and other variables)} \tag{10}$$

Temperature Effects.—Strain measurements are affected by temperature. This was amply demonstrated early in the test. To isolate this variable, several 24-hr studies were made during the spring and fall seasons to take advantage of daily variation in ambient temperature. Numerous investigations of the data (strains, air temperatures, and internal slab temperature) indicated that a consistent variable for study was the temperature differential, top to bottom of a 6.5-in. thick PCC slab. These analyses led to the following model for best fit.

$$\frac{\text{strain}}{\text{axle load}} = f \text{ (design \& random variables)} \times 10^{f(\text{slab temp})} \tag{11}$$

General Strain Equation.—Dynamic edge strain data from Rounds 4, 5, 8, and 9, gathered between April and August 1959, were selected for use in determining the most representative empirical relationship between edge strain, design, load and temperature. These rounds cover spring, summer and fall seasons when a large majority of the sections were still in good condition.

Plots of the data and preliminary analyses along with load and temperature studies were helpful in selection of a model. The final analysis indicated that the design variables, reinforcing and subbase thickness, were not significant. The following equations resulted:

Single-axle loads:

$$\frac{\epsilon}{L_1} = \frac{20.54}{10^{0.0031T} D_2^{1.278}} \tag{12}$$

Tandem-axle loads:

$$\frac{\epsilon}{L_1} = \frac{3.814}{10^{0.0035T} D_2^{0.8523}} \tag{13}$$

in which

ϵ = estimated edge strain at the surface of the concrete slab;
L_1 = nominal axle load of the test vehicle (a single axle or a tandem-axle set);
D_2 = nominal thickness of the concrete slabs; and
T = the temperature (° F) at a point ¼ in. below the top surface of the 6.5-in. slab minus the temperature at a point ½ in. above the bottom surface, determined at the time the strain was measured (the statistic T may be referred to occasionally as "the standard differential").

Residuals from the analyses that are less than the average root mean square residual determined in the two analyses correspond to observations that range from 83 to 120 percent of the predicted values.

Using the theory of elasticity given in Report 5, Appendix E (2), Eqs. 12 and 13 were converted to the following stress equations:

Single-axle loads:

$$\sigma_{es} = \frac{139.2L_1}{10^{0.0031T} D_2^{1.278}} \tag{14}$$

Tandem-axle loads:

$$\sigma_{et} = \frac{25.86L_1}{10^{0.00335T} D_2^{0.8523}} \tag{15}$$

in which

σ_{es} = predicted stress under single-axle load; and
σ_{et} = predicted stress under tandem-axle load.

L_1, T, and D_2 are as previously described.

Special No-Traffic Loop Stresses

Between October 9, 1959, and November 2, 1960, a series of eight experiments, designed to furnish information regarding the distribution of load stress in the surface of concrete slabs, was conducted on the sections comprising the experiment on the no-traffic loop (Table 1).

A rapidly oscillating load was applied to the pavement through two wooden pads on 6-ft centers, each approximating the loaded area of a typical dual tire assembly loaded to 22.4^k (Fig. 3). This dynamic loading was intended to simulate that of a typical single-axle vehicle used in the main loop experiments.

Dynamic Load.—The vibrating loader was mounted on a truck (Fig. 4). The essential parts were two adjustable weights rotating in opposite directions in a vertical plane in such a manner that all dynamic force components except those in a vertical direction were balanced by equal and opposite components. The deadweight necessary to prevent the upward components from lifting the truck from the pavement was provided in the form of concrete blocks resting on a platform located directly above the rotating weights.

TABLE 1

EXPERIMENT DESIGN FOR SPECIAL STUDIES OF LOAD STRESSES IN THE SURFACE OF CONCRETE SLABS

Subbase Thickness (in.)	No. of Sections					
	5.0-In. Slab, 12,000-Lb Load		9.5-In. Slab, 22,000-Lb Load		12.5-In. Slab, 30,000-Lb Load	
	No Reinf.	Reinf.	No Reinf.	Reinf.	No Reinf.	Reinf.
0	2	1	1	2	2	1
6	2	1	1	2	2	1

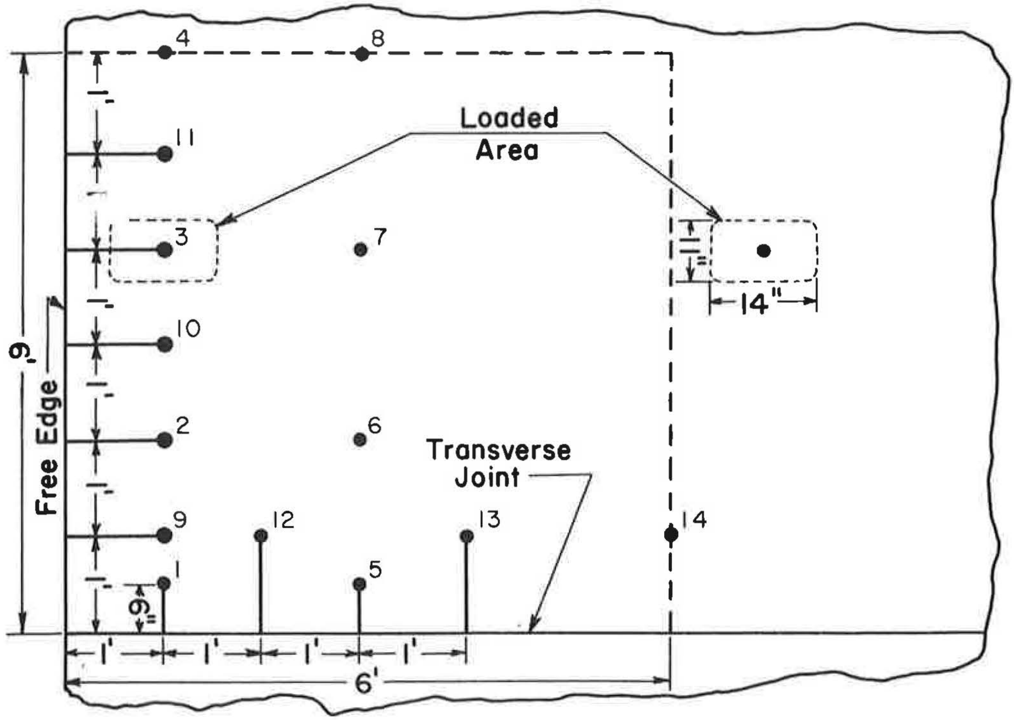

Figure 3. Load positions for special strain studies.

Figure 4. Truck-mounted vibrator in position on pavement.

The load was transmitted through inverted A-frames which could be folded upward against the side of the vehicle when not in use. Contact with the pavement being loaded was solely through the wooden pads.

During each of the eight experiments (rounds), the simulated single-axle load was applied at three or more of the positions indicated in Figure 3. Data from Round 7, taken in September 1960 during the early morning hours when panel corners were curled upward and the strains were among the highest observed, were selected for complete analysis and are presented in the Road Test report and used herein. Other data are available in Road Test file, DS 5205.

Field Procedures.—Strains were measured by means of 33 electrical resistance strain gages cemented to the upper surface of the pavement slab. The gages were laid out over the corner 6-sq ft area of the slab in each section (Fig. 5).

The use of delta rosettes at the 9 interior points permitted the computation of the magnitude and direction of the principal strains at those points. Only single gages were used along the edge and transverse joint, it being assumed that the strain perpendicular to the edge or joint could be calculated by use of Poisson's ratio for the concrete. No gages were required at the intersection of joint and edge as the strain there was assumed to be zero. Figure 6 shows the points at which gages were assumed to act.

Load cells for measuring the vibratory loads were developed at the project and were calibrated on the project's electronic scales. A continuous record of loading was made while the strain gage output was being recorded.

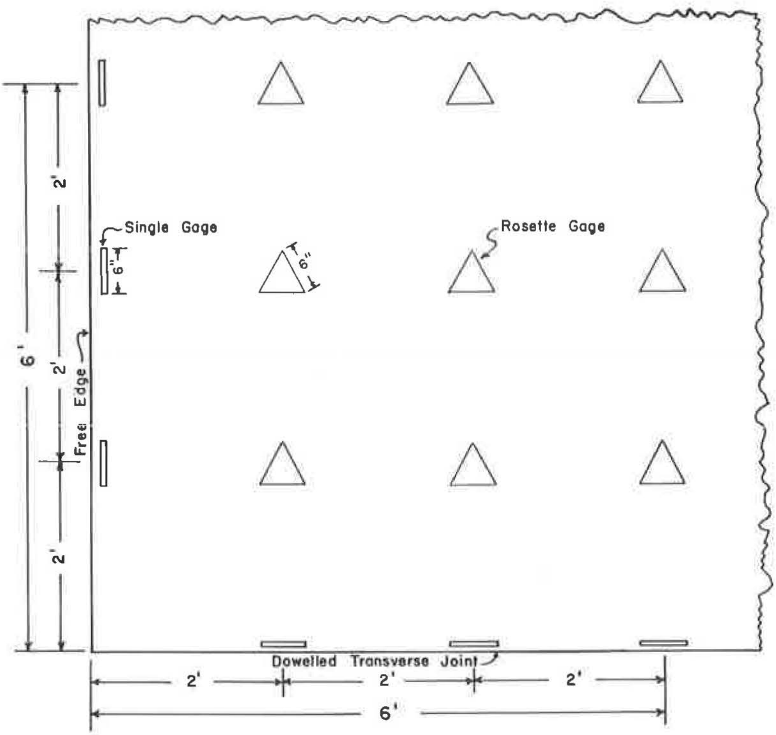

Figure 5. Typical gage layout, no-traffic loop strain experiment.

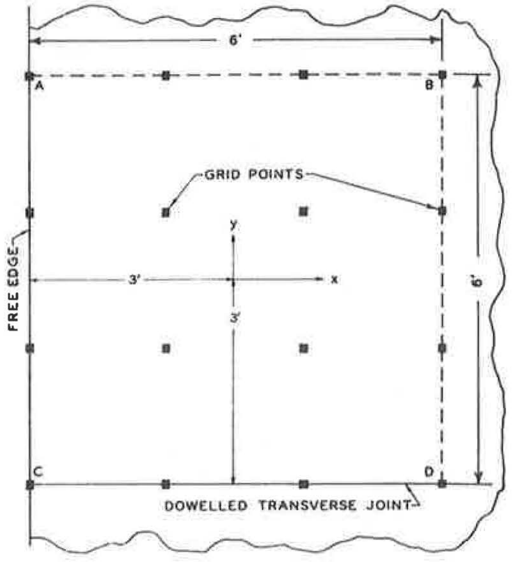

Figure 6. Control points for special strain studies.

In normal operation, the load was varied sinusoidally with time at a frequency of 6 cps, from a minimum value of about 500 lb on each contact area to a maximum value which depended upon the thickness of the pavement being tested (Table 1). The measured strain also varied sinusoidally with time, very nearly in phase with the load, and of course, at the same frequency. From examination of simultaneous traces of the load wave and strain wave it was possible to determine the amplitude of each as well as the nature (tension or compression) of the strain.

Data Collection.—Data were taken on the test sections in random order within the experiment. All load positions selected for a particular round were completed on a section before measurements were made on the next section. With the load in one of the selected positions, the recording equipment was switched to each of the 33 pavement gages in succession. The output of each pavement gage was recorded on paper tape, along with the record from the load gages. The overall time required to complete the measurements associated with one load position on one section, including the time required to set up the vibrating loader, was about 30 min, of which about 5 min were spent in recording the strains.

Data Processing.—The first requirement for each experiment was to derive by statistical techniques a pair of empirical equations for each load position, of the following general forms:

Major principal strain = a function of pavement design, load and the coordinates of the gage point (16)

Minor principal strain = a function of pavement design, load and the coordinates of the gage point (17)

(The coordinate system used was that shown in Figure 6.)

The second requirement was to compute from Eqs. 16 and 17, and the appropriate plane stress equations linking stress and strain, the estimated value of major and minor principal stresses at closely spaced points in the pavement surface within the 36 sq ft area of observation.

Examination of the data indicated that variations in the strain observed on sections at the same level of slab thickness but at different levels of reinforcing and/or subbase thickness were small and apparently random in nature. Therefore, within each round and for the same load position, the readings of gages with the same coordinates x and y installed on panels of the same slab thickness (irrespective of subbase thickness and reinforcing) were averaged to obtain a set of data representing the round-load position-slab thickness combination.

Thus, for one load position within an experiment, the processing resulted in three sets of data corresponding to the three levels of slab thickness (5.0, 9.5, and 12.5 in.) with each set consisting of 33 averaged strain gage readings. As the third step in processing, each such set was converted from strain gage readings to magnitude and direction of major and minor principal strains at the 15 gage points on a panel employing standard techniques based on elastic theory.

As the fourth and final step before analysis, each principal strain was divided by the corresponding load in accordance with experimental evidence (as described herein) that strain is directly proportional to load. Thus, as a result of the four-step processing of the data, the only remaining independent variables to be considered in the analysis of strain were the coordinates x and y of a gage point and the thickness D_2 of the slab.

Typical Stress Distribution Results.—Analysis of Strains.—The three sets of data corresponding to each round-load position combination were analyzed using statistical procedures. The strain data were represented by a linear model whose 48 terms (3 slab thicknesses by 16 combinations of x and y) were mutually orthogonal polynomials in x, y, and D_2. As a result of the elimination of reinforcing and subbase thickness as independent variables, there were 6 sections within each round-load position-slab thickness combination whose variation in strain furnished a measure of residual effects. The residual effects, in turn, were used to determine the statistical significance of each coefficient. (The coefficients from each analysis, with significant terms indicated, are available in Road Test file DS 5211.) Of the 48 original coefficients only those that were found to be significant at the 1 percent level were used in the calculations to be described below.

Distribution of Principal Stresses.—As previously indicated, the analyses of data from load positions 1, 2, 3, and 4 of Round 7 were selected for complete study. The stresses determined were used in plotting contours of equal principal stress (see Fig. 9). In these plots all stresses are recorded in pounds per square inch with the usual sign convention—tensile stresses positive, compressive stresses negative.

Critical Stresses (Edge Load Condition).—Maximum values of tensile stresses and maximum values of compressive stresses for the edge load positions studied were taken

TABLE 2

MAXIMUM TENSILE AND COMPRESSIVE STRESSES FOR 1-KIP SINGLE-AXLE LOAD (Data from Design 1, Loop 1, Lane 2)

Load Position	Slab Thickness (in.)		
	5.0	9.5	12.5
(a) Maximum Tensile Stress, psi			
1	12.47	4.21	2.62
2	9.39	3.27	2.05
3	8.58	2.85	1.38
4	6.94	2.60	1.52
(b) Maximum Compressive Stress, psi			
1	- 3.78	-1.61	-1.12
2	-17.97	-7.41	-4.71
3	-18.82*	-7.82	-4.89
4	-17.57	-8.10*	-5.57*

*Maximum for indicated slab thickness.

from Figure 7 and recorded in Table 2. Figure 7 shows the load position and the stress distribution when these critical stresses occurred.

According to an assumption commonly made in the application of elastic theory to a slab resting on an elastic foundation (4), the stresses at points on a vertical line through the slab are equal but opposite in sign at the slab surfaces and exceed, in absolute value, the stress at any other point on the line. If this assumption is made in the present instance, then each stress marked with an asterisk in Table 2 is equivalent, in absolute value, to the critical tensile stress for the indicated slab thickness and load position. These stresses occur along the pavement edge with the center of the outer loaded area at a distance of 1 ft from the edge and 4 to 6 ft from the nearest transverse joint (edge load conditions).

The following empirical equation is fitted to the three pairs of values of D_2 and critical stress given in Table 2.

$$\sigma_{ev} = \frac{160 L_1}{D_2^{1.33}} \tag{18}$$

in which

σ_{ev} = the critical load stress, in psi, as determined under a vibratory load on the no-traffic loop (edge load);
L_1 = single-axle load, in kips; and
D_2 = slab thickness, in in.

or in terms of wheel load (L_W):

$$\sigma_{ev} = \frac{320 L_W}{D_2^{1.33}} \tag{19}$$

Eq. 18 (Fig. 8) predicts the three critical stresses denoted by asterisks in Table 2 with an error of less than 2 percent. The critical load stress for any combination of single-axle load and pavement thickness, within the range observed, presumably may be estimated from Eq. 18. Additional stresses which may be present as a result of temperature or moisture fluctuations, of course, are not included in the stress estimated from this curve or from the contours (Fig. 7). It is also probable that stresses arising from static loads would be greater than those estimated from the strains measured in this study.

Stress Distributions for Corner Loading Conditions.—Previous research has indicated that the corner loading condition is of considerable importance in the study of pavement behavior. To provide a basis for comparison with previous data for this case of loading, the results of the corner load position of the Loop 1 strain experiments are

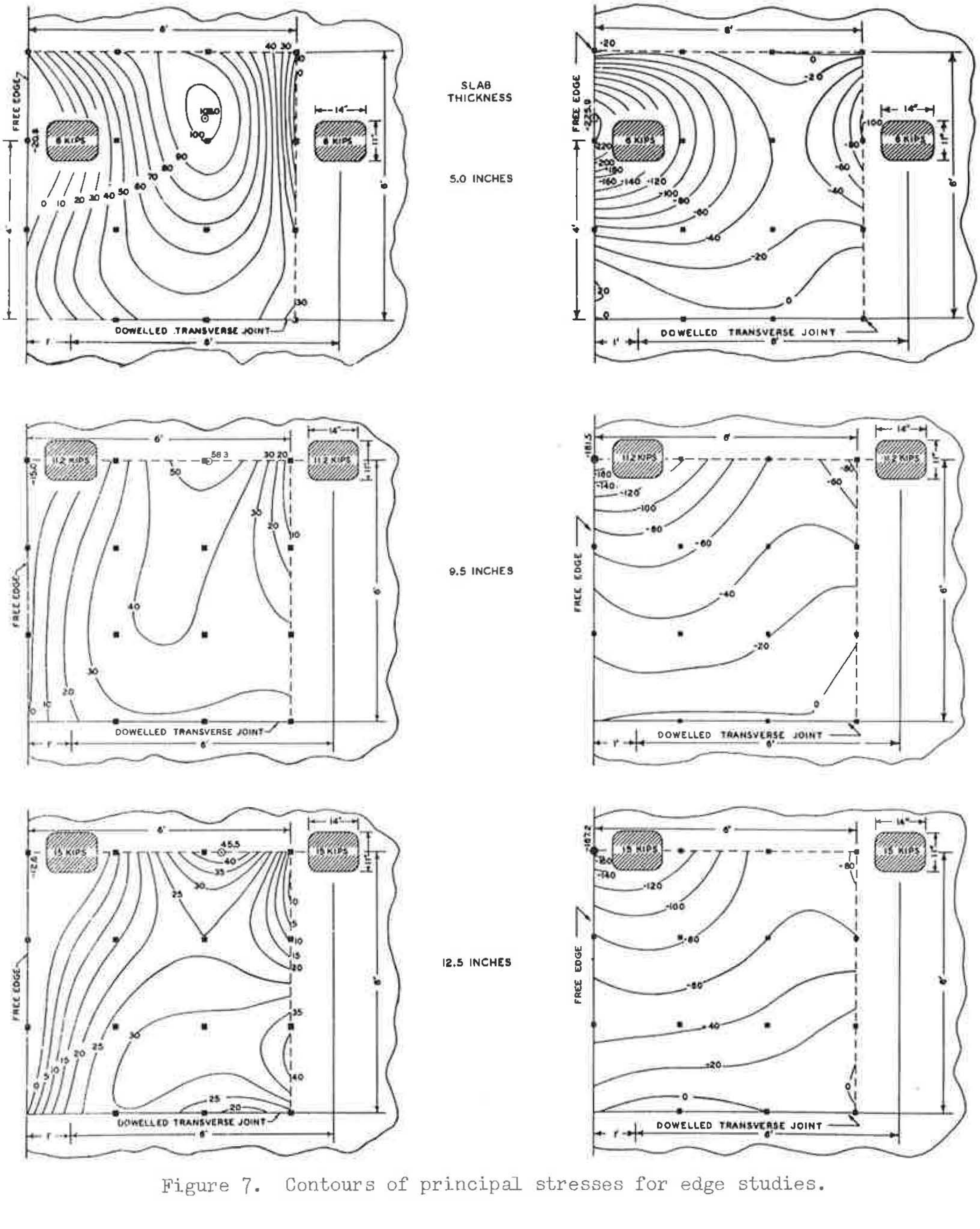

Figure 7. Contours of principal stresses for edge studies.

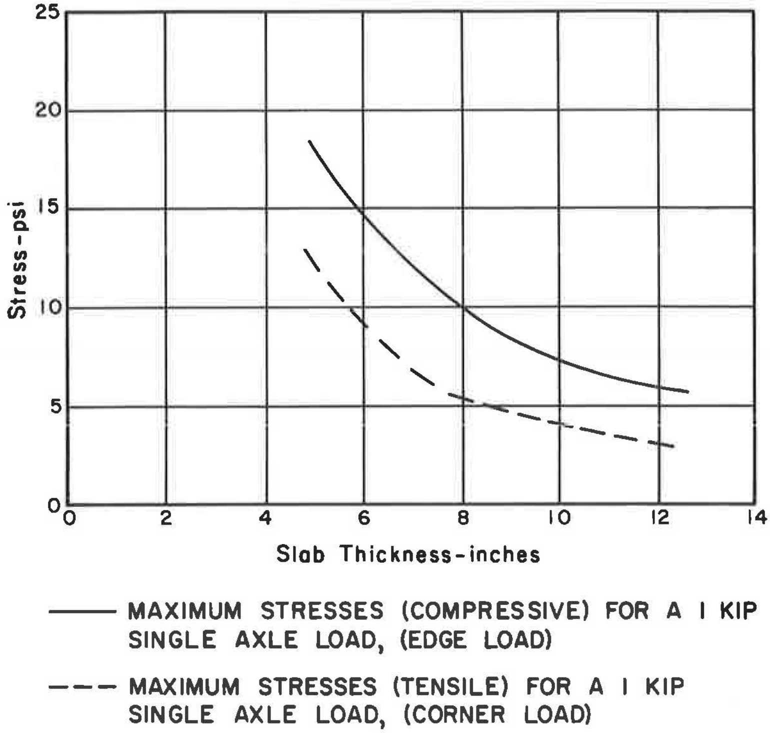

Figure 8. Plot of AASHO Road Test stress equation.

given in Figure 9; the directions of the principal stresses are given in Figure 10. These stress directions have not previously been reported although the stress contours are part of the Road Test reports.

Maximum stresses indicated for corner loading can be obtained from Figure 9. Using these values a corner stress equation can be developed exactly as Eq. 18 was developed for edge loading.

$$\sigma_{cv} = \frac{193L_1}{D_2^{1.7}} \tag{20}$$

in which

σ_{cv} = maximum load stress, in psi, as determined in Loop 1 for corner load.

L_1 and D_2 are as previously defined. In terms of wheel load L_w this equation becomes

$$\sigma_{cv} = \frac{386L_w}{D_2^{1.7}} \tag{21}$$

(Eq. 20 is also shown in Figure 8.)

Comparison of Main Loop and No-Traffic Loop Stresses

The use of dynamic loaders (such as the vibrator used in the no-traffic loop) in future experiments would facilitate the study of pavement strains under dynamic load conditions However, such studies will be useful only if the stresses observed under this dynamic

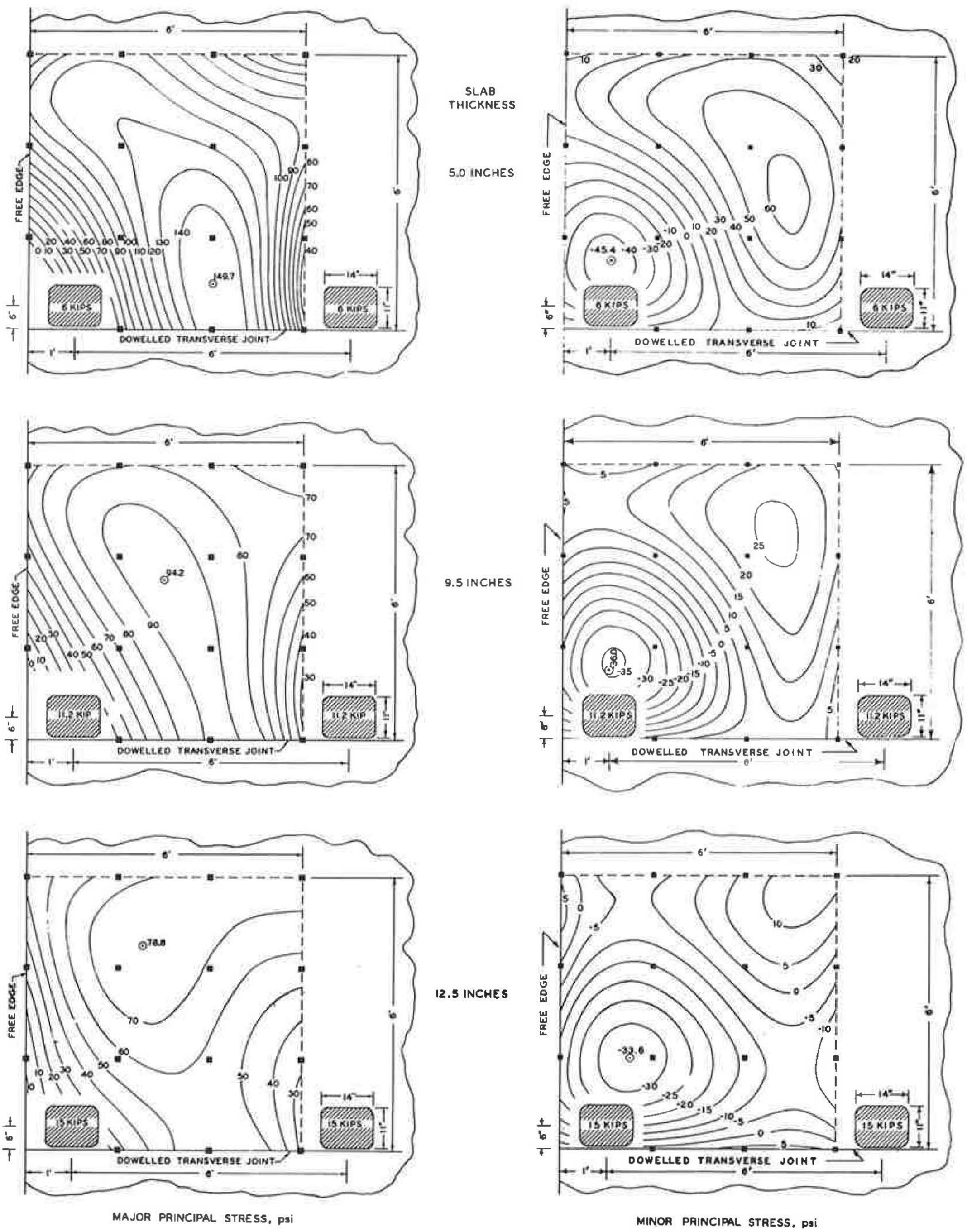

Figure 9. Contours of principal stress for corner load.

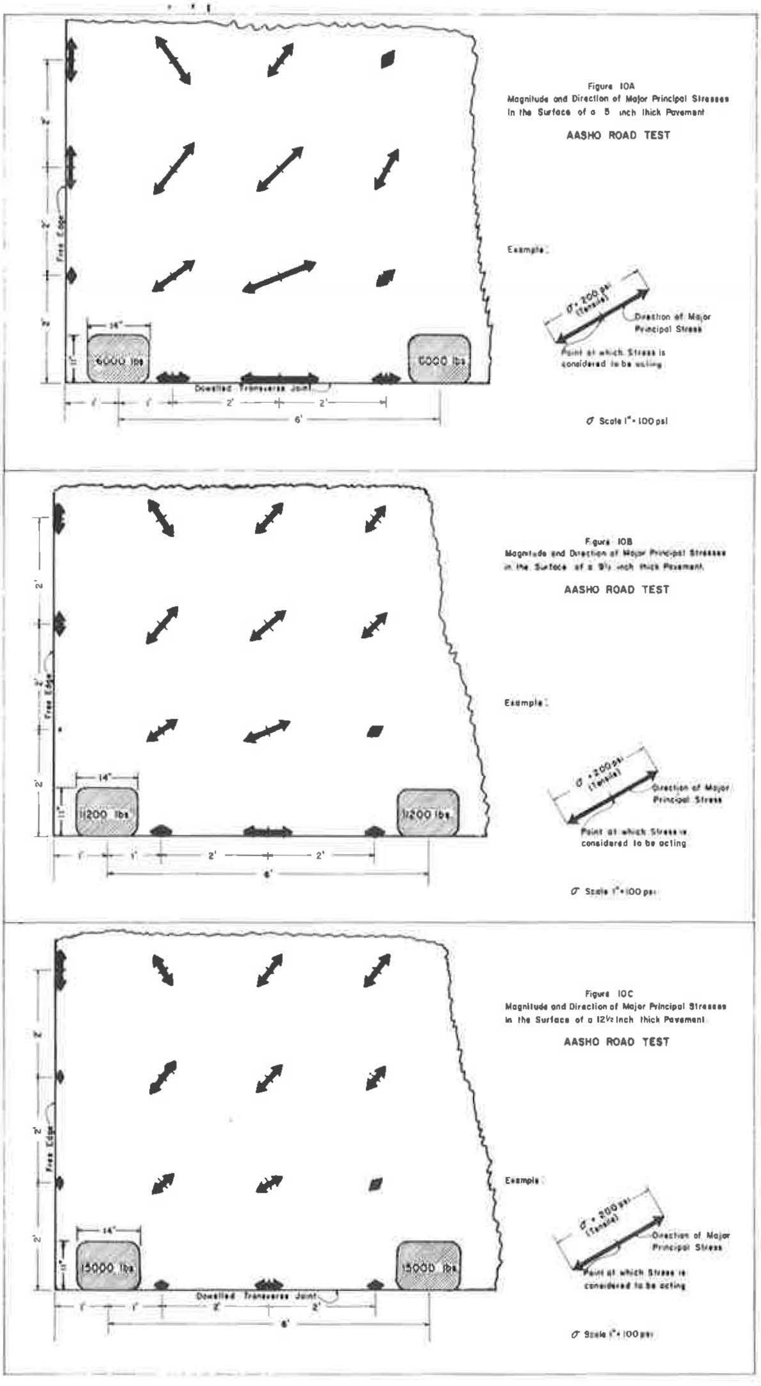

Figure 10. Magnitude and direction of major principal stresses.

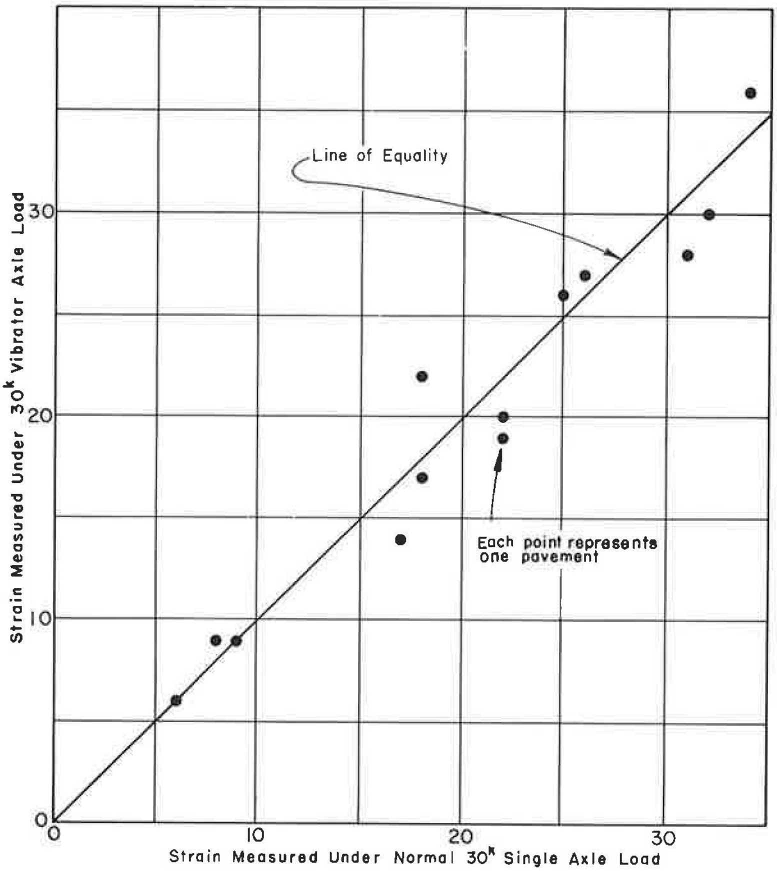

Figure 11. Correlations of vibratory loads and normal load.

loading device are comparable to stresses under normal traffic. It seems reasonable to compare the stress equations obtained for the two loading conditions to evaluate this device. It is also desirable to compare the observed stresses for selected pavement slabs under both routine truck traffic and the vibrator loaded to the same axle weight.

Figure 11 indicates that strains measured under a normal 30-kip single-axle vehicle and a 30-kip vibratory load are substantially equal.

If T is made equal to zero the main loop equation for edge stresses under single-axle loads (Eq. 4) becomes

$$\sigma_{es} = \frac{139.2\ L_1}{D_2^{1.278}} \tag{22}$$

Eq. 22 gives stresses nearly equal in value to those computed from the Loop 1 critical edge stress equation (Eq. 18) as shown in Figure 12. When D is 11 or 12.5 in., the stresses are numerically equal. The difference between these two equations could be due to one or more of the following reasons among others:

1. σ_{ev} are maximum stresses and their location varies with slab thickness, whereas σ_{es} is calculated for a fixed edge location.

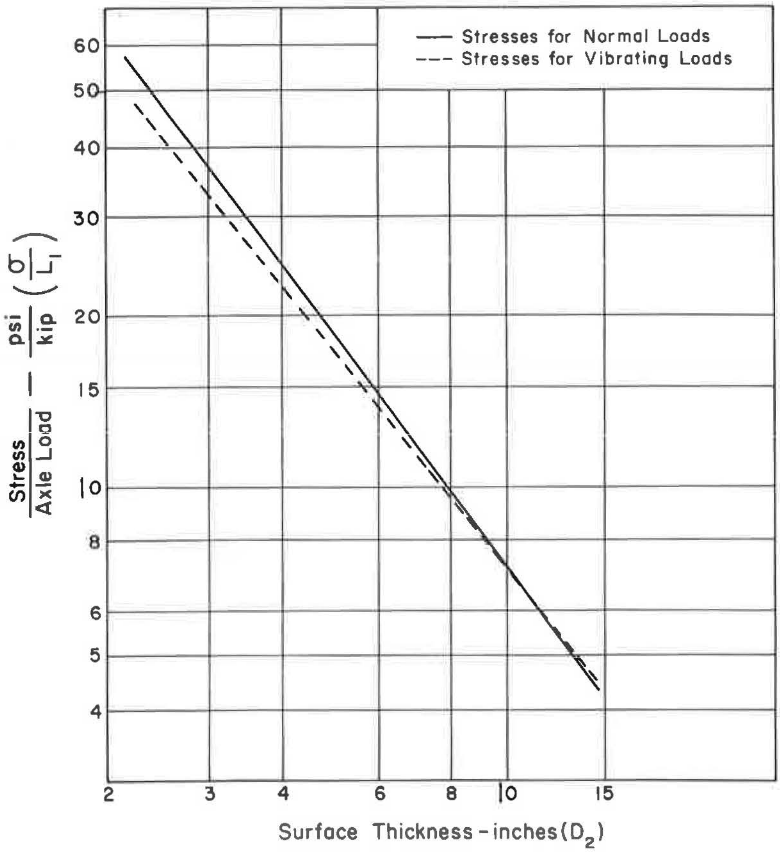

Figure 12. Comparison of normal load and vibratory load edge stress equation.

2. The loads used to induce σ_{ev} were applied through a wooden contact area of fixed size; σ_{es} were induced by normal tires and in general the contact area increased with slab thickness.

3. Both σ_{ev} and σ_{es} occurred with the load near the pavement edge; however, the centroid of the loaded area was slightly closer to the location of σ_{ev} than to the location of σ_{es}.

This close agreement between these stress equations supports the thesis of using the dynamic loader for future experiments with dynamic stresses.

PREVIOUS THEORETICAL AND EXPERIMENTAL WORK

This section compares the AASHO Road Test strain experiments with the theoretical equations developed by Westergaard, as well as the observed stresses and the resulting empirical equations from:

1. Bureau of Public Roads Tests conducted at Arlington, Va., 1933 to 1942, by Bureau of Public Roads' personnel and reported by Teller and Sutherland (4). Equation was developed and reported by Kelley (9).
2. Iowa State College Tests conducted indoors, 1930 to 1938, by Spangler (5).
3. Maryland Road Test, strain measurements made on the Maryland Road Test pavements 1950 (12) Highway Research Board Special Report 4.
4. Pickett Equation, mathematical work done by Pickett (11) in an effort to make an empirical equation which has rational boundary conditions as well as fit observed data previously reported by others.

These comparisons and analyses are broken into four categories: corner load conditions, edge load conditions, miscellaneous comparisons, and general overall comparisons. Necessary descriptive data relative to comparisons with the Road Test data are given.

Bureau of Public Roads' Arlington Tests

In 1930, the BPR began a research project, a portion of which had as its objective, "a study of the deflections, strains, and resulting stresses caused by highway loads placed in various positions on concrete slabs of uniform thickness." The data obtained from this project were analyzed using Westergaard's 1926 equations primarily.

Description of the Project.—Concrete Pavement.—The investigation was carried out on 10 full-size concrete pavement slabs especially constructed near Arlington, Va. Each of these slabs was 40 by 20 ft overall, divided by 1 longitudinal and 1 tranverse joint to produce 20-by 10-ft panels. Each slab was separated from those adjoining it by a 2-in. open joint. Slabs of uniform thickness of 6, 7, 8, and 9 in. were constructed. All slabs were nonreinforced (plain concrete). The static modulus of elasticity for concrete control specimens after 12 months' storage in a normal laboratory atmosphere averaged 4,500,000 psi for summer conditions and 5,500,000 psi for winter conditions. Poisson's ratio was assumed to be 0.15. Coarse aggregate was 1½-in. maximum size limestone. The concrete was proportioned to provide an average 28-day flexural strength of 765 psi. The average compressive strength at 28 days was 3,525 psi.

Subgrade Conditions.—The supporting soil for the slabs was a uniform brown, silty loam, Class A-4. The subgrade was plowed to a depth of about 10 in. before construction of the slab. After remaining in this loose condition for several weeks it was compacted with a 5-ton tandem roller followed by a loaded 5-ton motor truck. Daily sprinkling was provided during construction to maintain a uniform moisture content. The soil had a liquid limit of 25, a plasticity index of 9, a shrinkage limit of 19, and a shrinkage ratio of 1.8.

Testing Procedures.—Loading Procedures.—For the corner and interior loading conditions circular metal bearing plates with 6-, 8-, 12-, 16-, and 20-in. diameters were used. For edge loadings the bearing plates were semicircular with the diameter acting at the slab edge. Static loads were applied through a jack and reaction loading system. It was found that from 1 to 5 min of load application was required to "develop maximum stress." Therefore, all loads were applied for 5 min with a recovery period of at least 5 min between loads. This long loading period should be kept in mind when these observed stresses (strains) are compared with stresses observed under normal momentary dynamic loads. Loads of 7,000, 9,000, 12,000 and 15,000 lb were applied, respectively, to the 6-, 7-, 8-, and 9-in. pavement slabs. These loads created maximum stresses which approximated one-half of the modulus of rupture of the concrete.

Determination of Modulus of Subgrade Reaction.—Westergaard's original equations involve a coefficient of subgrade stiffness k called the subgrade modulus. To make practical use of the Westergaard equations, it is necessary to assign a value to this subgrade modulus for the conditions prevailing during the test. At the time of this particular investigation no determinations of the value of such a soil coefficient had been made. There was, therefore, no previous experience to indicate either the probable range of values of coefficients or a procedure by which values might be obtained. It was decided, however, that the factor used should simulate the action of a loaded slab. As a part of this experiment, tests were made to develop a proper testing procedure for determination of k. The procedure selected was that of loading a 30-in. diameter steel plate on the subgrade until a deflection of 0.05 in. was reached. Unit load required to produce this deflection was divided by 0.5 in. resulting in the coefficient k in pounds per square inch per inch of deflection.

It is important to note at this point that the k value used by the Bureau of Public Roads in its analysis of this test was not derived from the described plate bearing test. Instead k was determined by substituting the observed deflection of a loaded slab in the theoretical equation for maximum deflection and solving the equation for the value of k. In general a pavement design would not have the advantage of this method of evaluating k and other correlating methods must be developed.

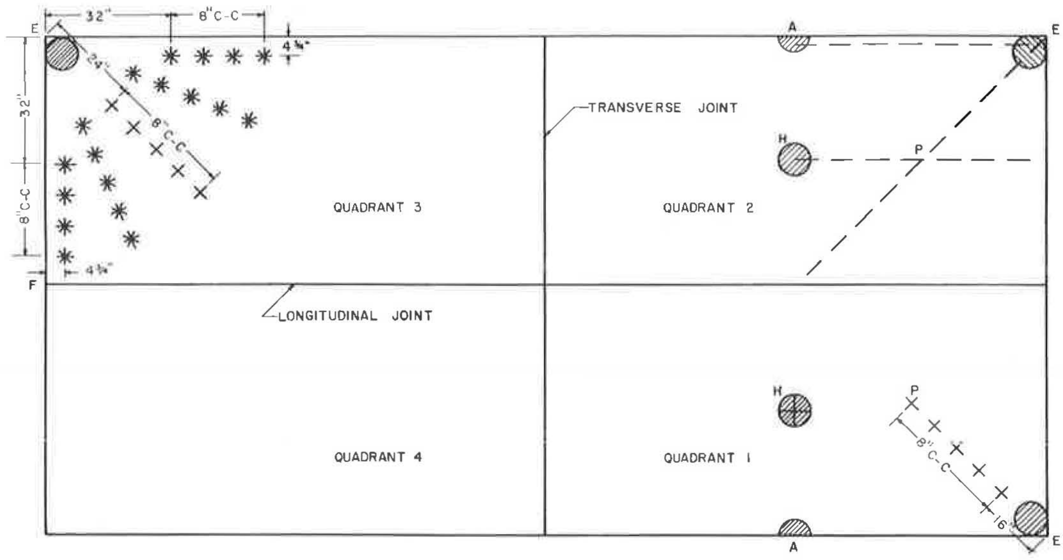

Figure 13. Plan of BPR test slab.

Strain Measurements and Stress Determinations.—Strain Measurements.—Strains were measured with a temperature compensating recording strain gage approximately 6.6 in. in length installed between metal plugs set in the top surface of the concrete slab. To evaluate the bottom strains it was assumed that the strain in the bottom of the slab was equal to the strain in the surface of the slab directly above it though opposite in sign. The assumption has previously been substantiated. Teller reported that in one test series the recording strain gages were attached to both bottom and top of a concrete slab which was supported on the ends only. Equal and opposite strains were recorded at both slab faces when load was applied. Additional research into this point would be very helpful because some tests at very high loads indicate a shift in the neutral axis of the slab with a resulting differential in the strain at top and bottom. However, the assumption of equal strains top and bottom is common to all the tests discussed in this paper. An example slab showing locations of applied load and arrangement of strain gages is shown in Figure 13.

Stress Determinations.—The measured strains were converted to stress by the use of elastic theory. The equations used are the same as those reported in Report 5, Appendix E, p. 290 for the Road Test measurements.

Iowa State College Tests

About 1930, research was begun at Iowa State College in an attempt to study corner stress conditions. The primary purpose was to provide experimental data for verification or modification of the original corner equation and the Westergaard corner equation for the design of concrete pavement slabs.

Description of the Project.—Concrete Pavement.—Five experimental slabs were constructed in a basement laboratory to provide controlled conditions for testing. Slab 1 was used primarily for development of procedure and measuring techniques. Details of the remaining slabs are given in Table 3. In the study of these slabs, slight tipping of the corner opposite the load was noted, but this was assumed to be negligible by the original author.

TABLE 3

PHYSICAL CHARACTERISTICS AND DIMENSIONS OF TEST SLABS[a]

Slab	Date Const.	Date Tested	Size (ft)	Thickness (in.)	W/C Ratio (by wt.)	Moist Curing	Avg. Properties of Control Specimens at Time Tested: Compression (psi)	Modulus of Rupture (psi)	Modulus of Elasticity (psi)	Poisson's Ratio
2	1932	1932-33	10 × 12	6	0.80	Earth	4,400	650	3,750,000	—
3	6/18/35	7/5 to 9/20/35	10 × 12	6	0.80	Burlap	3,300	520	2,270,000	0.20
4	6/24/36	7/15 to 8/15/36 1/9 to 2/23/37	12 × 12	6	0.75	Burlap	4,700	680	4,000,000	0.25
5	6/2/38	7/8 to 8/8/38	12 × 12	4	0.80	Burlap	3,080	490	2,430,000	0.23

[a]No reinforcement; high-early strength cement; limestone coarse aggregate; mix, by weight, 1:4:4; control specimens were beams and cylinders.

Subgrade.—The subgrades for the experimental slabs were constructed by tamping moist, yellow, clay loam in thin layers within a 12- by 14-ft wooden crib for slabs 2 and 3, and a 14- by 14-ft crib for slabs 4 and 5. All the subgrades were 2-ft thick above the concrete floor. Values of k, subgrade modulus, were assigned by dividing the unit load at any point within the slab by the deflection of the slab at that point. For analysis, the value of k was taken to be 100. Spangler reports that under the slab the value of k decreases as the radial distance from the corner increases. For example, under slab 5, k varied from 650 psi per in. at the corner to about 50 psi per in. at a distance of 40 in. from the corner. This is not consistent with the original Westergaard assumption that k is considered uniform at every point under the slab. Westergaard later reports, however, that k probably varies under the slab with the deflection.

Load Procedures.—Static loads were applied to slabs through a circular cast-iron 6.72-in. diameter bearing plate. A cushion of corn-stalk insulation board was used between the plate and the slab to help distribute the load uniformly over the circular area. Loads were measured with a pair of calibrated springs mounted between two cast-iron plates. Load magnitudes are given in Table 4.

Stress Determinations.—Strains were measured by means of optical levered extensometers approximately 3 in. long. These extensometers were placed in a rosette pattern and provided data for calculation of the maximum and minimum principal strains by graphical construction. These principal strains were then converted to stresses by the equations given in Report 5, Appendix E (2).

Maryland Road Test Strain Measurements

During the last six months of 1950, controlled traffic tests were run over a 1.1-mi section of PCC pavement constructed in 1941 on US 301 approximately 9.0 miles south of LaPlata, Md. The pavement consisted of two 12-ft lanes each having a 9-7-9-in. cross-section and reinforced with wire mesh. Expansion joints were spaced at 120 ft intervals with 2 intermediate contraction joints at 40 ft spacings. All transverse joints had ¾-in. diameter dowels on 15-in. spacing, and the adjacent lanes were tied together with tie bars 4 ft long spaced at

TABLE 4

LOAD VALUES USED IN IOWA STATE TESTS

Slab	Loads for Which Strains Recorded		
2	1,000	200	3,000
3	3,000	4,000	5,000
4	3,000	4,000	5,000
5	2,500	—	—

4-ft intervals. These pavements had been under normal traffic for approximately 9 years. There were very slight and localized systems of distress which indicated that their design was adequate for the traffic carried before the test. The test pavements were divided into four separate sections. Each section was subjected to repetitions of a single load. The four loads were 18-kip single axle, 22.4-kip single axle, 32-kip tandem axle, and 44.8-kip tandem axle.

Description of the Project.—Concrete Pavements.—The concrete in these slabs had an average compressive strength of 6,825 psi, an average modulus of rupture of 785 psi. The design cross-section thickness was closely approximated in construction according to field measurements. The static modulus of elasticity varied from 4,200,000 to 5,003,000. A value of 5,000,000 was used for all strain-to-stress conversion. The sonic or dynamic modulus averaged 5,700,000 for air-dried conditions and about 5,900,000 for wet specimens.

Subgrade Conditions.—The subgrade classifications and variation for the four test sections are given in Table 5.

Program of Strain Measurements.—Strains were measured for a variety of loads including the standard cases of interior loading, edge loading and corner loading. The results of the free edge load and the corner load conditions are primarily dealt with herein. Figure 14 shows these loadings with reference to the slab. Various studies were made on these test pavements. Those discussed in this comparison are load-stress relationships, speed-stress relationships, variation of stress with temperature differentials with the slab and variation of stress with subgrade support conditions.

Strains were measured with SR-4, type A9 (6-in. length electrical resistance) strain gages. All strain values were recorded with a direct-writing oscillograph. The strain gages were cemented into place on the slab surface and sealed with appropriate waterproof protection. Conversion of strain to stress was made using the appropriate elastic equations given in Report 5, Appendix E (2).

Pickett's Mathematical Studies

Pickett noted that several of the theoretical and empirical formulas developed for corner stresses in concrete pavement had poor boundary conditions. For example, the

TABLE 5

SUBGRADE CONDITIONS—MARYLAND ROAD TEST

Load No.	Max. Axle Loading (lb)	HRB Classification Group[a]				
		A-1	A-2-4	A-4	A-6	A-7-6
1	18,000 (single)	27	2	4	56	11
2	22,400 (single)	25	6	4	54	11
3	32,000 (tandem)	0	0	14	68	18
4	44,800 (tandem)	0	0	14	65	21

[a]Percent of total number of slabs in each lane supported by indicated soil.

Note: In general, the ratings of soils within these groups as a subgrade material are: (1) excellent for A-1; (2) good to fair for A-2-4; (3) fair to poor for A-4; and (4) poor for A-6 and A-7-6.

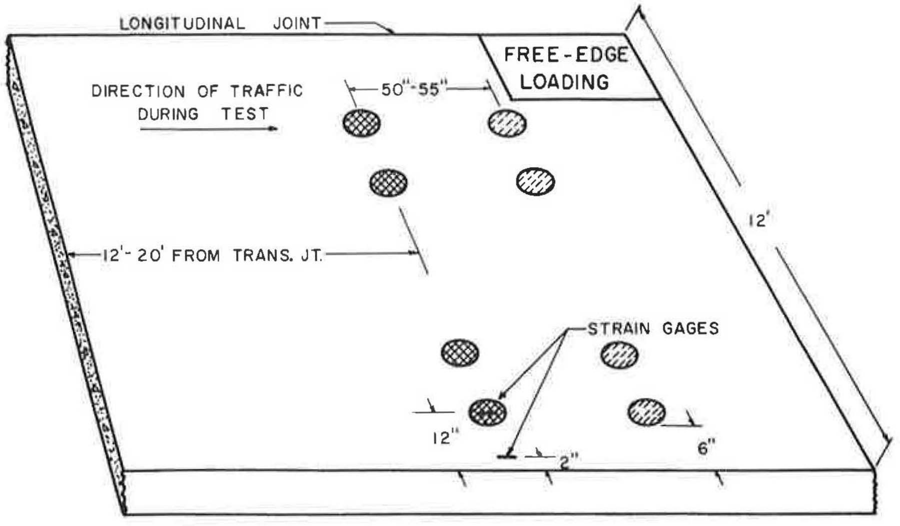

POSITION OF WHEELS AND LOCATION OF STRAIN GAGES FOR MEASUREMENT OF CRITICAL STRAINS FOR FREE-EDGE LOADING

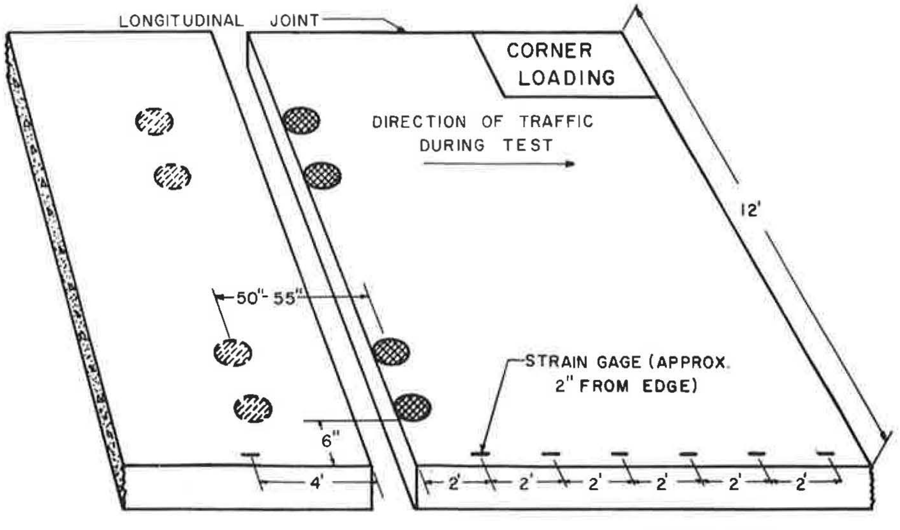

POSITION OF WHEELS AND LOCATION OF STRAIN GAGES FOR MEASUREMENT OF CRITICAL STRAINS FOR CORNER LOADING

Figure 14. Wheel positions for critical edge and corner strains.

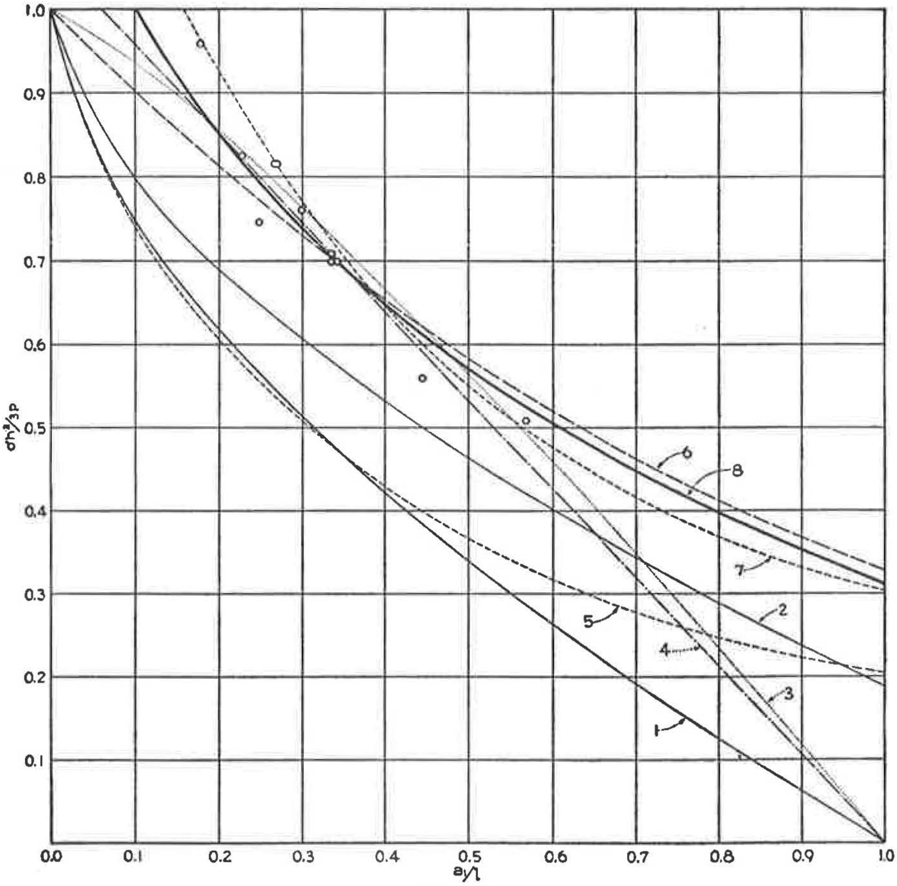

LEGEND

Curve 1 (Westergaard)	$\frac{\sigma h^2}{3P} = 1 - \left(\frac{a_1}{l}\right)^{0.6}$	Curve 5, Theoretical ————	Full subgrade support
Curve 2 (Bradbury)	$\frac{\sigma h^2}{3P} = 1 - \left(\frac{a_1}{\sqrt{2}\,l}\right)^{0.6}$	Curve 6, Theoretical ————	Partial subgrade support
Curve 3 (Kelley)	$\frac{\sigma h^2}{3P} = 1 - \left(\frac{a_1}{l}\right)^{1.2}$	Curve 7, Theoretical ————	50% Increase over Curve 5
Curve 4 (Spangler)	$\frac{\sigma h^2}{3P} = \frac{3.2}{3}\left[1 - \frac{a_1}{l}\right]$	Curve 8, Semi-empirical ——	$\frac{\sigma h^2}{3P} = 1.4\left[1 - \frac{\sqrt{a_1/l}}{1.1 + \frac{0.185 a_1}{l}}\right]$

° Plotted points represent experimental data furnished by the Public Roads Administration

Figure 15. Comparison of theory with existing stress equations.

Westergaard, Kelley, and Spangler equations all indicate stress to be zero when the ratio of the radius of the loaded area to the radius of relative stiffness equal 1.0 (Fig. 15). Because of these observations, Pickett has worked toward the development of a formula which has the shape and characteristics of the Westergaard equation, but which has more rational boundary conditions.

COMPARISON OF THEORETICAL AND OBSERVED STRESSES FOR CORNER LOAD CONDITIONS

Many of the concrete pavement design equations used in the past 30 years have been corner equations. Thus, it is interesting to compare all available information with the Road Test experimental results for the case of corner loads.

BPR Arlington Tests

Effect of Modulus of Elasticity on Indicated Stresses.—Figure 16 shows in solid lines the comparison of indicated and theoretical stresses in the 6-, 7-, 8-, and 9-in. slabs. The stresses were obtained by using an average value of E determined for the corner load conditions. Table 6 indicates that this value of E is considerably lower than E determined from the other two load conditions. The authors of the BPR report therefore calculated the values shown in dashed lines by using the average E for interior and edge loading. In their opinion, the theoretical (Westergaard) and observed stresses agree closely for the 6- and 8-in. slabs because these slabs were tested when warped

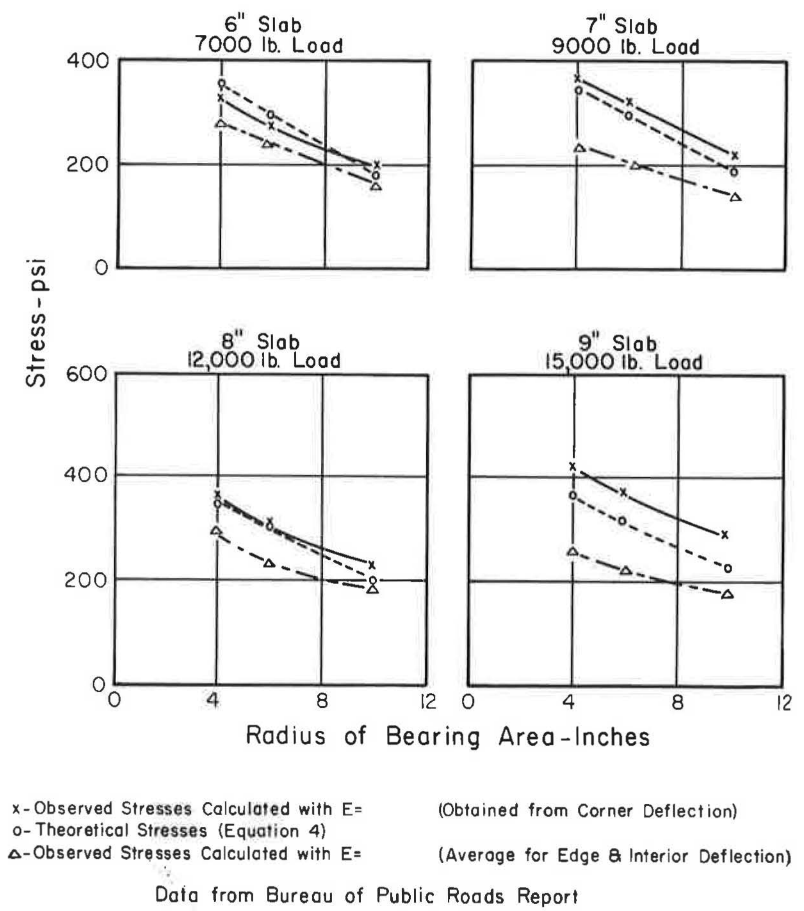

Figure 16. Comparison of theoretical and observed stresses for corner load.

TABLE 6

VALUES FOR VARIOUS COEFFICIENTS, WESTERGAARD EQUATIONS, DETERMINED FROM MEASURED DEFLECTIONS, BPR TESTS[a]

Load Position	Testing Time	Slab Thickness (in.)	l (in.)	k (pci)	K (psi)	D (psi)	E (psi)
Corner	Late summer	6	26	143	3,708	96,400	3,540,000
	Winter	7	28	161	4,515	126,400	3,390,000
	Winter	8	30	227	6,825	204,700	4,220,000
	Late fall	9	33	168	5,535	182,600	3,200,000
Interior	Late summer	6	25	195	4,880	122,000	4,140,000
	Winter	7	29	238	6,895	200,000	5,750,000
	Summer	7	28	222	6,230	174,400	4,670,000
	Winter	8	31	260	8,065	250,000	5,500,000
	Late fall	9	36	203	7,315	263,200	5,490,000
	Summer	9	33	220	7,290	240,500	4,210,000
Edge	Late summer	6	26	171	4,440	115,400	4,235,000
	Winter	7	29	212	6,145	178,200	5,125,000
	Winter	8	30	279	8,365	251,000	5,175,000
	Late fall	9	34	243	8,260	280,800	5,220,000

[a]Source: Public Roads, 23:8, p. 187.

downward. Observed stresses for the 7- and 9-in. slabs were higher than theory indicates because they were tested while warped upward. Additional tests on the 7- and 9-in. slabs while warped down seem to verify these observations. The following conclusions were drawn:

1. Values of E calculated for corner leading conditions are unrealistic.
2. If the conditions are such that the corner is receiving full subgrade support, values of critical stress for corner loading (Case 1) computed from the Westergaard equation can be used with confidence. When full support does not exist the computed stresses will be too low.

Variation of Critical Stresses with Slab Curling or Warping.—The authors compared critical or maximum load stresses observed for three positions of the slab: (a) corners warped up, (b) flat, and (c) corners warped down. Table 7 gives a compilation of these values with the comparative values of maximum stress observed at the Road Test (formulas were used to interpolate for the correct load and slab thickness).

Figure 17 shows the stress-slab thickness comparisons for the Arlington and Road Test experiments as well as for several stress equations. The Road Test stresses are considerably smaller than the BPR stresses or the theoretical stresses. The Road Test stresses are those due to dynamic (transient) loads (load time $1/12$ sec), whereas the BPR stresses are those under a static load (load time 5 min). The Road Test stresses were also measured at a corner with a doweled joint, whereas the BPR slabs had free joints and edges. Based on a comparison of other strain studies at the Road Test it appears likely that one-fourth to one-third of the load is transferred to the adjacent slab, thus reducing the induced strains and, thus, stresses in the study by 25 to 33 percent.

Directions of Maximum Principal Stresses.—In connection with the main studies, the BPR made some supplementary studies to indicate the direction and magnitude of the principal stresses induced by corner loads (Figs. 18 and 19). An 8-in. uniform

TABLE 7

COMPARISON OF CRITICAL STRESSES
BPR ARLINGTON TEST AND AASHO ROAD TEST

Wheel Load	Slab Thick (in.)	Arlington BPR			Theoretical Westergaard Case 1	AASHO Road Test	
		Warped Up	Flat	Warped Down		Warped Up[a]	Warped Down[b]
5^k	6	288	274	228	200	91	46
7^k	7	325	308	253	218	95	48
10^k	9	290	277	220	210	92	47

[a]Night. [b]Day.

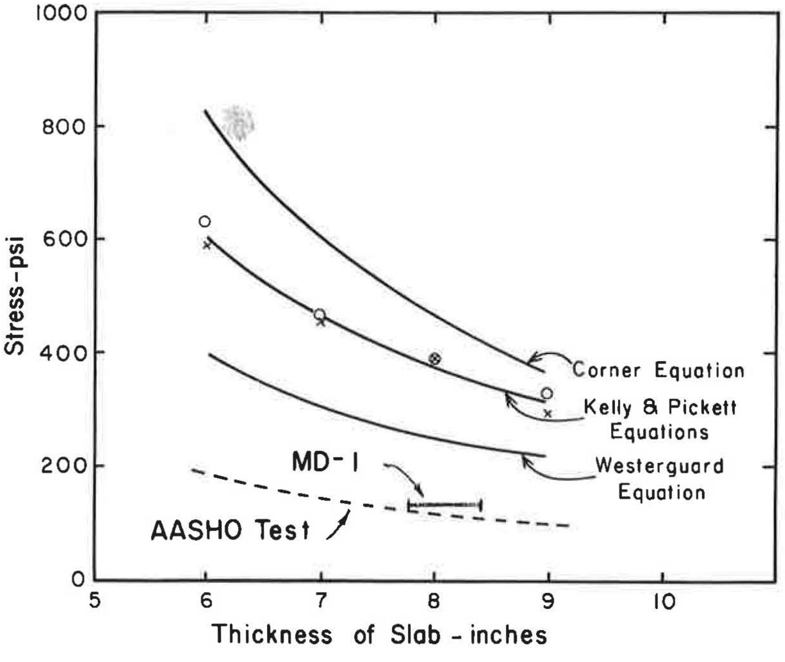

NOTE:

1. Plotted points represent data from B.P.R. Arlington Tests with 10,000 pound load, 12 inch diameter bearing area.

2. Dotted curve represents observed stresses from AASHO Road Test. Fitted Equation: $\sigma_c = \frac{385 L_w}{h^{1.7}}$

Figure 17. Comparison of observed stresses with four stress equations.

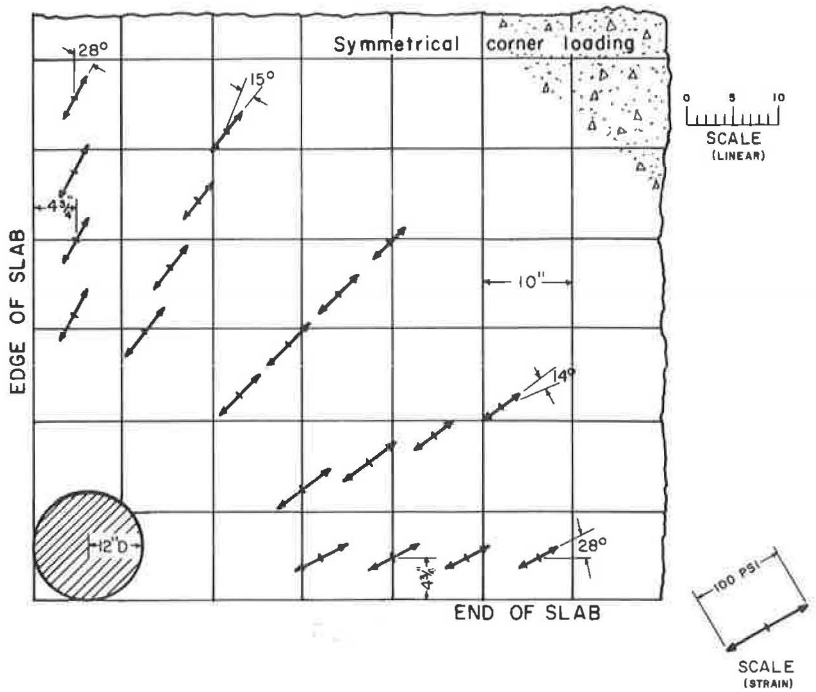

Figure 18. Direction of stresses, BPR Arlington tests, symmetrical corner loading.

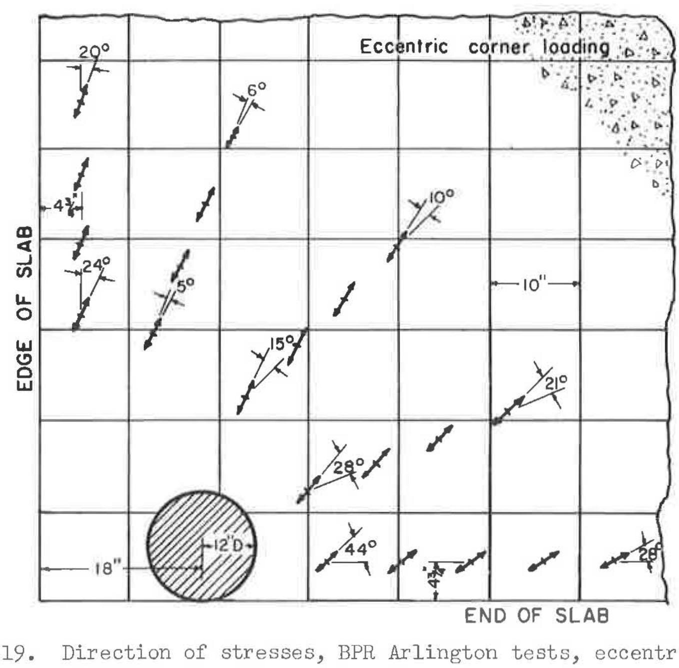

Figure 19. Direction of stresses, BPR Arlington tests, eccentric corner loading.

thickness slab and a 9-6-9-in. slab were compared with a symmetrical corner load and an eccentric corner load (Fig. 19). Moving the load from the corner toward the centerline 18 in. caused a shift in the direction of maximum stresses. The shifts were counter-clockwise angular displacements of 7 to 14 degrees.

Kelley's Empirical Equation.—To summarize their work on corner stresses the authors of the BPR report indicate that the Westergaard equation for Case 1 (Eq. 4) gives an accurate indication of maximum load stress when the pavement corner is in full contact with the subgrade. In the BPR investigation this condition was attained only when the corner was warped downward. If Eq. 4 is used for computing load stress, the condition of corner warping due to temperature would be such as to create a moderate compressive stress in the upper surface of the slab in the region where the load would create the maximum tensile stress. Thus the combined stress would be slightly lower than the load stress.

For other cases when the slab corner is not in complete bearing on the subgrade due to upward warping, Eq. 4 will give load stress values somewhat lower than those which are actually developed. For this condition the Arlington experiments indicate an empirical equation which gives computed values which are more nearly in accord with those observed. This equation was reported by Kelley in 1939 (9).

$$\sigma_c = \frac{3P}{h^2}\left[1 - \left(\frac{a_1}{\ell}\right)^{1.2}\right] \tag{23}$$

in which

σ_c = maximum tensile stress, in psi;
P = load, in lb;
h = thickness of concrete slab, in in.;
a_1 = the distance, in in. from the corner of the slab to the center of the area of load application; it is taken as $a\sqrt{2}$ where a is the radius of a circle equal in area to the loaded area;
$\ell = \frac{Eh^3}{12(1-\mu^2)k}$ = radius of relative stiffness;
E = Young's modulus for the concrete, in psi;
k = subgrade modulus, in psi/in.; and
μ = Poisson's ratio for the concrete.

To summarize, as a general rule the most critical condition for the corner loading is at night when the corner tends to warp upward; the subgrade support is least effective at that time. Any warping stress in the corner is also additive to the load stress.

Iowa State College Tests

New Hypothesis for Stress Distribution in Corner Region.—The Westergaard corner equation and the Older corner equation both imply the same assumption of uniform distribution of the maximum tensile stresses along a line normal to the corner bisector. Observations of stress and observation of structural corner breaks both in the laboratory and the field, led Spangler to the hypothesis that the locus of maximum moment produced in a concrete pavement slab by a corner load is curved line which bends towards the corner as it approaches the edge of the slab. It appears that the locus may lie anywhere between a straight line normal to the bisector (Westergaard assumption) and a circular curve tangent to that bisector having the corner as its center. Under this hypothesis the maximum stress will occur when the locus is a circular curve inasmuch as this is the shorter of the two limiting sections.

Figure 20, from the Spangler report, shows these limiting conditions along with a typical corner break.

Stress Direction and Magnitude.—Figures 21 and 22 indicate the direction and magnitude of principal stresses in slab 4 (6-in. thickness) under a 5,000-lb static load.

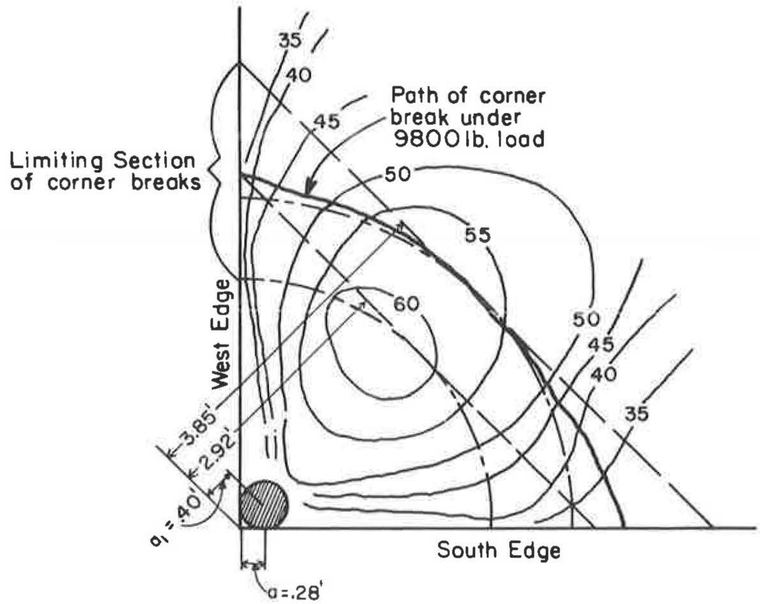

Figure 20. Stress contours for Iowa State College tests.

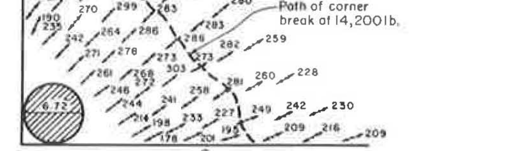

Figure 21. Magnitude and direction of maximum principal stresses.

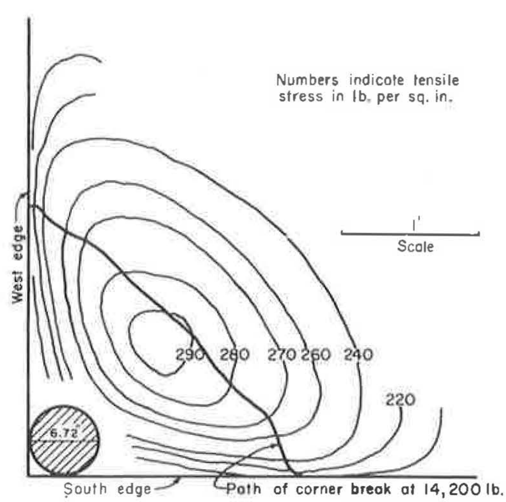

Figure 22. Stress diagram for maximum principal stress Iowa State College tests.

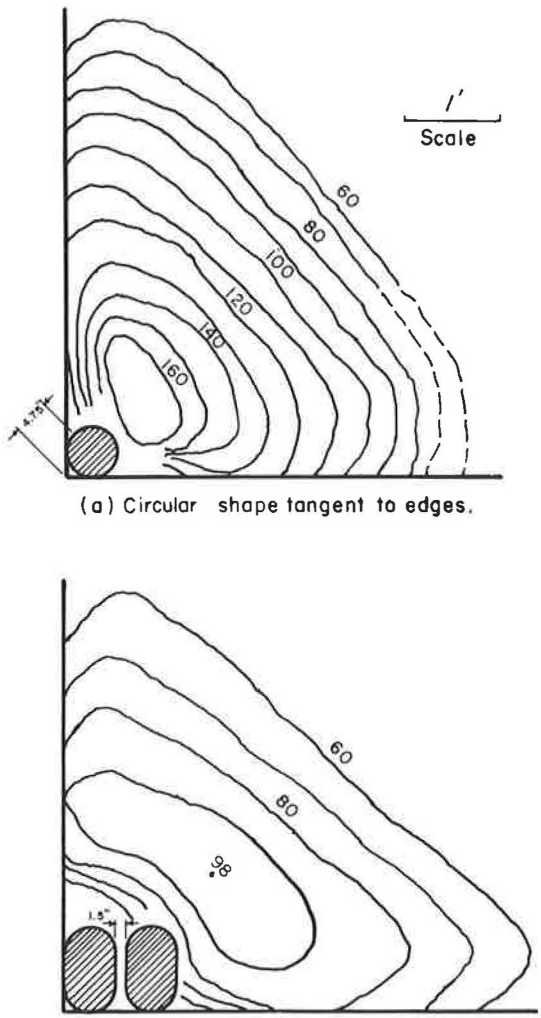

(a) Circular shape tangent to edges.

(b) Dual tire shape tangent to edges.

Note: Contours connect points of equal intensity of principal tensile stress. Values given are in lb. per sq. in.

Figure 23. Stress contours for slab 3, Iowa State tests.

These values were obtained by averaging readings from three separate loadings of the slab.

Slab 3 (6-in. thickness) was a smaller experiment than slab 4. Figure 23 shows the approximate principal stress contours observed on this slab for a circular and an elliptical load. As in slab 4, there is a considerable area over which the stress in slab 3 does not vary greatly. Although the slabs were of the same nominal thickness and approximately the same size, the maximum stress in slab 3 was only about 50 percent of that in slab 4. Spangler makes the following observations: "This is probably due to the fact that the subgrade under Slab 3 was stiffer than that under Slab 4 and that the modulus of elasticity of the concrete in Slab 3 was less than of Slab 4. It is difficult, however, to account for such a divergence in stress in this way since published analyses of stresses indicate that large variations in either or both of these coefficients cause relatively small variations in stress."

Iowa Study Conclusions

Table 8 compares the observed stresses in these studies with existing stress equations. It was concluded that in these studies observed stresses were in general agreement with the equation proposed by Kelley. The Kelley equation actually gives calculated stresses that closely agree with the observed stresses only for slab 2.

The Westergaard equation shows excellent agreement with the observed stresses for both slabs 4 and 5 and does not show too large a variation for slab 2. Since these slabs were constructed and tested in a closely controlled environment, to eliminate temperature and moisture curling, it would appear that the observed stresses should check the Westergaard equation more closely than the Kelley equation.

Maryland Road Test—Corner Load

The corner load-strain measurements at the Maryland and AASHO Road Tests were not as complete as the edge measurements. For that reason these comparisons will not be extensive. Comparisons will be made of load vs stress relationships and effects of corner warping (temperature differential).

These comparisons are further complicated by the nonuniform slab thickness of the Maryland pavements. In an effort to overcome this difficulty, results for several thicknesses from the AASHO tests have been compared with the Maryland data.

In the analysis of data from the Maryland test, static modulus of elasticity was used in the conversion of strains to observed stresses, whereas in the AASHO results

TABLE 8

COMPARISON OF STRESS EQUATIONS AND OBSERVED STRESSES—CORNER LOADING
(Iowa State College Tests)

Stress	Slab 2	Slab 4	Slab 5	Avg.
Westergaard Eq.	170	260*	255*	228*
Kelley Eq.	215*	350	415	326
Corner Eq.	250	410	470	376
Observed	230	285	215	243

*Indicates equation giving closest prediction for that slab.

dynamic E was used. It seems that a common type of E must be used if comparisons are to be valid. In the following work dynamic E has been used since the loads involved were dynamic or moving loads.

Load vs Stress.—Figure 24 shows a comparison of load-stress relationships at the two road tests. The MD-1 report indicates that a curvalinear relationship was found for slabs warped upward (early morning); whereas a straight-line relation existed with the slab warped down (day measurements). At the AASHO test after 26 series of such experiments, it was concluded from regression analyses that the relationship was a straight line within the limits of significant statistical error. There was some indication, however, that the relationship might be curvilinear for weaker subgrades.

Figure 24 shows that the indicated stresses from the MD-1 test approximate the stresses in a 7-in. slab at the AASHO test for conditions of upward warping. For conditions of downward warping, the MD-1, 9-7-9-in. slab acted much like an 8-in. slab at the AASHO test. This last comparison is considered to be the more valid since strain measurements of a slab on two different reasonably hot afternoons will agree without significant variation; whereas strains measured on two different mornings may vary considerably depending on moisture and temperature. Therefore, the general condition of downward warping is more stable than upward warping.

Effect of Corner Warping.—Additional complications arise with this comparison since quantitative information is not available about temperature differentials which existed at the time strains were measured. (The report merely indicates slabs warped up, flat or warped down.) The amount of warping, or more specifically the exact temperature differential of top minus bottom of the slab is very important in absolute strain existing. It can generally be concluded that the apparent effect of warping or curling was much the same for the Maryland and the AASHO Road Tests.

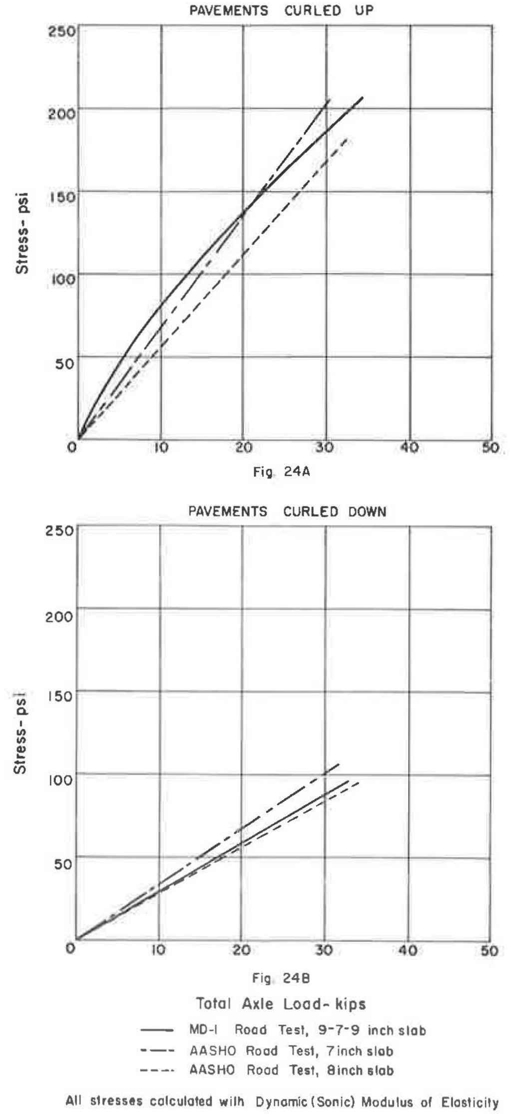

Figure 24. Load stress comparisons and effect of corner warping on stresses.

COMPARISON OF THEORETICAL AND OBSERVED STRESSES FOR EDGE LOADING

Edge loading was one of the three cases originally investigated by Westergaard. Study of these edge stresses has become more important with the advent of load transfer devices to help limit corner stresses. The use of longer joint spacing on reinforced concrete slabs and finally the development of continuously-reinforced concrete pavements have increased the need to study edge stresses. The largest strain experiment at the AASHO Road Test was measurement of edge strains. The most important edge strain experiments reported prior to the AASHO Test include the Bureau of Public Roads' Arlington Tests (4) and the Maryland Road Test (12).

In the AASHO tests, stresses under edge loads were generally higher than the stresses under corner loads. Figures 7 and 9 show some of the results of these tests. In all cases the maximum edge stresses occurred directly opposite the load. For tandem axles the maximum occurred opposite one of the pair of axles, usually the rear axle.

BPR Arlington Tests

The conditions of the BPR test and the AASHO Road Test have previously been discussed. It was necessary to adjust the AASHO results to conditions approximating the BPR test to compare the results. The following adjustments in the equation were made using experimental results from the Road Test:

1. Stresses will be 22 percent higher at creep speed, which is as nearly static as was tested.
2. Stresses will increase 24 percent due to change in placement of loaded wheels to approximate BPR placement.

The resulting equation for stresses at the Road Test which can be compared to the BPR tests is

$$\sigma_e = \frac{211\ L_1}{10^{0.0031T}\ D^{1.28}} \qquad (24)$$

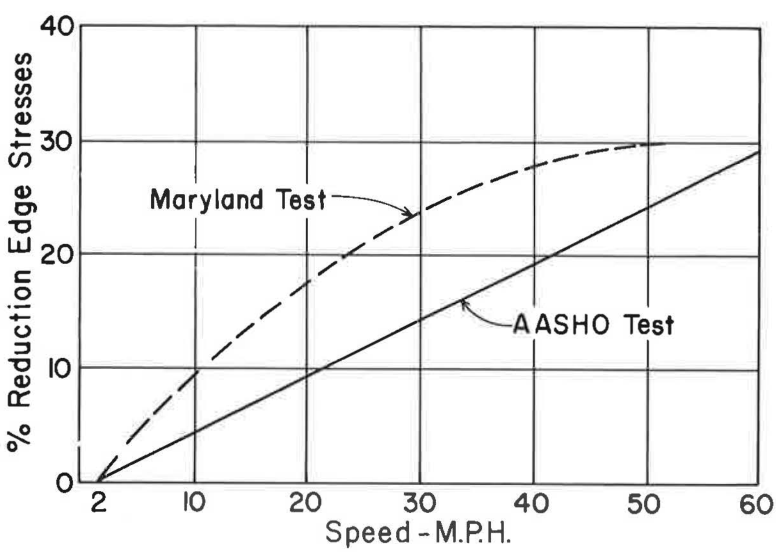

Figure 25. Effect of vehicle speed on pavement edge stresses.

or

$$\sigma_e = \frac{422\ P}{10^{0.0031T}\ D^{1.28}} \tag{25}$$

in which L is the axle load and P is a half axle load or wheel load. Other terms have previously been defined.

A static modulus has been used to convert the BPR strains because the load was static of 5-min duration. A dynamic modulus is assumed to apply for the AASHO Road Test since the load was always moving.

Stress Variation with Load.—To compare load study result, T is set equal to zero since no mention of warping conditions was made in this regard (4, Fig. 26). The results of this comparison are shown in Figure 26 for a 7-in. and 9-in. uniform thickness concrete slab. The load vs stress relationships are linear in all cases and the results for a given thickness very nearly agree. This indicates that the effect on stress of increasing the load might be expected to be the same on two pavements if the major physical variables such as temperature differential, load placement, and slab thickness are equal for the two pavements.

Stress Variation with Slab Thickness.—In the BPR report the effect of slab thickness was illustrated (4, Fig. 43). These data are shown in Figure 27. The basic information presented is for a study with pavement edges curled up. A similar curve for flat slabs has been developed by adjusting BPR data to a common load of 10,000 lb. Road Test data for both the curled up and flat positions are shown. A comparison of these curves indicates that the effect of curling was probably more severe on the BPR pavements than on the Road Test. This is to be expected because the BPR slabs had

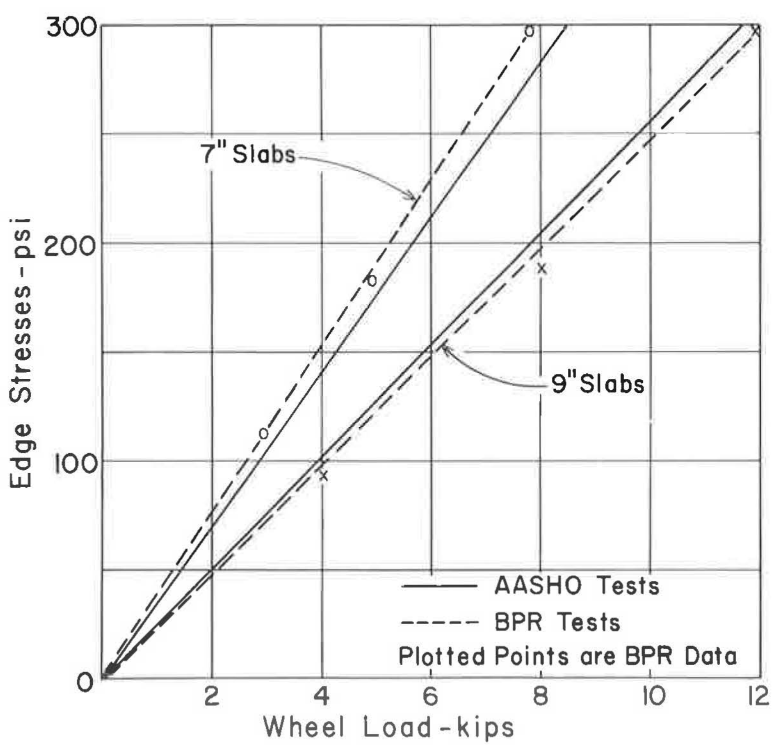

Figure 26. Comparison of load studies, BPR and AASHO tests.

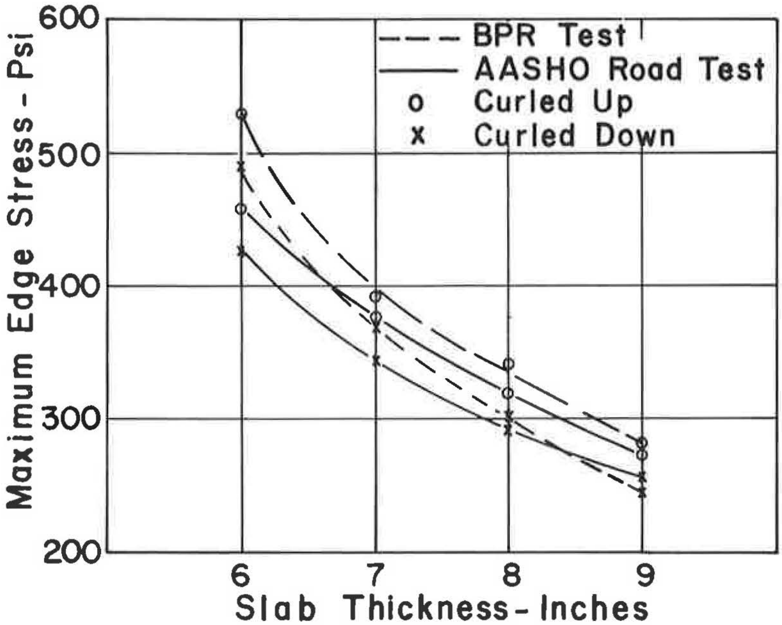

Figure 27. Effect of slab thickness, BPR and AASHO.

no adjacent slab giving restraint, whereas the Road Tests slabs were doweled to adjacent slabs. Further examination shows a variation in the shape of the curves which results in a cross at 8 in., thus explaining why Figure 26 shows BPR stresses higher on 7-in. slabs, but lower on 9-in. slabs. Figure 28, a plot of Westergaard's equation (Eq. 8) for the BPR physical conditions, agrees almost perfectly with the BPR "flat condition" data.

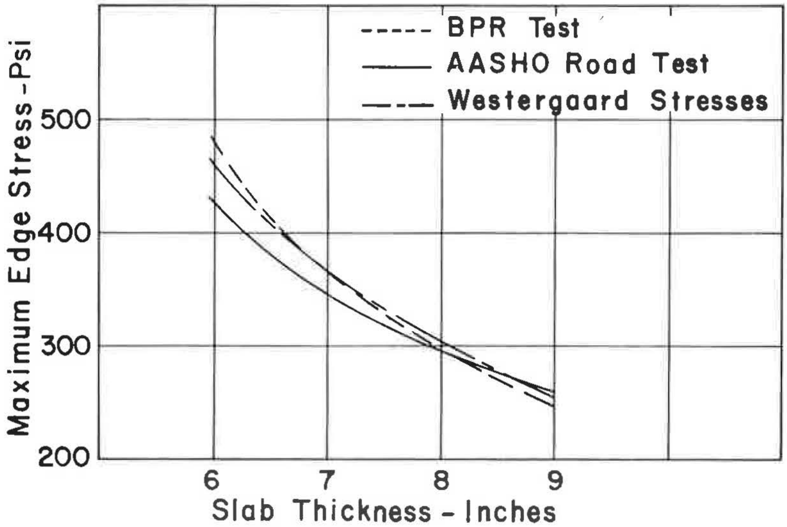

Figure 28. Comparison of BPR and AASHO with Westergaard equations for curled down pavements.

Maryland Road Test

To compare results, certain adjustments must be made in the AASHO stress equation and the Maryland data. Where reliable data were developed as part of the tests, the following changes were required:

1. The standard placement for the Maryland test was 3 to 4 in. nearer the edge than the AASHO Test. (For the AASHO Test the centroid of the loaded area was located 20 inches from the pavement edge.) Using published data (12, Fig. 13), Maryland results were adjusted to the AASHO placement.
2. In some cases the AASHO equation was adjusted to creep speed.
3. The Maryland tests involved normal dynamic vehicle loads.

At the AASHO Road Test the decision was made to use dynamic modulus of elasticity (E_d) with dynamic loads. For comparisons, the Maryland report gives results of load studies for pavement "warped or curled" up. To compare these results with the AASHO data, T (Eqs. 14 and 15) was taken as 7 degrees, a condition of moderate upward curl (-10° was the maximum negative temperature differential T observed at the Road Test). Figure 29 compares the load vs stress curves for the Maryland and AASHO Road Tests.

For single-axle loads the stresses on the 9-7-9-in. Maryland pavements were approximately equal to the stresses in a 9-in. uniform thickness pavement at the AASHO test. This indicates effective reduction of edge stresses by use of edge thickening.

For tandem-axle loads the stresses in a 8-in. AASHO Road Test slab closely approximate the stresses observed for the Maryland slabs. This indicates an averaging effect of the 9- and 7-in. portions because the stresses, although smaller than might be expected in a 7-in. thick slab, are not as small as they probably would have been for a 9-in. uniform thickness slab. The difference in the action of the 9-7-9-in. slab under the two types of load may be due to the broader stress patterns of the tandem loads. In other words, the tandem axles spread the load in such a way that a larger percentage of the 7-in. portion of the Maryland slabs comes into action. The apparent difference may be only experimental error in testing conditions though it is not likely since averages are used in the comparisons and no major known biasing effect is involved.

The load vs stress studies in the Maryland test indicate non-linear action (Figs. 29 and 30). The AASHO results show a linear effect. It is important to note that during the AASHO Test several individual studies indicated non-linear action. For the total picture, a linear equation always fits the data better than a non-linear one.

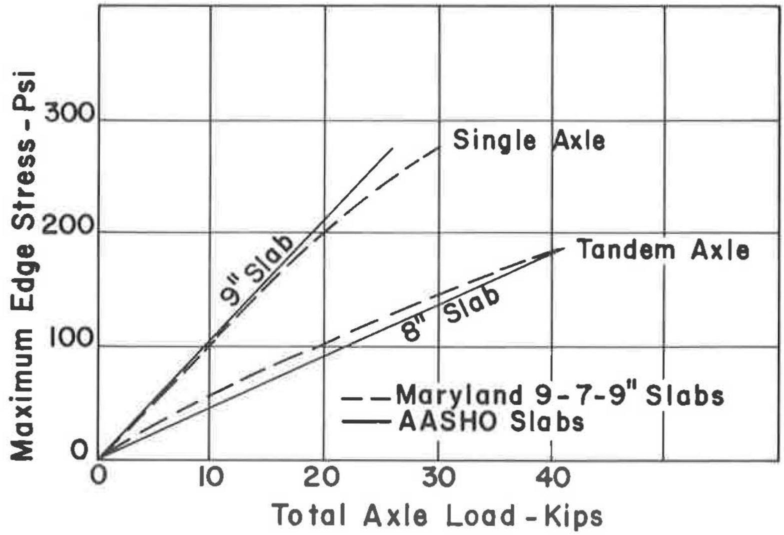

Figure 29. Comparison of load studies, Maryland and AASHO.

It was the conclusion at the AASHO Test that the load effect was linear, and it is believed that this holds true in general. It appears, however, that unexplained interaction effects may result in non-linear behavior for any given case study. Inasmuch as the Maryland tests were primarily case studies, this could explain the non-linear effect.

Variation of Stresses with Curling.—Curling, the warping of concrete pavements due to vertical internal temperature differential in the slab, affects the stresses in a concrete slab. A pavement which is curled upward will ordinarily exhibit higher compression stresses in the top than one which is curled downward. This was found to be true for both the Maryland and the AASHO Road Tests.

Figure 30 compares stresses in the AASHO and Maryland test pavements curled upward and downward. For both the single- and tandem-axle loads, the Maryland pavements indicate a greater reduction in stress from curled up to curled down condition than do the AASHO pavements. The stresses in the Maryland pavements were 28 percent smaller for the curled down condition than for the curled up condition, whereas the stresses for the AASHO pavements were 19 percent smaller for the down than for the up condition.

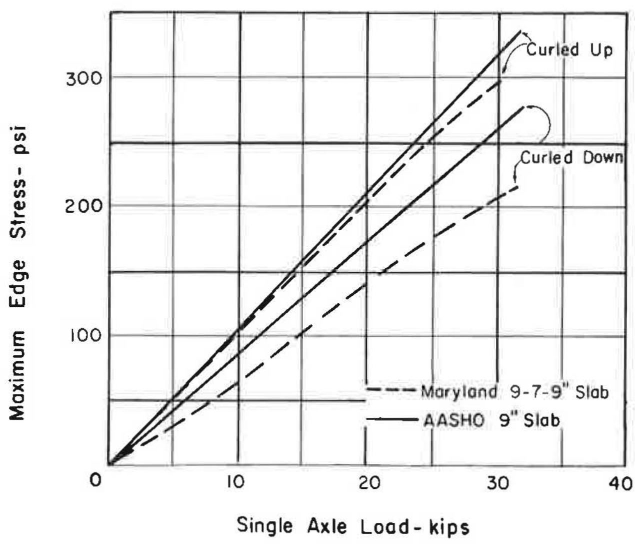

Fig. 30A

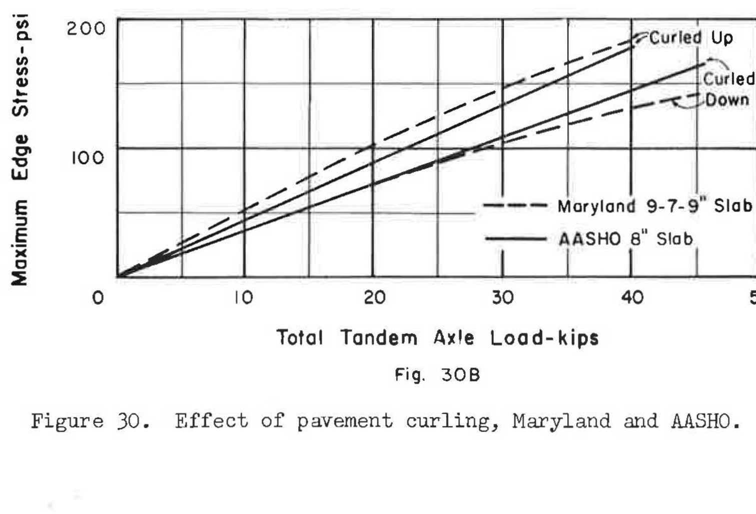

Fig. 30B

Figure 30. Effect of pavement curling, Maryland and AASHO.

This situation is hard to explain because during a 2-yr period on the AASHO Test only 1 percent of the observations of pavement temperature differential shows T greater than +20°. This was, therefore, taken as the maximum downward curl condition and used in these comparisons. The minimum differential was -10° for the up condition. Either the maximum temperature differential was greater in the Maryland test for the days involved or other conditions affecting curling warping (moisture, humidity, etc.) affected the results.

Summary of Edge Stress Comparisons

1. For equivalent conditions of load placement, vehicle speed, temperature differential within the slab, and physical constants, slab stresses vary in direct linear proportion to the load.
2. The load effects in the BPR test and the AASHO tests were equivalent within the limits of experimental error.
3. The edge stresses observed for the 9-7-9-in. slabs on the Maryland test were equivalent to the stresses in a 9-in. AASHO slab for single axles and an 8-in. AASHO slab for the tandem axles.
4. The variation of stress with slab thickness was regular for both the BPR and the AASHO tests. The BPR data for the flat or curled down condition is closely approximated by the original Westergaard equation. The Road Test results, however, show a smaller effect of thickness.
5. The general effect of pavement curling was observed to be the same in all tests. However, the effect of curl on stresses reported for the Maryland test was greater than any observed at the AASHO Road Test.

SUMMARY OF NEEDED RESEARCH

As a result of these dynamic studies, it appears that there is a need to study the effect of physical constants with relation to dynamic loads. It is believed that such a study would ultimately lead to a design equation relating all these factors in a manner similar to that proposed in the AASHO Rigid Pavement Design Guide, May 1962.

It would be desirable to study the effect of dynamic loads as related to modulus of elasticity, modulus of subgrade support, and strength of the concrete. There is sufficient proof available from the AASHO Road Test to indicate that such a study is both physically and economically feasible by employing a vibrating loader similar to that introduced at the Road Test.

Additional studies should be made on numerous factors including: (a) various types of load transfer devices, and (b) various types of supporting media including granular materials and various stabilized materials.

A large area of research is the combination of load-stresses with warping stresses in order to investigate the ultimate failure stresses in the pavement.

SUMMARY OF FINDINGS

Corner Load Stress Comparisons

1. The stresses predicted by the Westergaard equation, the corner load equation, or the Pickett equation are considerably higher than those observed at the AASHO Road Test. This is probably because (a) the effect of dynamic loads is not as great as a sustained static load of the same magnitude, and (b) the Road Test slabs were doweled to adjacent slabs and were not as free to deflect as theoretical equations predict.
2. The stresses observed for the Maryland test 9-7-9-in. slabs approximated those of 7- and 8-in. slabs at the AASHO Road Test in a curled up and curled down condition.
3. The directions of principal stresses are not symmetrical about the corner bisector for dual-tire loadings. The pattern is further altered if the slab joints are not free from restraint by other slabs.
4. The effect of slab warping or curling was observed to be much the same for the Maryland and AASHO Road Tests.

5. The load vs stress relationships at the Maryland and AASHO Road Tests were approximately equal and linear. There is some indication that slabs curled upward show non-linear variation of stress with load as the bottom support increases with increased load.

6. In future studies of pavement stresses a special effort should be made to obtain complete information concerning the physical factors affecting these stresses, including modulus of elasticity, modulus of subgrade support and concrete strength.

Edge Load Stress Comparisons

1. For equal load placement, vehicle speed, temperature differential within the slab, and physical constants, slab stresses vary in direct linear proportion to the load.

2. The load effects in the BPR tests and the AASHO tests were equivalent within the limits of experimental error.

3. Edge stresses observed for the 9-7-9-in. slabs on the Maryland test were equivalent to the stresses in a 9-in. AASHO slab for single axles and an 8-in. AASHO slab for tandem axles.

4. The variation of stress with slab thickness was regular for both the BPR and the AASHO tests. The BPR data for the flat or curled down condition is closely approximated by the original Westergaard equation. The AASHO Road Test results however show a smaller effect of thickness.

5. The general effect of pavement curling was observed to be the same in all tests. However, the effect of curl on stresses reported for the Maryland test was greater than any observed at the AASHO Road Test.

ACKNOWLEDGMENTS

This report was made possible through the work of the AASHO Road Test committees, staff and workers, particularly Frank Scrivner, Rigid Pavement Research Engineer. Appreciation is due to Bert Colly for assistance in the Road Test strain experiments and for his leadership in this field.

Recognition is also due to the Texas Highway Department personnel who participated in the preparation of this report, particularly Miss Patsy White. This work was done under the general supervision of T. S. Huff and M. D. Shelby, whose continued encouragement in the preparation of this report is appreciated.

REFERENCES

1. Carey, W. N., Jr., and Irick, P. E., "The Pavement Serviceability-Performance Concept." HRB Bull. 250, 40-58 (1960).
2. "The AASHO Road Test: Report 5—Pavement Research." HRB Special Report 61E, 352 pp. (1962).
3. "The AASHO Road Test: Report 2—Materials and Construction." HRB Special Report 61B, 173 pp. (1962).
4. Teller, L. W., and Sutherland, E. C., "The Structural Design of Concrete Pavements." Public Roads, 16:8, 9, and 10; 17:7 and 8; 23:8.
5. Spangler, M. G., "Stresses in the Corner Region of Concrete Pavements." Iowa Engg. Exp. Sta. Bull. 157 (1942).
6. Westergaard, H. M., "Stresses in Concrete Pavements Computed by Theoretical Analysis." Public Roads, 7:2 (April 1926).
7. Westergaard, H. M., "Analytical Tools for Judging Results of Structural Tests of Concrete Pavements." Public Roads, Vol. 14 (1933).
8. Westergaard, H. M., "New Formulas for Stresses in Concrete Pavement of Airfields." ASCE Proc. 73:5 (May 1947).
9. Kelley, E. F., "Application of the Results of Research to the Structural Design to Concrete Pavements." Public Roads, Vol. 20 (1939).
10. "Concrete Pavement Design." Portland Cement Association, Chicago (1951).
11. Pickett, Gerald, Raville, M. E., Janes, W. C., and McCormick, F. J., "Deflections, Moments and Reactive Pressures for Concrete Pavements." Kansas State College Bull. No. 65, Engg. Exp. Sta. (Oct. 15, 1951).

12. "Final Report on Road Test One-MD." HRB Special Report 4, 142 pp. (1952).
13. "Results of Modulus of Subgrade Reaction Determination at the AASHO Road Test Site by Means of Pavement Volumetric Displacement Tests." Corps of Engineers, U.S. Army, Ohio River Division Laboratories (April 1962).

Appendix A

ELASTIC CONSTANTS—AASHO ROAD TEST PAVEMENTS

TABLE 9

MODULUS OF SUBGRADE SUPPORT (k)

Outer wheelpath	107
Inner wheelpath	109
Average	108

TABLE 10

DYNAMIC TESTS ON 6- x 6- x 30-IN. BEAMS

Max. Aggregate Size (in.)	Age	Dynamic Modulus of Elasticity, E (10^6 psi)			Poisson's Ratio, μ		
		No. Tests	Mean, $\overline{X}$	Std. Dev., S	No. Tests	Mean, $\overline{X}$	Std. Dev., S
2½	8 mo	11	6.14	0.31	11	0.28	0.047
	1 yr	11	6.14	0.38	11	0.27	0.044
1½	8 mo	10	6.39	0.25	10	0.28	0.075
	1 yr	10	6.20	0.61	10	0.25	0.035

TABLE 11

STATIC AND DYNAMIC TESTS ON 6- x 12-IN. CYLINDERS

Max. Aggregate Size (in.)	Age	Static Modulus of Elasticity (10^6 psi)			Dynamic Modulus of Elasticity (10^6 psi)		
		No. Tests	Mean, $\overline{X}$	Std. Dev., S	No. Tests	Mean, $\overline{X}$	Std. Dev., S
2½	3 mo	10	4.57	0.80	—	—	—
	1 yr	11	5.15	0.57	10	6.25	0.33
1½	3 mo	9	4.61	0.68	—	—	—
	1 yr	11	5.25	0.40	10	5.87	0.74

TABLE 12

SUMMARY OF TEST RESULTS ON HARDENED CONCRETE
(Obtained from Data System 2230)

Max. Aggregate Size (in.)	Loop	Flexural Strength[1], 14 Days			Compressive Strength, 14 Days		
		No. Tests	Mean (psi)	Std. Dev. (psi)	No. Tests	Mean (psi)	Std. Dev. (psi)
2½	1	16	637	46	8	3,599	290
	2	20	648	37	9	3,603	281
	3	71	630	44	38	3,723	301
	4	96	651q	38	48	4,062	288
	5	96	629	28	48	4,196	388
	6	99	628	51	48	3,963	325
	All	398	636	45	199	3,966	376
1½	1	4	676	65	2	4,088	162
	2	39	668	44	19	4,046	295
	3	24	667	47	14	3,933	440
	All	67	668	46	35	4,004	352

[1] AASHO Designation: T97-57 (6- x 6- x 30-in. beams).

TABLE 13

SUMMARY OF STRENGTH TESTS
(Obtained from Data System 2231)

Max. Aggregate Size (in.)	Age	No. Tests	Flexural Strength (psi)	
			Mean	Std. Dev.
2½	3 days	11	510	23
	7 days	11	620	34
	21 days	11	660	51
	3 mo	11	770	66
	1 yr	11	790	61
	2 yr	11	787	66
1½	3 days	12	550	37
	7 days	12	630	35
	21 days	12	710	53
	3 mo	12	830	41
	1 yr	10	880	53
	2 yr	12	873	48

Appendix B

CHARACTERISTICS OF MATERIALS—RIGID PAVEMENT
(AASHO Road Test)

TABLE 14

PORTLAND CEMENT CONCRETE

Item	Pavement Thickness	
	5 In. and Greater	$2\frac{1}{2}$ and $3\frac{1}{2}$ In.
Design characteristics:		
Cement content[1], bags/cu yd	6.0	6.0
Water-cement ratio, gal/bag	4.8	4.9
Volume of sand, % total agg. vol.	32.1	34.1
Air content, %	3-6	3-6
Slump, in.	$1\frac{1}{2}$-$2\frac{1}{2}$	$1\frac{1}{2}$-$2\frac{1}{2}$
Maximum aggregate size[2], in.	$2\frac{1}{2}$	$1\frac{1}{2}$
Compressive strength, psi:		
14 days	4,000	4,000
1 year	5,600	6,000
Flexural strength, psi:		
14 days	640	670
1 year	790	880
Static modulus of elasticity (10^6 psi)	5.25	5.25
Dynamic modulus of elasticity (10^6 psi)	6.25	5.87

[1] Type I cement.
[2] Uncrushed natural gravel.

TABLE 15

SUBBASE MATERIALS

Item	Value
Aggregate gradation, % passing:	
$1\frac{1}{2}$-in. sieve	100
1-in. sieve	100
$\frac{3}{4}$-in. sieve	96
$\frac{1}{2}$-in. sieve	90
No. 4 sieve	71
No. 40 sieve	25
No. 200 sieve	7
Plasticity index, minus No. 40 material	N.P.
Max. dry density, pcf	138
Field density, as per-cent compaction	102

Appendix C

LIST OF SYMBOLS

a = radius of area of load contact, in in.; the area is circular in case of corner and interior loads and semicircular for edge loads.

a_1 = the distance, in in. from the corner of the slab to the center of the area of load application—taken as $a\sqrt{2}$ where a is the radius of a circle equal in area to the loaded area.

b = radius of equivalent distribution of pressure at the bottom of the slab.

D_2 = nominal thickness of the concrete slabs.

E = modulus of elasticity of the concrete, in psi.

h = thickness of the concrete slab, in in.

k = subgrade modulus, in pci.

ℓ = radius of relative stiffness.

L_1 = nominal axle load of the test vehicle (a single axle or a tandem-axle set).

P = point load, in lb.

T = the temperature (° F) at a point $\frac{1}{4}$ in. below the top surface of the 6.5-in. slab minus the temperature at a point $\frac{1}{2}$ in. above the bottom surface, determined at the time the strain was measured (the statistic T may be referred to occasionally as "the standard differential").

ϵ = estimated edge strain at the surface of the concrete slab.

μ = Poisson's ratio for concrete.

σ_c = maximum tensile stress, in psi, at the top of the slab, in a direction parallel to the bisector of the corner angle, due to a load applied at the corner.

σ_e = maximum tensile stress, in psi, at the bottom of the slab directly under the load at the edge, and in a direction parallel to the edge.

σ_i = maximum tensile stress, in psi, at the bottom of the slab directly under the load, when the load is applied at a point in the interior of the slab at a considerable distance from the edges.

σ_{cv} = maximum load stress, in psi, as determined in Loop 1 for corner load.

σ_{es} = predicted stress under single-axle load.

σ_{et} = predicted stress under tandem-axle load.

σ_{ev} = the critical load stress, in psi, as determined under a vibratory load on the no-traffic loop (edge load).